diversity

MDPI

Article

Improving Scientific Knowledge of Mallorca Channel Seamounts (Western Mediterranean) within the Framework of Natura 2000 Network

Enric Massutí [1,*], Olga Sánchez-Guillamón [2], Maria Teresa Farriols [1], Desirée Palomino [2], Aida Frank [1], Patricia Bárcenas [2], Beatriz Rincón [3], Natalia Martínez-Carreño [2], Stefanie Keller [1], Carmina López-Rodríguez [2], Julio A. Díaz [1], Nieves López-González [2], Elena Marco-Herrero [4], Ulla Fernandez-Arcaya [3], Maria Valls [1], Sergio Ramírez-Amaro [1], Francesca Ferragut [1], Sergi Joher [1], Francisco Ordinas [1] and Juan-Tomás Vázquez [2]

[1] Centre Oceanogràfic de les Balears, Instituto Español de Oceanografía (IEO–CSIC), 07015 Palma, Spain; mt.farriols@ieo.es (M.T.F.); aida.frank@ieo.es (A.F.); stefanie.keller@ieo.es (S.K.); julio.diaz@ieo.es (J.A.D.); maria.valls@ieo.es (M.V.); sergio.ramirez@ieo.es (S.R.-A.); isferragutperello@gmail.com (F.F.); sergi.joher@ieo.es (S.J.); xisco.ordinas@ieo.es (F.O.)

[2] Centro Oceanográfico de Málaga, Instituto Español de Oceanografía (IEO–CSIC), 29640 Fuengirola, Spain; olga.sanchez@ieo.es (O.S.-G.); desiree.palomino@ieo.es (D.P.); patricia.barcenas@ieo.es (P.B.); natalia.martinez@ieo.es (N.M.-C.); carmina.lopez@ieo.es (C.L.-R.); nieves.lopez@ieo.es (N.L.-G.); juantomas.vazquez@ieo.es (J.-T.V.)

[3] Centro Oceanográfico de Santander, Instituto Español de Oceanografía (IEO–CSIC), 39004 Santander, Spain; beatriz.rincon@ieo.es (B.R.); ulla.fernandez@ieo.es (U.F.-A.)

[4] Centro Oceanográfico de Cádiz, Instituto Español de Oceanografía (IEO–CSIC), 11006 Cádiz, Spain; elena.marco@ieo.es

* Correspondence: enric.massuti@ieo.es

Abstract: The scientific exploration of Mallorca Channel seamounts (western Mediterranean) is improving the knowledge of the Ses Olives (SO), Ausias March (AM), and Emile Baudot (EB) seamounts for their inclusion in the Natura 2000 network. The aims are to map and characterize benthic species and habitats by means of a geological and biological multidisciplinary approach: high-resolution acoustics, sediment and rock dredges, beam trawl, bottom trawl, and underwater imagery. Among the seamounts, 15 different morphological features were differentiated, highlighting the presence of 4000 pockmarks, which are seafloor rounded depressions indicators of focused fluid flow escapes, usually gas and/or water, from beneath the seabed sediments. So far, a total of 547 species or taxa have been inventoried, with sponges, fishes, mollusks, and crustaceans the most diverse groups including new taxa and new geographical records. Up to 29 categories of benthic habitats have been found, highlighting those included in the Habitats Directive: maërl beds on the summits of AM and EB, pockmarks around the seamounts and coral reefs in their rocky escarpments as well as fields of *Isidella elongata* on sedimentary bathyal bottoms. Trawling is the main demersal fishery developed around SO and AM, which are targeted to deep water crustaceans: *Parapenaeus longirostris*, *Nephrops norvegicus*, and *Aristeus antennatus*. This study provides scientific information for the proposal of the Mallorca Channel seamounts as a Site of Community Importance and for its final declaration as a Special Area of Conservation.

Keywords: geomorphology; geodiversity; biodiversity; habitats; benthic communities; trawl fishing; seamounts; Natura 2000 network; Balearic Islands; Mediterranean

Citation: Massutí, E.; Sánchez-Guillamón, O.; Farriols, M.T.; Palomino, D.; Frank, A.; Bárcenas, P.; Rincón, B.; Martínez-Carreño, N.; Keller, S.; López-Rodríguez, C.; et al. Improving Scientific Knowledge of Mallorca Channel Seamounts (Western Mediterranean) within the Framework of Natura 2000 Network. *Diversity* **2022**, *14*, 4. https://doi.org/10.3390/d14010004

Academic Editors: Carlo Nike Bianchi, Carla Morri and Michael Wink

Received: 31 October 2021
Accepted: 17 December 2021
Published: 22 December 2021

1. Introduction

The protection of marine species and ecosystems is especially relevant in the Mediterranean, which has been described as a hot spot of biodiversity [1]. Marine protected areas (MPAs) are recognized as useful tools for managing and enhancing marine species and ecosystems. MPAs can constitute a globally connected system for safeguarding biodiversity and maintaining the health of marine ecosystems and the services they provide. Through

the Protocol Concerning Specially Protected Areas and Biological Diversity in the Mediterranean (SPA/BD Protocol), the Contracting Parties to the Barcelona Convention promote cooperation in the management and conservation of natural areas as well as in the protection of threatened species and their habitats. The Marine Strategy Framework Directive (MSFD) also includes a requirement for the European countries of the Mediterranean to establish an ecologically coherent network of MPAs to help protect vulnerable species and habitats [2]. In the European Union, the main instrument for protecting biodiversity is the Natura 2000 network, which seeks the stable maintenance or, where appropriate, the restoration to a favorable status of certain habitats and species including the marine environment.

The Natura 2000 network is composed of Sites of Community Importance (SCI), which are subsequently declared as Special Areas of Conservation (SAC). These protection regimes seek to ensure the long-term preservation of these areas and their flora and fauna as well as the sustainability of human activities carried out therein through the implementation of management plans. As a result of the LIFE INDEMARES project (https://www.indemares.es/en (accessed on 15 December 2021)) developed between 2009 and 2014 in Spain, 10 large marine areas were declared as SCI, half of them sited in the Mediterranean. With this, the total protected sea surface off Spain increased from <1% to >8%, thus contributing to the objective of the Convention on Biological Diversity to protect 10% of marine regions by 2020.

The current LIFE IP INTEMARES project (https://intemares.es/en (accessed on 15 December 2021)) has the aim to complete this work. The scientific exploration of seamounts in the Mallorca Channel (Balearic Islands, western Mediterranean), developed within this project, is to improve the scientific knowledge of this area for its inclusion in the Natura 2000 network. The main objective is to map and characterize the benthic habitats and species of special interest for conservation, the most important human threats, and the vulnerability of the area to propose it as a SCI for the subsequent development of management plans and its final declaration as a SAC.

Seamounts are isolated undersea topographical elevations on continental margins and oceanic domains, which are considered as hotspots of biological activity and biodiversity in the deep-sea [3]. These relevant seafloor reliefs span a broad depth range, being influenced by different oceanographic processes [4] and located in diverse geodynamic settings. Therefore, they comprise heterogeneous habitat types [5], some of them structured by fragile, sessile, slow-growing, and long-lived species sensitive to fishing and other types of disturbance, being internationally recognized as Vulnerable Marine Ecosystems [6]. The scientific knowledge on Mediterranean seamounts is marked by large gaps and an asymmetry between the number of geological studies and biological ones [5].

Up to 60 seamounts and seamount-like structures have been identified in the western Mediterranean [7,8]. Among these are the Ses Olives (SO), Ausias March (AM), and Emile Baudot (EB) seamounts, currently studied within the INTEMARES project (Figure 1). Previous studies on these seamounts have analyzed the demersal fisheries targeted on deep water decapods crustaceans [9,10], the geomorphology and geodynamics [11,12], and the benthic species and habitats [13–17], suggesting their high ecological value. For this, the protection of these seamounts is recommended [18]. The present study includes the first results obtained in the INTEMARES project regarding the mapping and characterization of seafloor, benthic species, and habitats as well as fishing activity on SO, AM, and EB seamounts and adjacent bottoms.

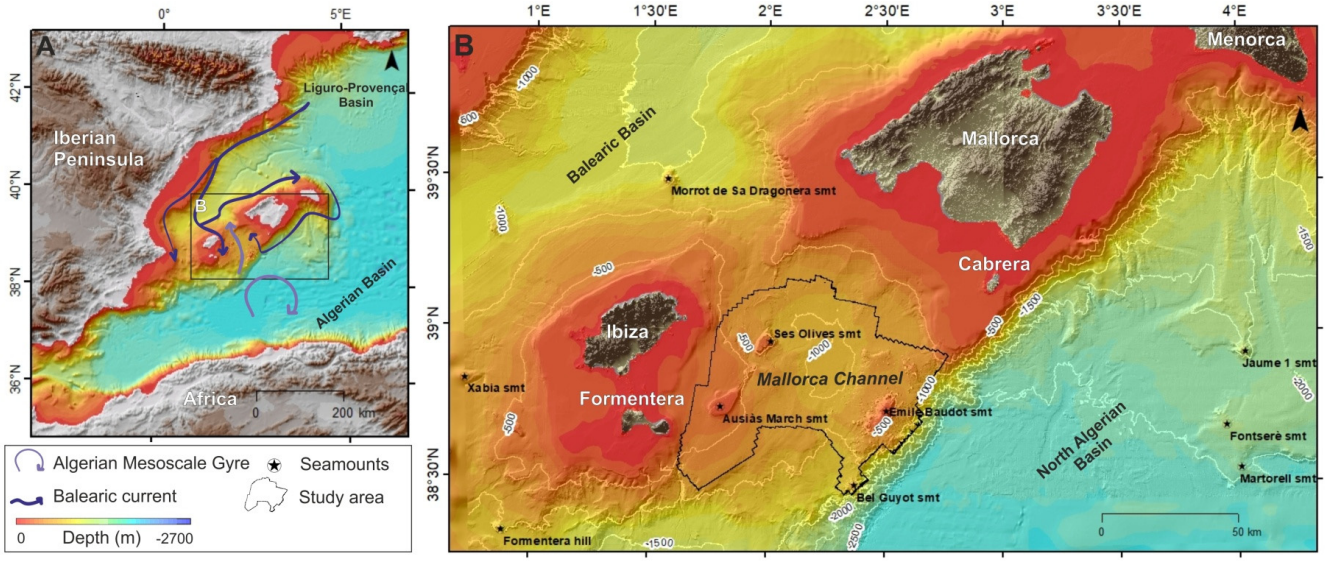

Figure 1. Map of the western Mediterranean showing (**A**) the Balearic Promontory and the (**B**) Ses Olives, Ausias March, and Emile Baudot seamounts and adjacent area of the Mallorca Channel currently studied within the INTEMARES project as well as other seamounts (smt) in the area. The western Mediterranean water mass circulation scheme is modified from López-Jurado et al. (2008).

2. Study Area

The Mallorca Channel corresponds to a seaway between the Ibiza and Mallorca islands, located southwest of the Balearic Promontory between the Valencia Trough to the west and the abyssal domain to the east (western Mediterranean). It can be described as an asymmetric channel, whose width varies between 100 and 200 km, narrowing toward the north and deepening up to 1050 m. It is characterized by the presence of a variety of morphological features such as seamounts, scarps, and depressions [8,19]. The three studied seamounts are located in this area, being situated east off Ibiza and the Formentera Islands in the case of SO and AM and south off Mallorca and the Cabrera Islands in the case of EB (Figure 1).

The Balearic promontory delimits the Balearic and Algerian sub-basins in the north and the south, respectively (Figure 1), with different oceanographic conditions [20]. The Balearic sub-basin is more influenced by atmospheric forcing and Mediterranean waters, which are colder and more saline, whereas the Algerian sub-basin is basically affected by density gradients and receives warmer and less saline Atlantic waters [21]. Different water masses can be found in both sub-basins [21,22]. The surface waters, coming from the Atlantic and called the Atlantic Waters (AW), have high seasonal temperature variation, ranging from 13 °C during winter to 26 °C during summer, when a strong vertical temperature gradient is established between a 50 and 100 m depth. The Western Mediterranean Intermediate Water (WMIW) is found at 100–300 m depths and exhibits variable thickness. It is formed during winter in the Gulf of Lions by deep convection, when sea–air heat flux losses are high enough, being characterized by a minimum temperature (~12.5 °C). The Levantine Intermediate Water (LIW), originating in the eastern Mediterranean, reaches the Balearic Islands after circulating through the northern part of the western Mediterranean. It shows maximum temperature and salinity (~13.3 °C and ~38.5, respectively) and is found at 200–700 m depths, just above the Western Mediterranean Deep Water (WMDW), which is located in the deeper part of the water column.

The regional circulation in the western Mediterranean is dominated by the Northern Current, which carries down these intermediate waters along the continental slope of the Iberian Peninsula and bifurcates when reaching the Ibiza Channel [21,23]. One significant part crosses this channel flowing southward, and the other part cyclonically returns along the northern Balearic Islands, forming the Balearic Current (Figure 1). The composition

of the waters passing through the Balearic channels are subject to inter-annual variations, depending on the amount of these waters reaching and passing these channels and the flows of the Atlantic Waters passing northward through Ibiza and Mallorca Channel [21,24,25].

Within the general oligotrophic environment of the Mediterranean, the waters around the Balearic Islands show more pronounced oligotrophy than the adjacent waters off the Iberian Peninsula and the Gulf of Lions, due to the lack of supply of nutrients from land runoff [26,27]. Frontal meso-scale events between Mediterranean and Atlantic waters [28] and input of old northern water into the channels [29] can act as external fertilization mechanisms that enhance productivity off the Balearic Islands.

These distinct hydrodynamic scenarios in the northern and southern Balearic Archipelago [30] could be on the basis of some differences observed in deep water ecosystems between the Algerian and the Balearic sub-basins: (i) trophic webs are supported more by plankton biomass than by benthic productivity, while supra-benthos plays a more important role, respectively [31,32]; and (ii) body condition of species is lower in the Algerian sub-basin than in the Balearic sub-basin, not only at an individual species level but also considering the whole assemblage [33]. The interannual variability in the meso-scale circulation above explained can influence the population dynamics of two of the most important demersal resources of the Mediterranean, the hake and the red shrimp as well as their accessibility to fishing exploitation [34,35].

Some demersal fisheries are developed in the Mallorca Channel, mainly focused on the deep water decapod crustaceans red shrimp (*Aristeus antennatus*) and the pandalid shrimp *Plesionika edwardsi* using bottom trawl in the adjacent bottoms of SO and AM and traps at the flanks and summits of the three seamounts, respectively [9,10], where commercial and recreational fishing fleets also operate more sporadically using bottom long-line and hand-lines, respectively, to capture large sparids and serranids. In all areas, there are also pelagic fisheries, mainly targeted to swordfish (*Xiphias gladius*) using pelagic and semi-pelagic long-lines [36] and to bluefin tuna (*Thunnus thynnus*) using purse-seine [37].

3. Materials and Methods

We developed a multidisciplinary approach including both geological and biological sampling, monitoring of the fishing fleet, and compilation and review of information from existing databases on fishing landings (Figure 2).

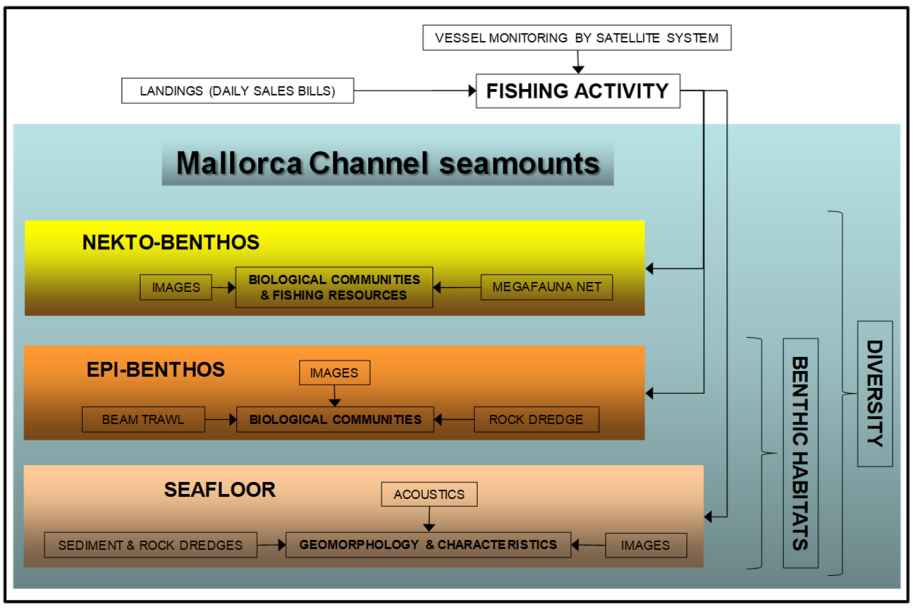

Figure 2. Scheme of the sampling strategy applied during the INTEMARES project in the study of the Ses Olives, Ausias March, and Emile Baudot seamounts of the Mallorca Channel (Balearic Islands, western Mediterranean).

3.1. Research Surveys

Between 2018 and 2020, four INTEMARES research surveys were developed (Table 1). High resolution geophysical techniques were applied to study the seafloor and dredges, where beam trawl and an experimental bottom trawl were used for sampling sediments, rocks, epi-benthic and nekton-benthic organisms as well as demersal fishing resources. A photogrammetric sledge and a remote operated vehicle (ROV) were also used to take videos of the seafloor communities. In 2020 and 2021, samples from the experimental bottom trawl were also collected during the three MEDITS surveys (Table 1).

Table 1. Summary of the research surveys developed in the Ses Olives, Ausias March, and Emile Baudot seamounts and adjacent bottoms of the Mallorca Channel (Balearic Islands, western Mediterranean) during the INTEMARES and MEDITS projects, showing the methods applied to obtain the data and samples: multibeam (MB) and parametric (P) echosounders, Shipek (SK), Box–Corer (BC) and rock (RD) dredges, beam trawl (BT), the experimental bottom trawl GOC-73 (GOC), photogrammetric sledge (ROTV), and remote operated vehicle (ROV).

Survey	Period	Research Vessel	Methods
INTEMARES_A22B_0718	25 July–8 August 2018	*Ángeles Alvariño*	MB, P, SK, BC, RD, BT
INTEMARES_A22B_1019	11–30 October 2019	*Ángeles Alvariño*	MB, P, SK, BC, RD, BT, GOC, ROTV
MEDITS_ES_GSA5_2020	24 June 2020	*Miguel Oliver*	GOC
INTEMARES_A22B_0720	19–29 July 2020	*Ángeles Alvariño*	MB, P, RD, BT
INTEMARES_A22B_0820	21–31 August 2020	*Sarmiento de Gamboa*	P, SK, BC, ROV
MEDITS_ES_GSA5_2021	23 June 2021	*Miguel Oliver*	GOC
MEDITS-PITIÜSES-2021	18, 19 and 25 August 2021	*Miguel Oliver*	GOC

3.1.1. Geophysical Methods

Bathymetric and backscatter data were obtained on board the R/V *Angeles Alvariño*, which is equipped with a Kongsberg EM710 multibeam echosounder transmitting from 40 to 100 kHz, depending on the changes in depth. During the acquisition, a sound velocity correction was applied using sound velocity profiles of the full water column (SVP+ from AML). An area of 4506 km^2 has been prospected, from 86 to 1720 m depths along 3250 km of parallel navigation lines (Figure 3A) with full coverage. At the same time, ca. 3000 km of high-resolution parametric profiles were acquired on board R/V *Angeles Alvariño* and R/V *Sarmiento de Gamboa* (Figure 3B) using Kongsberg TOPAS PS018 and Atlas Parasound P-35 sub-bottom profilers, respectively. These data allowed us to analyze the geomorphological features of the area.

3.1.2. Sediments and Rocks

A total of 137 surface sediment samples were collected using Shipek and Box–Corer grabs between 86 and 1062 m depths (Figure 3C, Appendix A). Recovered sediments were photographed and described on board. The topmost 5 cm layer of sediments recovered using the Box–Corer grab were sub-sampled using two sterilized bottles of 50 g each, which were stored at −18 °C for subsequent analysis in the laboratory.

A total of 55 samples were taken using a rock dredge between 89 and 1191 m depth, mainly at the summit and upper flanks of the seamounts (Figure 3D, Appendix B). This dredge is composed of a metallic rectangular mouth with beveled edges, equipped with a 1 cm mesh cod-end, protected by another net of 2 cm meshes and leather covers on bottom and top sides. It was trawled in an upward direction over the seafloor, collecting rock fragments, together with the associated flora and fauna. Sampling was conducted at 0.5–1 knots, with an effective duration from 5 to 10 min.

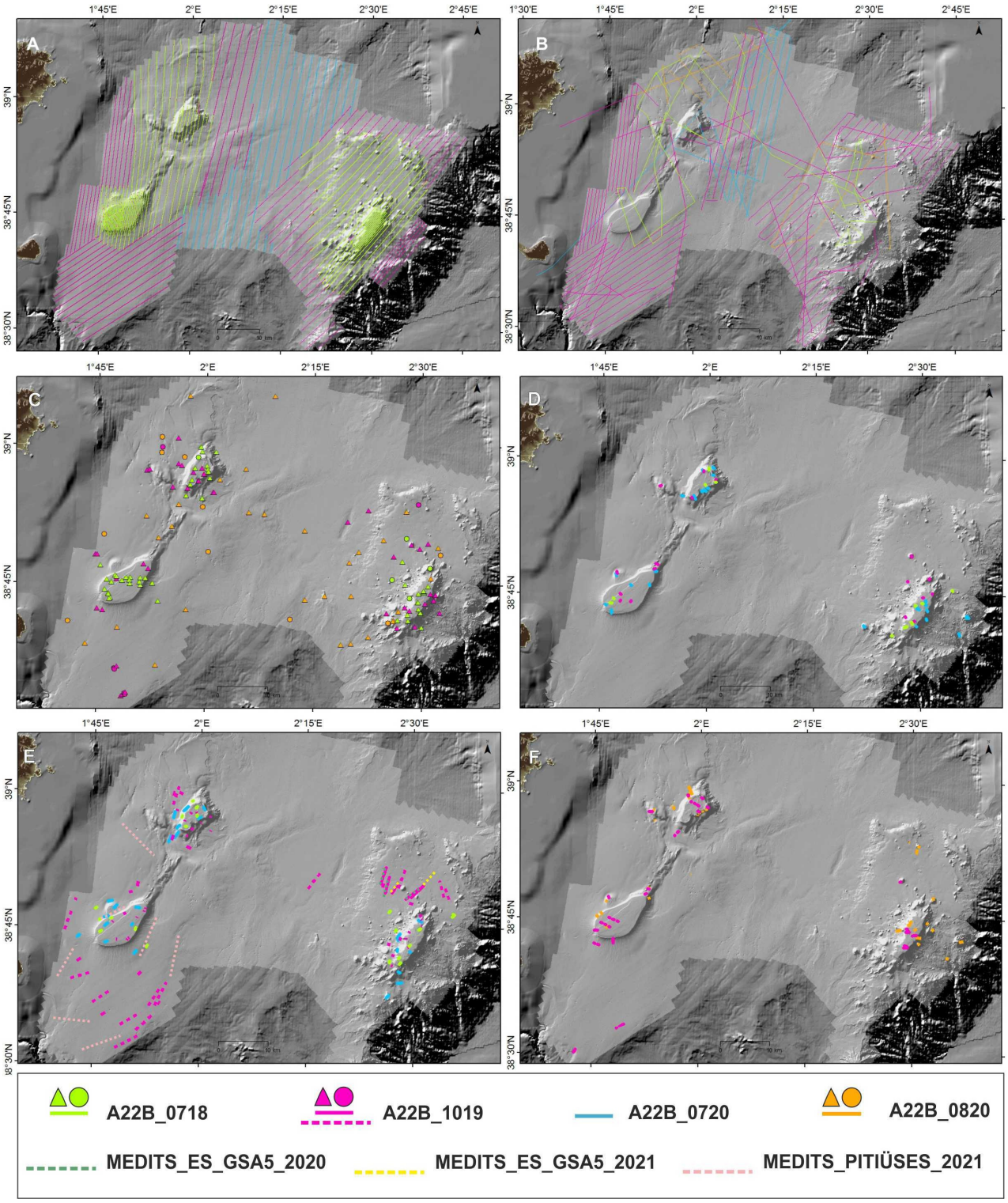

Figure 3. Map of the study area around the Ses Olives, Ausias March, and Emile Baudot seamounts in the Mallorca Channel (Balearic Islands, western Mediterranean) showing the sampling developed in each research survey (plotted in different colors): (**A**) multibeam echosounder; (**B**) high-resolution sub-bottom profilers; (**C**) Box–Corer in circles and Shipek in triangles; (**D**) rock dredges; (**E**) beam trawl (continuous lines) and GOC (dashed lines); and (**F**) ROTV (dashed lines) and ROV (continuous lines).

3.1.3. Epi-benthos

Samples were collected with a standard beam trawl described by Jennings et al. (1999) [38], and efficiency was estimated by Reiss et al. (2006) [39]. It has horizontal and vertical openings of 2 and 0.5 m, respectively, and a cod-end mesh size of 5 mm. Sampling was conducted at 2 knots and between 5 and 15 min of effective sampling duration. A total of 85 sampling stations were covered between 99 and 764 m depths (Figure 3E, Appendix C).

The megafauna was sorted on board, identified to species level or to the lowest possible taxonomic level, counted, and weighed. For the calculation of the abundance of colonial ascidians or cnidarians, a foot or colony was counted as one unit or individual. Some species of sponges and algae appeared fragmented and only their biomass was estimated. In the case of calcareous algae, only the biomass of living rhodoliths was measured.

Unidentified specimens were preserved in absolute ethanol or formaldehyde depending on the taxon for further identification at the laboratory. Abundance and biomass of living organisms were standardized by species or taxon to 500 m^2 using the horizontal opening of the net and the effective towing distance over the bottom in each haul. This distance was estimated using a global positioning system (GPS) and a SCANMAR net probe attached to the headline of the beam trawl to control depth and its arrival and departure to the bottom.

3.1.4. Nekto-Benthos and Demersal Resources

Samples were collected using the experimental bottom trawl GOC-73, widely used along the northern Mediterranean by the MEDITS program to estimate the abundance and distribution of demersal resources and the impact of the fishing activity on the ecosystems [40,41]. This gear has horizontal and vertical net openings ranging 18–22 and 2.5–3 m, respectively, and a cod-end mesh size of 10 mm. Its sampling efficiency has been estimated by Dremière et al. (1999) [42] and Fiorentini et al. (1999) [43]. Sampling was conducted at 2.8 knots and between 45 and 60 min of effective sampling duration, depending on depth. A total of 29 sampling stations were covered between 237 and 1028 m depths in the adjacent fishing grounds of AM and EB (Figure 3E, Appendix D).

Samples were sorted on board, identified to species level, counted, and weighed following the above-mentioned criteria. Length frequency sampling of fishes, decapod crustaceans, and cephalopod mollusks was also estimated. Abundance and biomass of species were standardized to one square km, using the horizontal opening of the net and the distance covered in each haul, obtained using the SCANMAR system and the GPS, respectively.

3.1.5. Visual Transects

Habitat and benthic communities were high resolution filmed from transects developed with the TASIFE photogrammetric sledge, a remotely operated towed vehicle (ROTV), and the ROV Liropus 2000. Each covered a different objective: The ROTV filmed sedimentary and flat areas, while the ROV filmed rockier areas and steeper slopes.

The ROTV transects were carried out with the vehicle moving at 0.5 knots and flying from 0.5 to 2.5 m above the seafloor. It was equipped with a Nano SeaCam piloting camera installed forward and a Nikon D800 video recording camera in the zenithal position, a spotlight system to illuminate the seafloor and three green laser beams, with a distance between them of 10 and 24 cm. Its accurate location over the bottom was obtained from the HiPAP® acoustic positioning of the R/V. The ROTV was also equipped with a precision altimeter and a SBE50 pressure sensor to control its distance to the bottom and depth, respectively. A total of 48 transects from 15 to 20 min were recorded with a ROTV between 87 and 708 m depths (Figure 3F, Appendix E), providing 13 h of video and a total explored area of 30,066 m^2: 8304 m^2 in SO, 19,124 m^2 in AM, and 2638 m^2 in EB.

The ROV transects were carried out with the vehicle moving at <0.3 knots and flying from 0.5 to 2.5 m above the seafloor. This ROV is equipped with a full HD color camera and a pal color camera installed forward and a mini camera in the rear part. It was also

equipped with a CTD SBE37Microcat, two laser pointers, a dual frequency SONAR Seaking DST, an altimeter (LPA200), an acoustic Beacon MST 324, two hydraulic manipulators, and a boxes system to store collected samples. The navigation system of this ROV includes a Tether Management System (TMS) and a Launch and Recovery System (LARS). The TMS is equipped with an extra low light back and white camera, a CTD, a current meter Midas Valeport, and an acoustic beacon MST 324. A total of 29 transects from one to four hours were recorded with ROV between 89 and 1162 m depth (Figure 3F, Appendix F), providing 52 h of video and a total explored area of 17,322 m^2.

3.2. Fishing Activity

The most important demersal fishery operating within the study area was assessed from Vessel Monitoring by satellite System (VMS) data of the bottom trawl fleet. The VMS database consists of records that contain data on the geographic position, date, time, and instantaneous velocity for each boat, approximately every two hours. In the study area, trawlers are only allowed to work 12–13 h per day (05:00–17:00 the insular fleet and 05:00–18:00 the peninsular fleet) and five days a week, from Monday to Friday. In order to remove VMS signals from boats transiting to fishing grounds or ports, only records with an instantaneous vessel velocity from 2 to 3.5 knots were selected, making sure vessels were fishing at the time of the emitted signal.

After filtering, a total of 115,764 VMS signals were retained during the period 2016–2019. These signals were used to estimate the trawling effort in the study area. Each signal was assigned to one of the trawl fishing grounds previously mapped by Guijarro et al. (2020) [44] around the Balearic Islands. Then, the fishing effort in each fishing ground was calculated as the number of fishing trips per year. In addition, data on the landings and their economic value were obtained from daily sales bills of the bottom trawl fleet. The marketing of their catches takes place the same day or the day after the catches, depending on the ports. These sheets detail, for each vessel, the kilograms auctioned by species commercial category as well as their first sale value. The daily VMS data of the vessels allowed us to assign their sales sheets, and therefore the landings, to the exploited fishing grounds. To assess the bottom trawling around the studied seamounts, we estimated the number of fishing days developed by trawlers in the fishing grounds closest to them as well as the catches extracted and revenues obtained.

3.3. Analysis of Samples in the Laboratory and Data Processing

3.3.1. Geomorphology

Bathymetric raw data were imported in a single project using CARIS HIPS and SIPS V. 11.3 software (© Teledyne) and were georeferenced to create a gridded base surface of a 2 × 2 m cell size in the shallower zones of the summit of the seamounts, of 8 × 8 m in the whole seamounts, and 16 x 16 in the deepest zones of the seafloor. The CUBE algorithm was used to create the surface and data were manually inspected and cleaned using the subset editor module. Tide correction was applied and the final processed data were exported as geotiff raster files. After cleaning, the backscatter mosaic was obtained using the SIPS backscatter module and Geocoder algorithm and exported as a geotiff raster with the same resolution. Bathymetric and backscatter processed data were integrated into an ArcGIS v.10.8 (© ESRI) project where the geomorphological analysis was conducted.

Parametric profiles were loaded in a Kingdom IHS Markit software for their interpretation. Time-to-depth conversion was conducted assuming a sound velocity of 1600 m/s for unconsolidated sediments [45].

The identification and counting of pockmarks were carried out using a sequence of well-defined ESRI ArcGIS tools for mapping and spatially delineated these features in individual polygons, which represent the areas of the seabed where pockmarks occur. The methodology used was based on the study developed in other pockmark fields located in the central North Sea [46].

3.3.2. Sediments

The sedimentological analysis for grain size distribution was carried out on 10–15 g of sediment pre-treated with 10% H_2O_2 to remove organic matter and sodium hexametaphosphate as a dispersing agent. Samples were wet sieved to separate the coarse fraction (gravel) using a 2 mm mesh size sieve. Particles <2 mm (sand, silt, and clay) were determined by using a laser diffraction analyzer (Mastersizer 3000, Malvern® Panalytical, Fuengirola, Spain). The textural classification of the sediments was based on Folk (1954) [47] ternary diagrams.

The organic matter (OM) and carbonate contents were obtained by the loss on ignition method (LOI) [48] in dry sediment samples (60 °C for 72 h). The percentages of OM and carbonates were estimated as the weight loss after the first (550 °C for 4 h) and second (950 °C for 2 h) ignitions, respectively.

3.3.3. Biological Communities and Fishing Resources

The standardized abundance and/or biomass by species or taxon at each beam trawl and experimental bottom trawl station were used to construct benthic and nekton-benthic species matrices, respectively. In the case of rock dredge stations, for which standardization was not possible, the data matrix only included the presence/absence data by species or taxon. Additionally, the length frequency distribution of the red shrimp *Aristeus antennatus*, the target fishing resource for the deep-water trawl fishery in the whole western Mediterranean [49], was also estimated from the experimental bottom trawl samples.

For multivariate analysis, data were square-root transformed and similarity between samples was calculated using the Bray–Curtis index. Cluster analysis and non-metric multidimensional scaling (MDS) were conducted to identify assemblages. The similarity percentage analysis (SIMPER) and the analysis of similarity (ANOSIM) were applied to characterize the species composition of assemblages and to test for differences in their composition, respectively.

For each assemblage, we calculated the following community and diversity indicators: mean standardized total abundance and biomass, number of species (S), Shannon–Wiener (H'), and Pielou evenness (J'). These analyses were performed with the PRIMER-E 6 and PERMANOVA software [50]. The index of diversity N90, especially sensitive to the fishing impact [51–53], was also applied to detect differences between assemblages. This was calculated following the R procedure described in Farriols et al. (2021) [54]. For statistical comparisons, the Student's *t*-test was used. The Shapiro–Wilk test was applied to check for normality. When this assumption was not met, a Kruskal–Wallis non-parametric test was applied.

3.3.4. Habitat Identification from Images

The analysis of video transects carried out thus far has been qualitative. Both ROTV and ROV were viewed using VLC Media Player 3.0.16 for Windows software. Video fragments not allowing for accurate identification of habitats or species, containing blurry images or not showing the two laser pointers, were considered not valid. Video recorded while the ROV stopped or was too far or too close from the seabed to properly visualize it was also considered not reliable for analysis.

In the case of ROTV, the coverage percentage of each habitat type was estimated with the time observed within a width of 0.5 m (based on the laser beams). The video fragments were divided into sections that showed only one habitat at a constant speed and the same distance from the seafloor. These fragments were considered the sampling units. The covered area was calculated by multiplying the sampling unit length by the field of vision width of the ROV camera, estimated from the laser pointers for scaling.

On each sampling unit, habitat and substrate type categories (fine sand, medium sand to gravel, cobbles and pebbles, rhodoliths, and rock) were defined and the biota was identified to the lowest possible taxonomic level and counted, with special focus on taxa considered vulnerable, as a conservation target and habitat-forming species. In some cases, especially for sponges, cnidarians and tunicates were catalogued in morphotype categories.

The habitat identification was carried out considering those included in the Habitats Directive 92/43/EEC such as sandbanks that are slightly covered by sea water all the time (Habitat code 1110), reef (Habitat code 1170), and underwater structures formed by gas leaking (Habitat code 1180). When none of these habitats was observed, it was categorized according to the Spanish Inventory of Marine Habitats and Species [55], guidelines for inventorying and monitoring dark habitats in the Mediterranean [56], and previous studies in the Balearic Islands [13,14,57–59].

4. Results

4.1. Geomorphological Features of the Seafloor

Six main morphological feature groups characterized the geodiversity of the Mallorca Channel (Figure 4). Based on their origin, these features were classified as (i) structural; (ii) fluid escape-related; (iii) volcanic; (iv) mass movement-related; (v) bottom current-related; and (vi) biogenic-related (Figure 4A). The near surface morphology and the sub-bottom sedimentary structure of these features as well as their location in each seamount and adjacent seafloor are explained below.

- Structural features

Features related to tectonics, with a morphological expression on the seafloor, were mapped in the entire study area. The main structures were seamounts, highs, ridges, tectonic depressions, and fault scarps.

Both SO and AM are NNE–SSW trending seamounts made up sedimentary rocky materials, corresponding to Balearic Promontory basement uplifted by tectonics. A linear fault scarp runs longitudinally across the summit of AM at 86–150 m depth (Figure 4C). It is 8.6 km long, up to 64 m deep in its SW edge and 23 m in its NE edge, with 32° of slope (Figure 4B). The sub-bottom profiles indicated a relatively thin sedimentary cover (<15 m) at the summits of the seamounts (Figure 4F).

Close to these seamounts, two minor highs named Greixonera and Dimoni are located, showing sharp flanks up to 40° of slope (Figure 4D). Greixonera, 230 m high and 6 km long, is located in western SO, whilst Dimoni is a 300 m high and 5 km long spike located at the edge of a structural spur in northern AM.

Moreover, two NE–SW ridges were located to the north and central area of the Mallorca Channel, having lengths of 10 to 12 km, respectively, and moderate slopes (Figure 4A,B). Several depressions and fault scarps with NNE–SSW to N–S trends are located to the northeast of the northern ridge, and to the north, south, and east of the central ridge, most likely associated with structural control.

- Fluid escape-related features

Pockmarks are the main feature related to fluid seepage, being mapped more than 3950 in a 300–1000 m depth range. They are extended in the whole study area, with the exception of the deep central basin area, which only presents some individual depressions. Most of these pockmarks had circular shapes with U to V-shaped cross sections (Figure 4D). Their length ranged from 10 to 500 m and up to 40 m in deep. Although most of them appeared randomly distributed, some were aligned, forming strings in mainly NW–SE, NE–SW, and N–S trends. In some cases, these strings developed elongated depressions and were emplaced on normal faults, recognized in the parametric profiles (Figure 4G).

- Volcanic features

The main volcanic element is the EB seamount that corresponds to a NNE–SSW oriented volcanic guyot, whose summit is located between 94 and 150 m in depth. It is constituted by the coalescence of several volcanic buildings, partially visible on the eroded summit of the seamount, which is also characterized by several terraced levels at 100–150 m depth and a volcanic cone of 130 m high in its northeastern edge.

In addition, a volcanic cone field was identified on the flanks and adjacent seafloor of EB between 215 and 915 m depths (Figure 4A,E). It comprises at least 170 spike and

flat-topped conical edifices that rise from 25 to 420 m, with maximum widths and lengths of 140 to 1785 m and slopes up to 50°. These are mostly circular, although some have irregular geometries.

- Mass-movement related features

Mass-movement features were one of the most widespread features in the Mallorca Channel. They comprise both erosive and depositional elements such as slide scars and mass-transport deposits (MTD). In addition, some gullies related to these features have been differentiated.

Erosive surfaces and gullies developed in the upper sector of the eastern flanks of EB and AM, forming a network of drainage that erodes their walls. They appear as narrow V incisions, separated by moderate to sharp ridges up to 30 m in depth. They have different orders of magnitude, being larger in EB than in AM. In general, they are 1 to 5 km long and have NW–SE and NE–SW to N–S trends, respectively (Figure 4C), with moderate slopes. Their heads are mainly sub-circular in shape and coalesce, forming major amphitheater scarps such as the one located northwestern EB, up to 4 km long (Figure 4C).

Slide scars were identified on the eastern flanks of SO and the western flank of EB as well as in the adjacent seafloor (Figure 4A,E). They have amphitheater geometry and high slopes of 40°, lengths of 1.5 to 2.2 km in SO, and up to 5 km long in EB. Those developed in the northern Mallorca Channel are evenly affected by pockmarks at the sharp walls.

MTDs were present along the Mallorca Channel slope, mainly at the foot of the slope of the seamounts at different depths, generating scarps of up to 20 m high at the seafloor. In parametric profiles, it was observed that most part of these deposits has nowadays been buried, but recent deposits affecting the seabed were also observed. Those MTDs were up to 50 m thick and recognized by the disappearance of sediment packages and the presence of sedimentary features. Moreover, some buried MDTs appeared stacked, representing at least three different events (Figure 4G).

- Bottom current related features

Bottom current features were mainly mapped at the base of AM. They comprised erosive elements such as contourite moats and furrows and depositional ones such as contourite drifts and sediment waves.

Contourite moats were elongated depressions located around seamounts. They are asymmetric and have U–shaped cross sections that deepen up to 30 m of incision and are mainly NE–SW oriented. In addition, a major 2 km long and 35 m deep moat was identified locally, associated with the western edge of AM. It is asymmetric, half-moon shaped, and NE–SW oriented (Figure 4C).

Several contourite drifts were identified associated with the moats, depressions, and the seamounts. These are mainly mounded and plastered drifts attached to the edges or bases of these features. These contourite drifts are occasionally disturbed by pockmarks and slide scars, and in some cases, older MTDs appear under the youngest drift deposits (Figure 4F).

Small scale sediment waves were identified in the southern AM at 300–400 m depths. They comprise slightly sinuous crests with NE–SW to N–S trends and occupy a total area of 17 km^2 (Figure 4C,H).

- Biogenic related features

Biogenic features were identified in the summits and upper flanks of SO, AM, and EB, being well represented in the western area of AM and central area of EB. They are mound-shaped to ridge features up to 2 to 15 m high and around 200 m long, that when coalesced reach lengths up to 1 km (Figure 4A,D). Biogenic mounds were formed by hard substrates, coming from bioclastic accumulations of fossil and contemporary calcareous framework-building organisms such as coralline algae (e.g., rhodoliths) and other skeleton-supported reefs of scleractianians and octorals as well as bivalve cement-supported reefs.

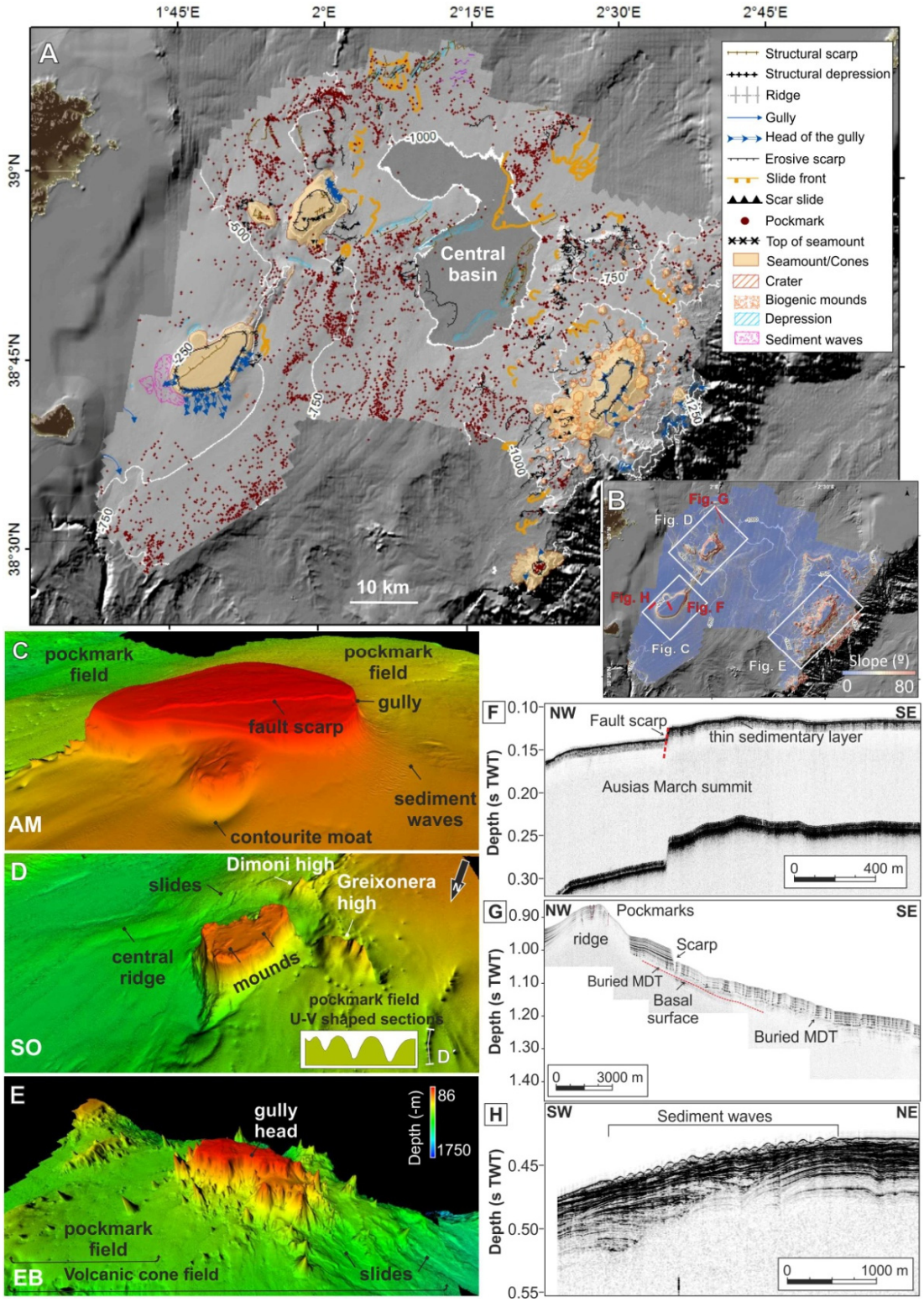

Figure 4. Bathymetry and geomorphology of the seafloor in the Mallorca Channel: (**A**) Morphological map showing the main morphological features and domains of the study area; (**B**) slope map showing bathymetric contours at each 250 m and the location of the 3D bathymetric models and parametric profiles; (**C**–**E**) overview 3D bathymetric map of the main edifices of the study area: Ses Olives, Ausias March, and Emile Baudot seamounts and Greixonera and Dimoni highs; (**F**–**H**) parametric profiles showing the internal structure of the main morphological features present in the study area.

4.2. Sediment Characterization

Sediments at the summit of AM were coarse and mixed (Figure 5A,B) with a texture ranging from gravelly sand (up to 35% gravel) to gravelly muddy sand (up to 28% mud). The nearest surrounding areas of this seamount were muddy to silty sand (up to 36% silt), evolving to a finer texture of sandy silt (up to 61% silt) toward the Dimoni high. The pockmark field at the southern area of the seamount was mostly sandy mud to sandy silt (53% average silt), with 22 and 25% clay and sand content, respectively (Figure 5A,B).

Sediments at the summit of SO show an average sand content of 90%, thus they were classified as sand and muddy sand becoming less sandy (68% on average) and more muddy (32%) toward the flanks (Figure 5A,B). The pockmark field observed at the northwest of this seamount was sandy mud in texture, where the silt content (40% on average) was higher than the clay (23%) and the sand (37%).

EB was quite heterogeneous in sediment texture, ranging from coarse sediments of gravelly sand (up to 92% sand) and mixed sediments of gravelly mud (up to 83% mud) at the summit, toward sand (up to 98%) to muddy sand (up to 48% mud) in some areas of the summit, the flanks, and in the nearest area of volcanic cones (Figure 5A,B). The pockmark field at the north of this seamount is sandy mud that evolves to coarser sediment, predominantly muddy sand toward northern areas. On average, the sediment was characterized by 42, 36, and 22% of sand, silt, and clay, respectively.

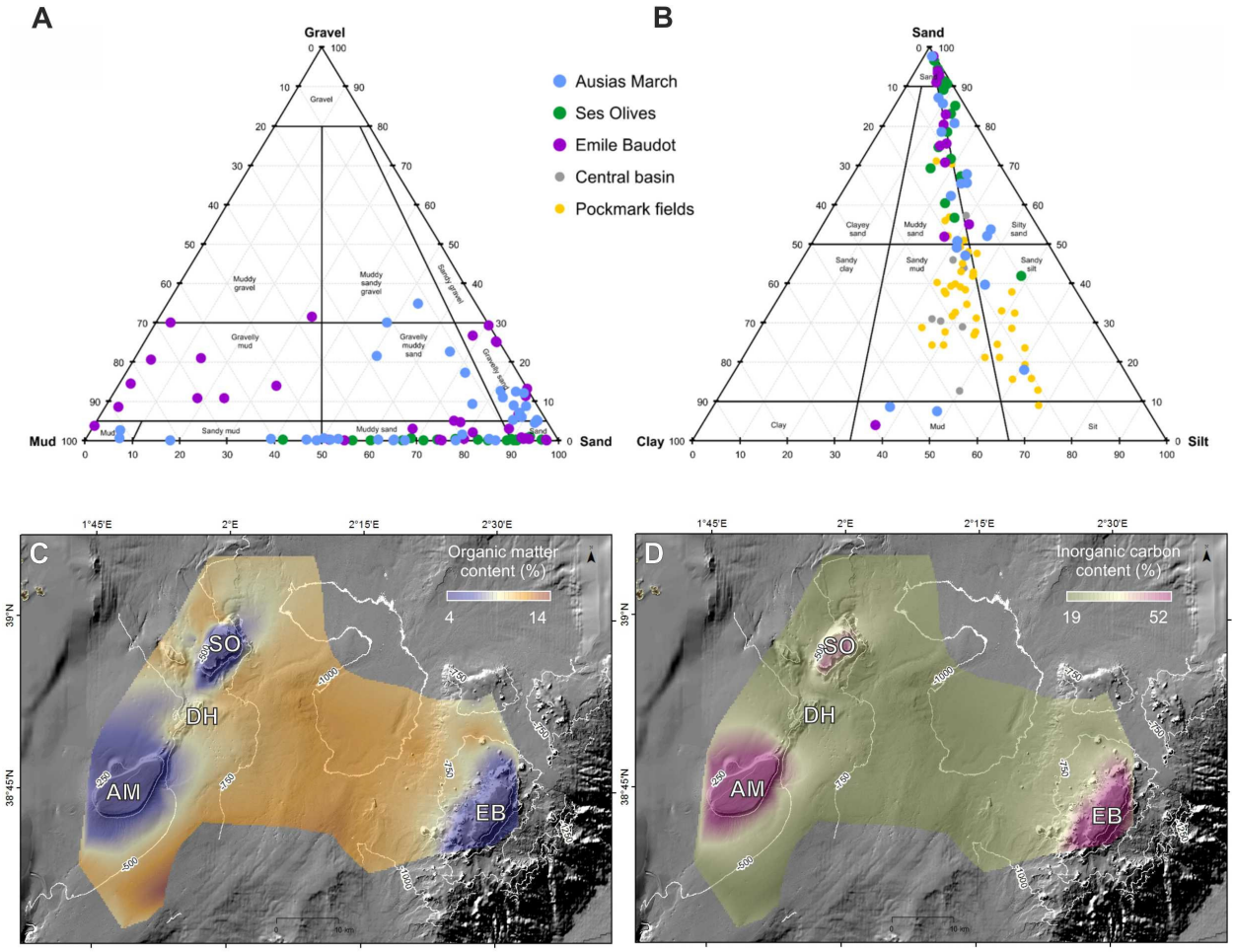

Figure 5. Surface sediment characteristics of the Ses Olives, Ausias March, and Emile Baudot seamounts, pockmark fields around them, and the central basin of the Mallorca Channel (Balearic Islands, western Mediterranean): (**A**,**B**) Folk (1954) classification diagrams indicating the particle size percentage variation of the surface sediment samples; (**C**) organic matter content percentage map; and (**D**) inorganic carbon content percentage map.

In general, the coarser sediments were observed in the summit of AM, followed by EB and SO. The main difference among the pockmark fields is the content of silt and sand, since the clay was similar in all of them. The coarser textures were observed in the pockmark field in northern EB, while the finer textures were present in the pockmark field in southern AM. Some samples in the central basin showed sediments of sandy mud texture (Figure 5A,B), with silt (up to 50%) as the dominant fine fraction.

The organic matter content in surface sediments ranged from 4 to 14.3% with a mean value of 10.4% (Figure 5C). The lowest values (4.6–9.3%) were observed on the summits of the three seamounts, extending along their flanks to 300–350 m depths. The rest of the studied area showed intermediate to high values of organic matter content (9.3–14.3%), with the highest values observed in the central basin.

The carbonate (inorganic carbon) content values of the surface sediments ranged from 19.5 to 52.2%, with an average value of 27.9% (Figure 5D). The spatial distribution showed maximum values (>43%) at the summits of AM and EB, extending on their flanks up to 250 m in depth. In general, the distribution was opposite to that of the organic matter content. The intermediate values (43–34%) were distributed from 250 to 350 m depths including the summit of SO. The rest of the studied area, from a 350 m depth onward, was covered by sediments with low carbonate content (<34%), reaching minimum values in the central basin.

4.3. Biodiversity, Species Assemblages and Fishing Resources

So far, a total of 547 different species or taxa have been identified (Appendix G), most of them identified from beam trawl (68%), while 30, 29, and 25% were identified from ROV, bottom trawl, and rock dredge sampling, respectively. There were also differences in the number of species or taxa identified by seamount, being 184 in SO, 413 in AM, and 369 in EB. The more diverse groups were sponges, followed by teleost fishes, mollusks, crustaceans, and echinoderms with 118 (22%), 105 (19%), 96 (18%), 91 (17%), and 49 (9%) species or taxa identified, respectively.

The cluster and MDS analyses of standardized biomass from beam trawl samples identified three epi-benthic assemblages on sedimentary bottoms, which were strongly influenced by depth (Figure 6A): (BT-a) the shallowest samples, between 102 and 169 m, at the summits of AM and EM; (BT-b) a group of samples from intermediate depths, between 227 and 574 m, at the summit of SO and flanks of SO, AM, and EB; and (BT-c) the deepest samples, between 500 and 756 m, at the base and adjacent bottoms of these three seamounts. The ANOSIM results ($R = 0.77$; $p < 0.01$) confirmed significant differences between these assemblages. The mean values for the estimated ecological parameters showed differences between these assemblages (Table 2). Both standardized abundance and biomass and the diversity indices S, H', and N_{90} decreased with depth. In contrast, the three assemblages showed similar values of equitability (J').

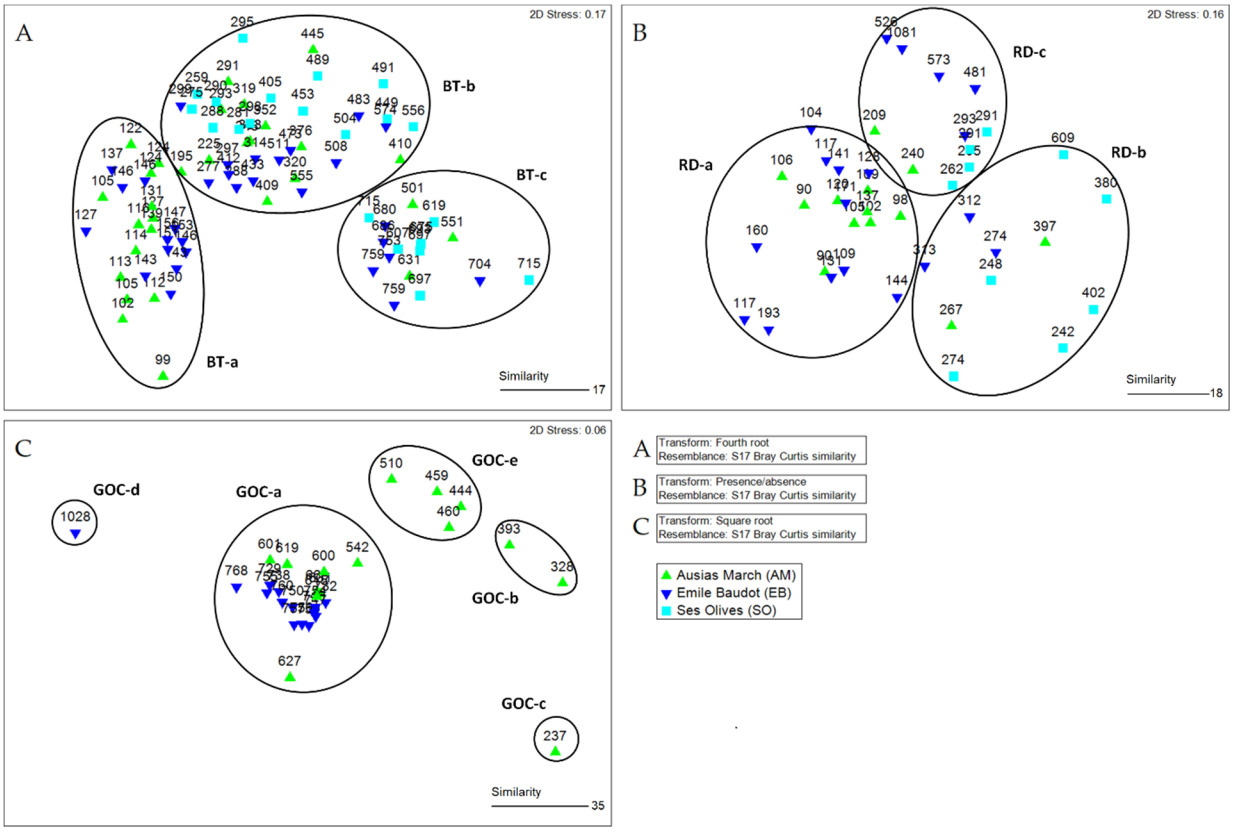

Figure 6. Multi-variant analysis of benthic assemblages, obtained in sedimentary and rocky bottoms of the Ses Olives (SO), Ausias March (AM) and Emile Baudot (EB) seamounts and adjacent area of the Mallorca Channel (Balearic Islands, western Mediterranean): (**A**) MDS and clusters at >17% similarity of epi-benthic species, identified from the analysis of beam trawl samples, in terms of standardized biomass (g/500 m^2), obtained in sedimentary bottoms; (**B**) MDS and clusters at >18% similarity of benthic species assemblages, identified from the analysis of presence/absence matrix from rock dredge samples, obtained in rocky bottoms; and (**C**) MDS and clusters at 50% similarity of necto-benthic species, identified from the analysis of experimental bottom trawl samples, in terms of standardized abundance (individuals/km^2), obtained in the fishing grounds adjacent to AM and EB. Labels and symbols correspond to sampling depth and area, respectively.

Table 2. Mean values (μ) and standard errors (SE) of standardized abundance and biomass, species richness (S), Shannon–Wiener (H′), and Pielou evenness (J′), estimated for each of the assemblages identified from multi-variant analysis of beam trawl, rock dredge, and experimental bottom trawl samples obtained at the Ses Olives, Ausias March, and Emile Baudot seamounts and adjacent area of the Mallorca Channel (Balearic Islands, western Mediterranean). The code (see Figure 7), number of samples analyzed (n), depth (D), number of species (Spp.) of each assemblage, and the significant differences (Kruskal–Wallis test; $p < 0.001$) between all assemblages (*) or between pairs of assemblages (1–2, 1–3) are also shown. In the case of beam trawl sample assemblages, mean (AvN_{90}) and standard deviation (SDN_{90}) values of the N90 diversity index are also shown, jointly with the associated average (AvSim) and the standard deviation (SDSim) values of within-group similarity.

				n/500 m^2		g/500 m^2		S		H′		J′					
Code	**n**	**D (m)**	**Spp.**	**μ**	**SE**	**μ**	**SE**	**μ**	**SE**	**μ**	**SE**	**μ**	**SE**	**AvN90**	**SDN90**	**AvSim**	**SDSim**
Beam trawl (BT)																	
BT-a1	25	99–156	407	33(*)	7	208.6(1,3)	69.2	52.0(*)	16.2	2.6(1,3)	0.7	0.7	0.2	45.62	1.08	11.43	0.48
BT-b2	40	195–574	354	10.3(*)	1.4	16.8(1,2)	4.8	38.9(*)	16	2.2	0.5	0.6	0.2	28.48	0.98	11.53	0.42
BT-c3	17	501–759	124	3.4(*)	0.9	9.7	2.8	20.5(*)	7.2	1.9	0.6	0.6	0.2	8.71	0.59	21.88	0.88
Rock dredge (RD)																	
RD-a	20	90–193	139					15.15	2.11								
RD-b	12	242–609	64					8.25	1.55								
RD-c	10	209–1081	56					9.8	1.9								
Experimental bottom trawl (GOC)																	
GOC-a	21	542–768	76	3.5×10^3	485.4	270.5	45.2	22	0.8	2.3	0	0.8	0				
GOC-b	4	444–510	66	15.1×10^3	3283.1	206.9	73.8	41.3	2.4	2.9	0.3	0.7	0.1				
GOC-c	2	328–393	60	44.8×10^3	20,958.7	1157	427.6	42	2	2.3	0.1	0.6	0				
GOC-d	1	237	25	6.3×10^3	-	749.2	-	25	-	2	-	0.6	-				
GOC-e	1	1028	4	150.1	-	0.42	-	4	-	1.1	-	0.8	-				

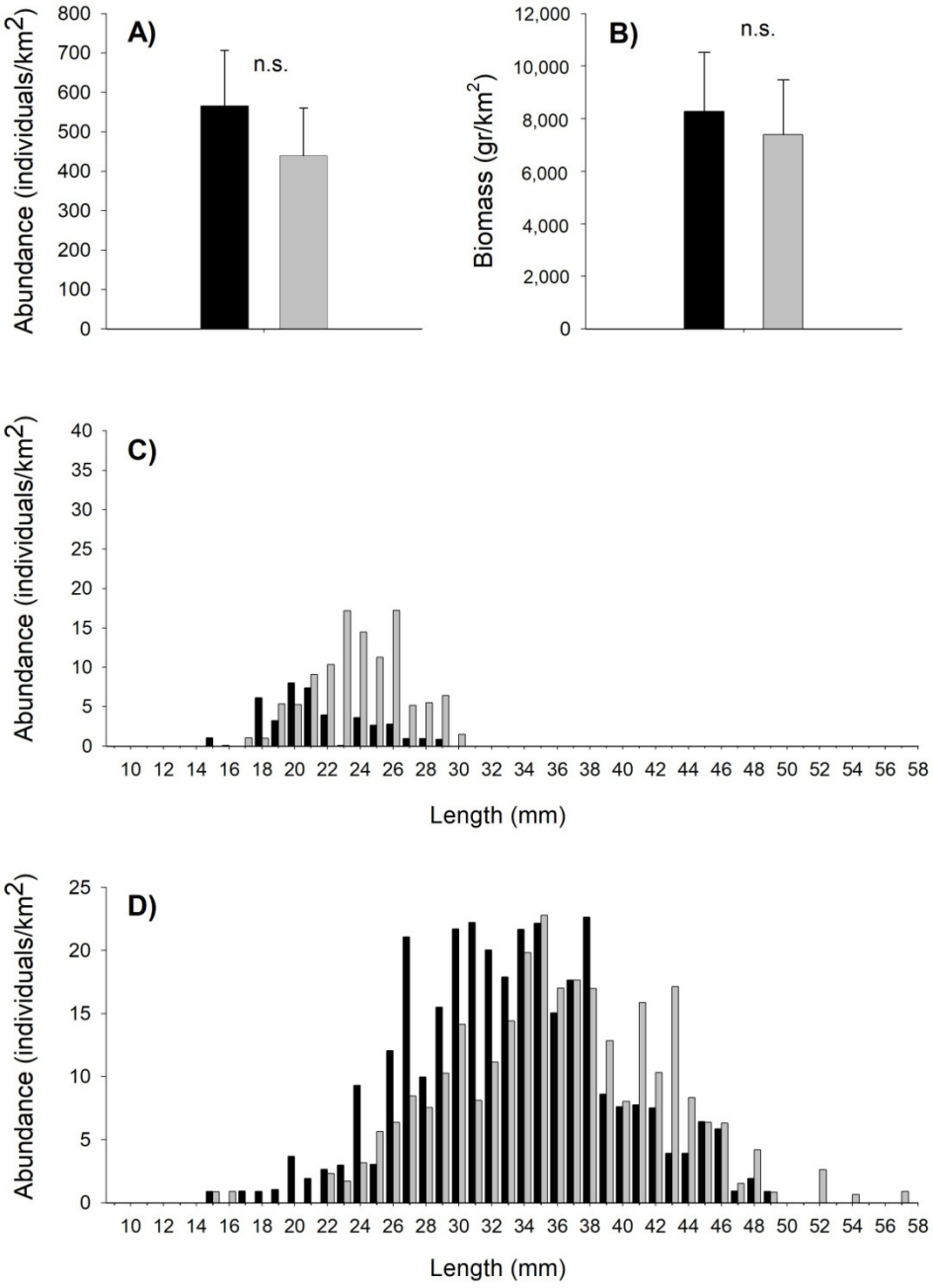

Figure 7. Mean standardized abundance (**A**) and biomass (**B**) and length frequency distribution by males (**C**) and females (**D**) of red shrimp (*Aristeus antennatus*) at fishing grounds adjacent to the Ausias March (black columns) and Emile Baudot (grey columns) seamounts of the Mallorca Channel (Balearic Islands, western Mediterranean). Standard error and results of the Student's *t*-test are also shown: n.s. (not significant).

SIMPER results (Table 3; Appendix H) showed that the main species contributing to within-group similarity in the BT-a assemblage were coralline red algae (10%), while the contribution of a high number of decapod crustaceans, sponges, brachiopods, and echinoderms, both sea urchins and sea stars, was much lower (1–3%). No species contributed much more than the others to the similarity of the BT-b assemblage, ranging between 2 and 7% of the contribution of ten species of crustaceans (decapods and the peracarid *Lophogaster typicus*), sponges, the brachiopod *Gryphus vitreus*, an echinoderm (the brittle star *Ophiura* (*Dictenophiura*) *carnea*), and the cephalopod mollusk *Sepietta oweniana*. Decapod crustaceans were the main species contributing to similarity of the BT-c assemblage, with only three

species (*Geryon longipes*, *Polycheles typhlops*, and *Calocaris macandreae*) summing more than 50% of this similarity.

Table 3. Summary of SIMPER results of the assemblages (see codes in Figure 7) identified from multi-variant analysis of beam trawl (BT), rock dredge (RD), and experimental bottom trawl (GOC) samples obtained in sedimentary and rocky bottoms of the Ses Olives (SO), Ausias March (AM), and Emile Baudot (EB) seamounts and adjacent area of the Mallorca Channel (Balearic Islands, western Mediterranean), showing the percentage of within-group similarity (Sim) and the number of species (Spp.) contributing up to 90% to this similarity. The percentage of between-group dissimilarity (Diss) comparing geographic differences (by seamount) in the identified beam trawl sample assemblages as well the number of species (Spp.) contributing up to 90% to this dissimilarity, is also shown.

Codes	Sim	Spp.	Areas	Diss	Spp.
BT-a	24.0	64	AM vs. EB	79.3	230
BT-b	21.9	59	SO vs. AM	79.7	144
			SO vs. EB	79.3	171
			AM vs. EB	78.7	170
BT-c	33.3	16	SO vs. AM	67.7	64
			SO vs. EB	67.4	68
			AM vs. EB	70.5	53
RD-a	23.4	13			
RD-b	23.6	7			
RD-c	15.4	8			
GOC-a	57.1	13	AM vs. EB	46.2	38
GOC-b	52.1	24			
GOC-c	53.4	14			

The geographic differences (by seamount) were also analyzed. SIMPER results (Table 3; Appendix H) showed an average dissimilarity of 79.3% between AM and EB summit samples, being coralline red algae and sponges (e.g., *Hexadella sp.*), both more abundant in AM, as the species with a higher contribution to this dissimilarity. The average dissimilarity values by comparing SO summit and flanks of the three seamount samples were 79% in all cases, being *G. vitreus* and *Desmacella inornata*, with larger biomass in AM and EB, respectively, the main species that contribute to this dissimilarity. The comparison of samples obtained in the base and adjacent bottoms of the seamounts showed lower values of dissimilarity: 67.7% (SO-AM), 67.4% (SO-EB), and 70.5% (AM-EB). The presence of *Isidella elongata* at SO and the higher abundance of the fishes *Nezumia aequalis* and *Lepidorhombus boscii* at AM and *G. vitreus* and *G. longipes* at EB contributed mostly to this dissimilarity.

The cluster and MDS analysis of the presence/absence matrix from the rock dredge also identified three benthic assemblages on rocky bottoms (Figure 6B): (RD-a) the shallowest samples between 90 and 193 m depths at EM and AM summits; (RD-b) samples from 242 to 609 m depths at SO, AM, and EB flanks; and (RD-c) a more heterogeneous group, between 240 and 1081 m depths, at the flanks of the three seamounts and volcanic cones surrounding EB. The ANOSIM results (R = 0.64; p = 0.001) confirmed significant differences between these assemblages. SIMPER results (Table 3; Appendix H) showed that main species contributing to within-group similarity of the RD-a assemblage were coralline red algae and the brachiopods *Megerlia truncata* and *Argyrotheca cordata*, summing up to 70% of similarity. The decapod crustaceans of the genus *Plesionika* (three species summing up to 45.7%) and the bivalve mollusk *Asperarca nodulosa* (31%) were the main species in the RD-b assemblage. The sponges *Haliclona poecillastroides*, *Hamacantha* (*Hamacantha*) sp. 1, Ancorinidae sp. 1, *Poecillastra compressa*, and other not identified sponges, summed up to 77.5% of similarity of the RD-c assemblage.

The cluster and MDS analysis of standardized abundance from the experimental bottom trawl GOC samples on the deep water trawl fishing grounds adjacent to the seamounts identified an assemblage between 542 and 768 m in depth at AM and EB (GOC-a), which is clearly separated from four samples at 444 and 510 m depth in AM (GOC-b), the two samples at 328 and 393 m depth in AM (GOC-c), and the shallowest and deepest samples at a 237 m depth in AM (GOC-d) and at a 1028 m depth in EB (GOC-e), respectively (Figure 6C). The ANOSIM results (R = 0.71; $p < 0.01$) confirmed significant differences between these assemblages. The mean values for the ecological parameters analyzed also showed differences between these assemblages (Table 2). While standardized abundance and the species richness (S) clearly decreased with depth, the standardized biomass and the other diversity indices H' and J' did not show this trend. In the GOC-a assemblage, the ANOSIM results showed low geographic differences between AM and EB (R = 0.24, $p < 0.002$). The dissimilarity between AM and EB in this group was 42.16% and the main species that contributed to this dissimilarity were the elasmobranch *Galeus melastomus* (7.9%) and the decapod crustaceans *Aristeus antennatus* (6.8%), *Geryon longipes* (5.9%), and *Phasiphaea multidentata* (5.3%).

The SIMPER results (Table 3; Appendix H) showed that the main species contributing to within-group similarity in the GOC-b assemblage were decapod crustaceans, teleost fishes, and one cephalopod mollusk, some of them of commercial interest: *Plesionika martia*, *Nephrops norvegicus*, *Parapenaeus longirostris*, *Phycis blennoides*, *Helicolenus dactylopterus*, *Lepidorhombus boscii*, and *Merluccius merluccius*. The main species that contributed to within-group similarity in the GOC-a assemblage were also decapod crustaceans, teleost fishes, and the elasmobranch *G. melastomus*. Some of these species (*P. martia*, *Hymenocephalus italicus*, *P. blennoides*, and *Hoplostethus mediterraneus*) were the same as the previous assemblage, but contributed with different percentages. Species of commercial interest also contributed to the similarity of the GOC-a assemblage: the target *A. antennatus* and its by-catch *P. martia*, *G. longipes*, *G. melastomus*, and *P. blennoides*.

The data obtained from the experimental bottom trawl GOC-37 samples from 542 to 768 m in depth at AM and EB allowed us to compare the density and population structure of red shrimp (*A. antennatus*) between the two fishing grounds adjacent to these seamounts (Figure 7). No significant differences were detected in the standardized abundance and biomass. However, length frequency distributions showed larger males in EB and smaller females in EB.

4.4. Bottom Trawling

In recent years, three different trawl fleets operate in the identified three fishing grounds around Ibiza and Formentera Islands, possibly impacting the SO and AM seamounts (Figure 8A): (i) up to nine local vessels from the ports of Sant Antoni de Portmany, Eivissa, and La Savina that focus their activity mainly on the continental shelf; (ii) up to 29 vessels from the ports of Denia, Calp, Altea, La Vila Joiosa, and Santa Pola on the Iberian Peninsula, that can carry out trips of 3–5 days to fish below 150 m depth; and (iii) only three vessels from the port of Andratx on Mallorca, that carry out daily trips to fish sporadically on the northern slope off Ibiza Island. In contrast, no trawling activity has been detected in adjacent bottoms of EB.

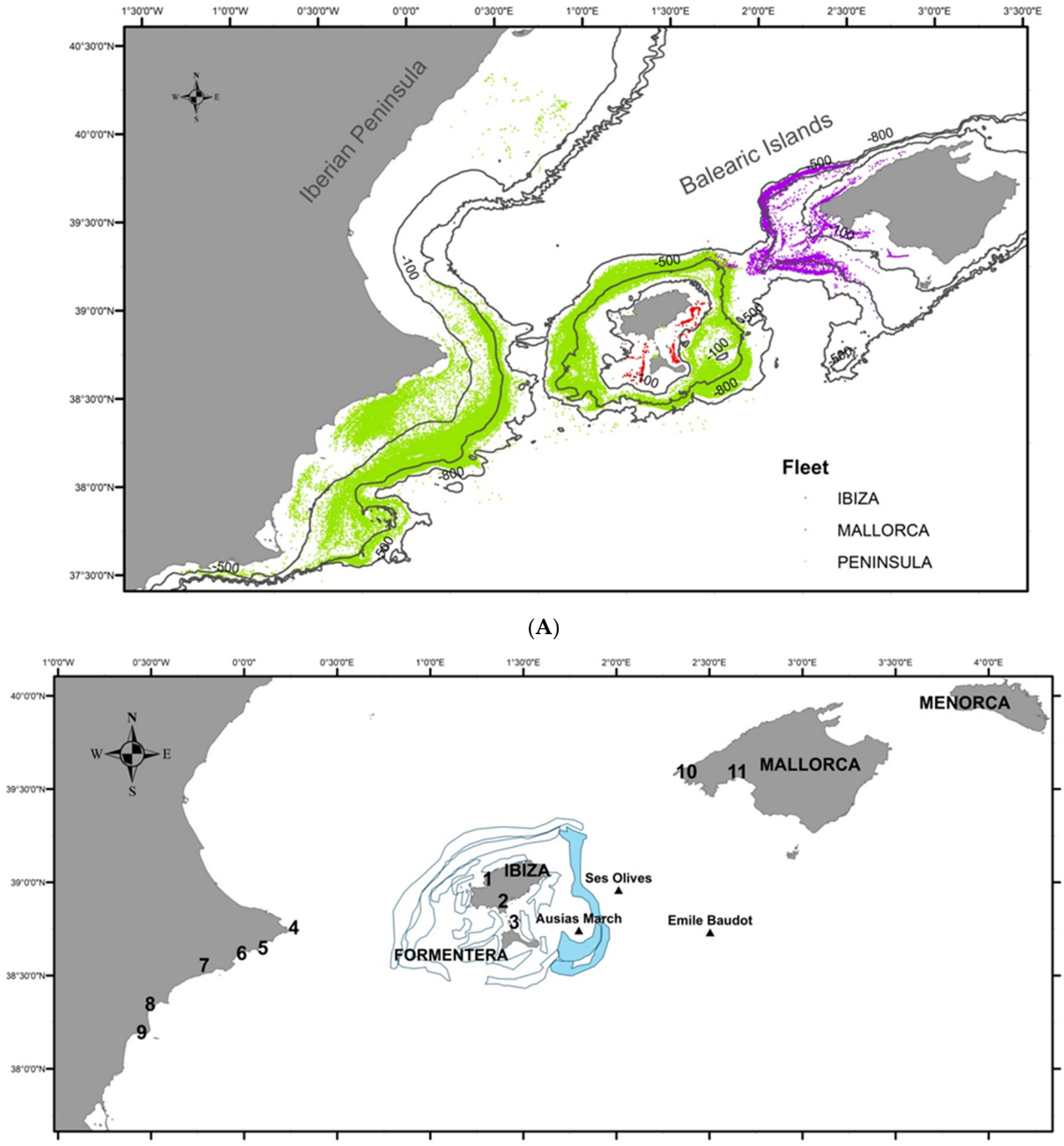

Figure 8. Bottom trawl fishing activity in the seamounts of the Mallorca Channel: (**A**) VMS signals during the period 2016–2019 of the fleets that operate around Ibiza and the Formentera Islands (red: vessels from ports on these islands; green: vessels from ports on the Iberian Peninsula; violet: vessels from ports on Mallorca Island), showing the three seamounts studied and the whole fishing areas of these fleets along the northwestern Mediterranean; and (**B**) fishing grounds located in adjacent bottoms of the Ses Olives and Ausias March seamounts, identified from the cartography of all fishing grounds around the Balearic Islands from VMS signals [60], showing the base port fleets operating in the study area: (1) Sant Antoni de Portmany; (2) Eivissa; (3) La Savina; (4) Xàvia; (5) Calp; (6) Altea; (7) La Vila Joiosa; (8) Alicante; (9) Santa Pola; (10) Andratx; and (11) Palma.

Three different fishing grounds were identified in the vicinity of SO and AM (Figure 8B): (i) one situated east and northeast of Ibiza Island, with its southern part including upper

and middle slope bottoms adjacent to SO and AM; and (ii) two situated east of Formentera, one including upper slope bottoms and the other including middle slope bottoms, in both cases adjacent to AM. These fishing grounds correspond to slope bottoms, where the insular trawling fleets of Ibiza and Formentera do not operate. They are mainly exploited by the trawling fleet from the Iberian Peninsula targeting deep water decapod crustaceans of high economic value such as rose shrimp (*P. longirostris*) and Norway lobster (*N. norvegicus*) on the upper slope and the red shrimp on the middle slope.

On average, these three fishing grounds represent 16% of the fishing days conducted by the trawl fleet around Ibiza and Formentera. They concentrated 28% of the fishing days conducted by the Iberian Peninsula fleet around these two islands and 13% of its fishing days with respect to the whole fishing area of this fleet including both insular and peninsular fishing grounds. The fleet from Mallorca only operates in the northernmost part of the fishing ground in eastern and northeastern Ibiza, which on average concentrates up to 45% of the fishing days developed by this fleet when operating near Ibiza and less than 6% of its fishing days with respect to its whole fishing area, mainly western and southern Mallorca.

Up to 16 species or commercial categories were identified as the most important catches of the trawling fleet operating on slope bottoms around Ibiza and the Formentera Islands (Table 4): rose shrimp, Norway lobster, red shrimp, the deep water crab *G. longipes* and other category of decapod crustaceans composed by species of the genus *Plesionika*, a category of cephalopod mollusk composed by the Ommastrephidae species *Illex coindetii*, *Todaropsis eblanae* and *Todarodes sagittatus*, the teleost fishes hake (*M. merluccius*), spotted flounder (*Citharus linguatula*), blackbelly rosefish (*H. dactylopterus*), blue whiting (*Micromesistius poutassou*), greater forkbeard (*Phycis blennoides*), monkfishes (*Lophius budegassa* and *L. piscatorius*), megrims (*L. boscii* and *L. whiffiagonis*), a category composed by species of the family Argentinidae (*Glossanodon leioglossus* and *Argentina sphyraena*), the elasmobranch blackmouth catshark (*G. melastomus*), and a category composed of species of the family Rajidae. These species or commercial categories represent >90% of total landings in terms of biomass and >92% in terms of economic value.

Table 4. Estimated annual landings, in terms of biomass (kg) and economic value (€ from first sale), for the main species or commercial categories extracted from the three bottom trawl fishing grounds in adjacent bottoms of the Ses Olives and Ausias March seamounts in the Mallorca Channel (Balearic Islands, western Mediterranean), and average values (± standard error) during the period 2016–2019. The location of these fishing grounds is shown in Figure 9B.

Species or Category	2016		2017		2018		2019		Average Whole Period			
	kg	€	kg	€	kg	€	kg	€	μ (kg)	SD (kg)	μ (€)	SD (€)
Argentinidae	318	849	4005	9223	6136	16,381	4726	14224	3796	2482	10,169	6899
Aristeus antennatus	3481	94,361	3633	93,128	6064	188,003	15,126	427,550	7076	5496	200,760	157,588
Citharus linguatula	2	4	1881	5527	10,837	40,892	8611	40,829	5333	5208	21,813	22,109
Galeus melastomus	98	368	96	492	875	2988	1493	5171	640	677	2255	2288
Geryon longipes	5657	27,320	8589	39,188	7026	32,608	9713	27,199	7746	1776	31,578	5665
Helicolenus dactylopterus	499	1717	2876	5131	9340	22,458	10,490	24,994	5801	4871	13,575	11,849
Lepidorhombus spp.	1582	8009	1675	8358	1616	7345	2489	14,066	1840	434	9445	3110
Lophius spp.	2453	23,449	4065	28,998	10,268	70,846	12,847	90,179	7408	4949	53,368	32,402
Merluccius merluccius	1672	11,949	3055	20,633	8992	46,242	13,416	90,701	6784	5444	42,381	35,350
Micromesistius poutassou	805	2264	2468	8704	2369	8810	13,400	45,650	4761	5810	16,357	19,767
Nephrops norvegicus	2977	72,615	5840	148,117	16,302	445,533	20,547	496,826	11,417	8358	290,773	211,623
Ommastrephidae	323	525	3242	8913	8929	23,541	5585	20,363	4520	3643	13,335	10602
Pandalidae	2302	17,213	2957	20352	4518	30,692	5784	43,262	3890	1568	27,880	11,761
Parapenaeus longirostris	136	1419	4541	50727	20,935	249,009	19,137	258,024	11,187	10401	139,795	132,899
Phycis blennoides	2005	4984	5191	15486	11,318	30,043	13,132	34,524	7912	5200	21,259	13556
Rajidae	285	958	1924	2676	2996	8085	4813	11,485	2505	1900	5801	4856
TOTAL	24,593	268,004	56,037	465652	128,523	1,223,475	161,309	1,645,048	92,616	63175	900,545	644,931

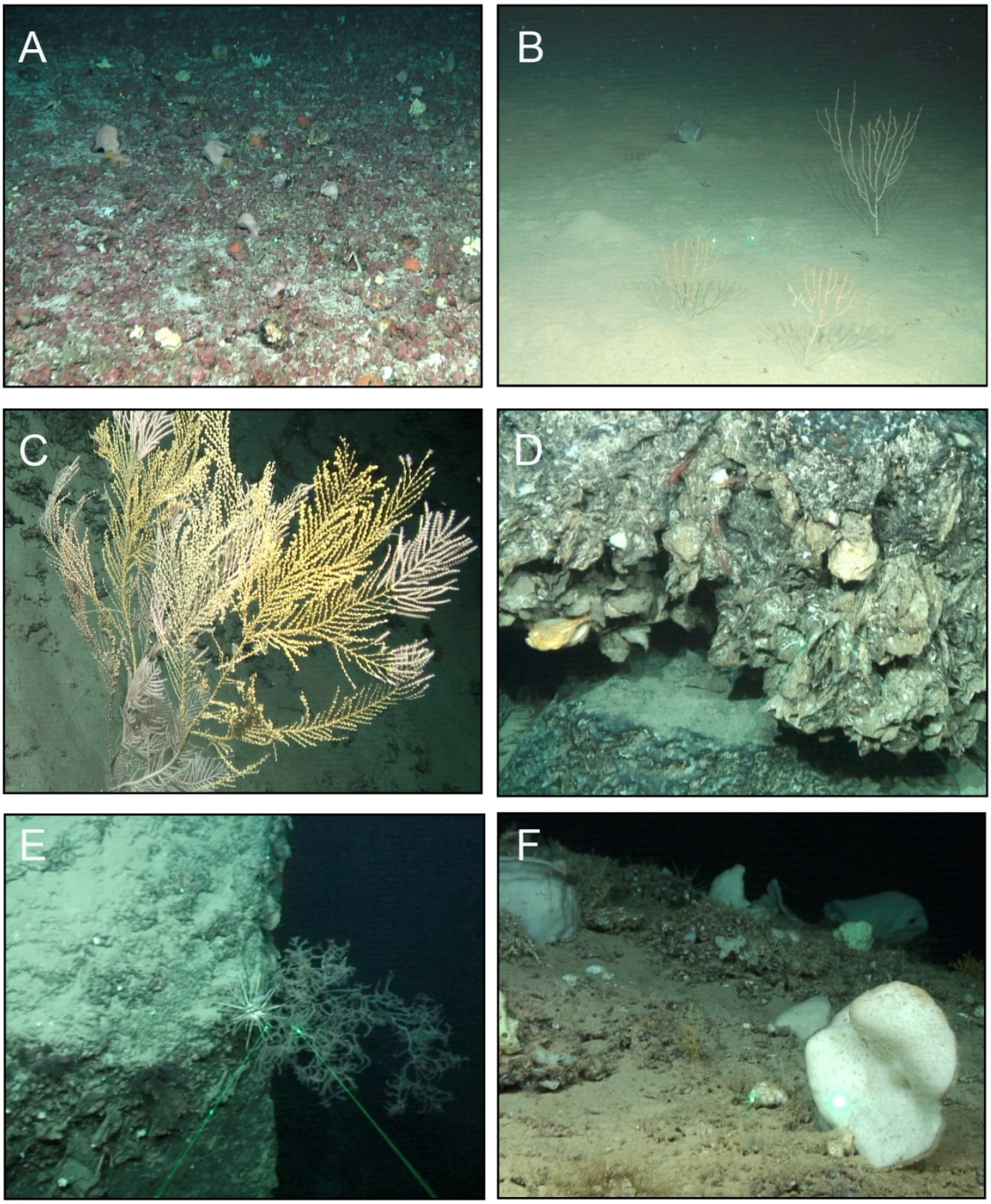

Figure 9. Habitats and biological communities identified in the Ses Olives (SO), Ausias March (AM), and Emile Baudot (EB) seamounts of the Mallorca Channel (Balearic Islands, western Mediterranean): (**A**) Rhodolith beds in EB at 113 m depth); (**B**) bathyal muds with Alcyonacea (*Isidella elongata*) in SO at a 590 m depth; (**C**) bathyal rock with Alcyonacea (*Callogorgia verticillata*) in EB at a 830 m depth; (**D**) upper bathyal biogenic Thanatocoenosis of giant ostreids in EB at a 417 m depth; (E) bathyal rock with Anthipataria (*Leiopathes glaberrima*) in EB at a 491 m depth; and (**F**) bathyal rocky bottoms with coarse sediments dominated by sponges in AM at a 365 m depth.

On average, the annual catches of these species or commercial categories obtained by the trawling fleet from the three fishing grounds adjacent to the SO and AM seamounts represent 24% of their landings from all trawl fishing grounds around Ibiza and Formentera and 25% in terms of their economic value (Table 4). These landings represent 35% of the annual biomass of these species extracted by the fleet from the Iberian Peninsula on the

fishing grounds around Ibiza and Formentera, and 7% from their landings obtained both on insular and peninsular fishing grounds. In terms of economic value, these figures were 32 and 7%, respectively (Table 4). Regarding the vessels from Mallorca Island, their landing obtained in the northernmost part of the fishing ground in eastern and northeastern Ibiza represent up to 83% of the annual biomass extracted by these vessels from the fishing grounds in this area and 84% of its economic value, but they only represented 2 and 1.5% of their total landings in terms of biomass and economic value, respectively (Table 4).

4.5. Habitats

Up to 29 different categories of benthic habitats were identified from ROTV and ROV video transects (Table 5; Figure 9). Two of them are considered protected habitats: rhodoliths beds and coralligenous bottoms. Five of them were designated as sensitive habitats: (i) bathyal muds with *Isidella elongata*; (ii) facies with crinoids, (iii) facies with red algae of the genus *Peyssonnelia*; (iv) rhodoliths beds; and (v) communities of bathyal detritic sands with *Gryphus vitreus*.

The analysis of video transects obtained with ROTV (Figure 10) showed that dominant habitats in SO were soft bottoms. Bathyal mud with burrowing mega-fauna dominated around the seamount and detritic bottoms on the summit, both habitats summing up 87.5% coverage. On the flanks, hard bottoms with bathyal rock, dominated by sponges were found, with 11.5% coverage. In the summit of AM there were rhodolith beds (16%), alternating with detritic bottoms (30%), while in the base, soft bottom with pockmarks (13%) and bathyal detritic bottoms (30%) predominated. On flanks, escarpments, rocky walls, and slopes with anthozoans and/or small sponges such as *Thenea muricata* were also found. Rhodolith beds with invertebrates, especially anthozoans (alcyonarians and gorgonians) and sponges, predominated on the EB summit (67% coverage), while muddy bottoms were found at the base and adjacent areas.

The analysis of the ROV (Figure 10) found that the SO seafloor consisted mostly of bathyal muds (69% of covered area), in some areas with burrowing megafauna, and to a lesser extent, detritic bathyal bottoms and rocky slopes covered by sponges (10 and 7% coverage, respectively). Pockmarks, soft bottoms with *G. vitreus* or *T. muricata*, and rocky areas dominated by the crinoid *Leptometra celtica* were also found. The circa-littoral seafloor of AM was defined by rhodolith beds (33%) and detritic sand (7%), dominated by alcyonids and sponges, while its bathyal areas were widely covered by sand or muddy sediments (41%), some of them dominated by the brachiopod *G. vitreus* (3%). The rocky slopes and escarps of AM were covered mainly by sponges (10%), but also by the cnidarians *Paramuricea hirsuta* (1.6%) and *Bebryce mollys* (1%). EB, with the widest depth range of visual deployments, showed a circa-littoral domain with detritic soft bottoms (38%), some dominated by the soft red algae *Phyllophora crispa*, the alcyonids *Alcyonium palmatum* and *Paralcyonium spinulosum*, and rhodolith beds. The bathyal transects showed mainly muddy or soft detritic sediments (22% and 38%, respectively), with dead coral mounds and pockmarks. The hard substrates were dominated by sponges, the crinoid *L. celtica*, and black corals.

The geographic distribution of the habitats (Figure 10) showed that the lowest number of habitats was observed in SO (11) and the highest in EB (21). AM presented an intermediate number of habitats (16), despite being the seamount with less video transect sampling. In general, thanatocoenosis of giant ostreids seemed to be distributed around the three seamounts and dead coral framework, and mounds were also found in some bathyal areas of their flanks.

Table 5. Categories of benthic habitats identified from ROTV and ROV video transects in th Ses Olives, Ausias March, and Emile Baudot seamounts of the Mallorca Channel (Balearic Islands, western Mediterranean) during the INTEMARES project. Their name, code, and hierarchical organization level (HOL; ranging from 1 for the more generalist and least detailed one to 5 for the level with the highest detail and knowledge) were assigned according to the Habitats Directive, with some exceptions (*) identified during the previous INDEMARES project (https://www.indemares.es/en (accessed on 20 December 2021)).

Habitat Name	Code	HOL	Habitat Assignment
Sandbanks which are slightly covered by sea water all the time	1110		Rhodoliths beds *
			Infralittoral and circalittoral detritic beds with rhodoliths dominated by invertebrates *
			Circalittoral detritic beds with *Alcyonium palmatum* and *Paralcyonium spinulosum* *
		5	Infralittoral and circalittoral detritic beds with rhodoliths dominated by invertebrates with sponges dominance *
		2	Circalittoral detritic bottoms
			Circalittoral and infralittoral detritic biogenic habitats *
			Circalittoral and infralittoral detritic biogenic habitats with *Phyllophora crispa* *
		3	Bathyal detritic bottoms
			Bathyal shelf-edge sedimentary bottoms with Brachiopoda *(Gryphus vitreus)* *
			Bathyal mud and sandy mud bottoms dominated by burrowing megafauna *
Reefs	1170		Bathyal rock with Scleractinia *
		5	Bathyal rock with Alctyonacea (*Paramuricea hirsuta)*
		4	Dead coral framework
		5	Dead coral mounds
		4	Bathyal rock with Anthipataria (*Leiopathes glaberrima)*
		4	Bathyal rock with Alcyonacea (*Callogorgia verticillata)*
		4	Bathyal rock with coarse sediments with *Bebryce mollis*
		4	Bathyal rock with coarse sediments with *Leptometra celtica*
		3	Coralligenous rock dominated by invertebrates
		3	Circalittoral rock invertebrate-dominated
		3	Bathyal rocky bottoms with sponges aggregations
		4	Bathyal rock with coarse sediments dominated by sponges
		5	Upper bathyal biogenic Thanatocoenosis of giant ostreids
		2	Bathyal muds
			Bathyal muds with small sponges (*Thenea muricata)* *
		4	Bathyal compact muds with Alcyonacea (*Isidella elongata)*
			Escarpments, rocky walls and slopes of seamounts with anthozoans (scleractinians, gorgonians, and antipatharians)
Submarine structures made by leaking gases	1180	3	Pockmarks

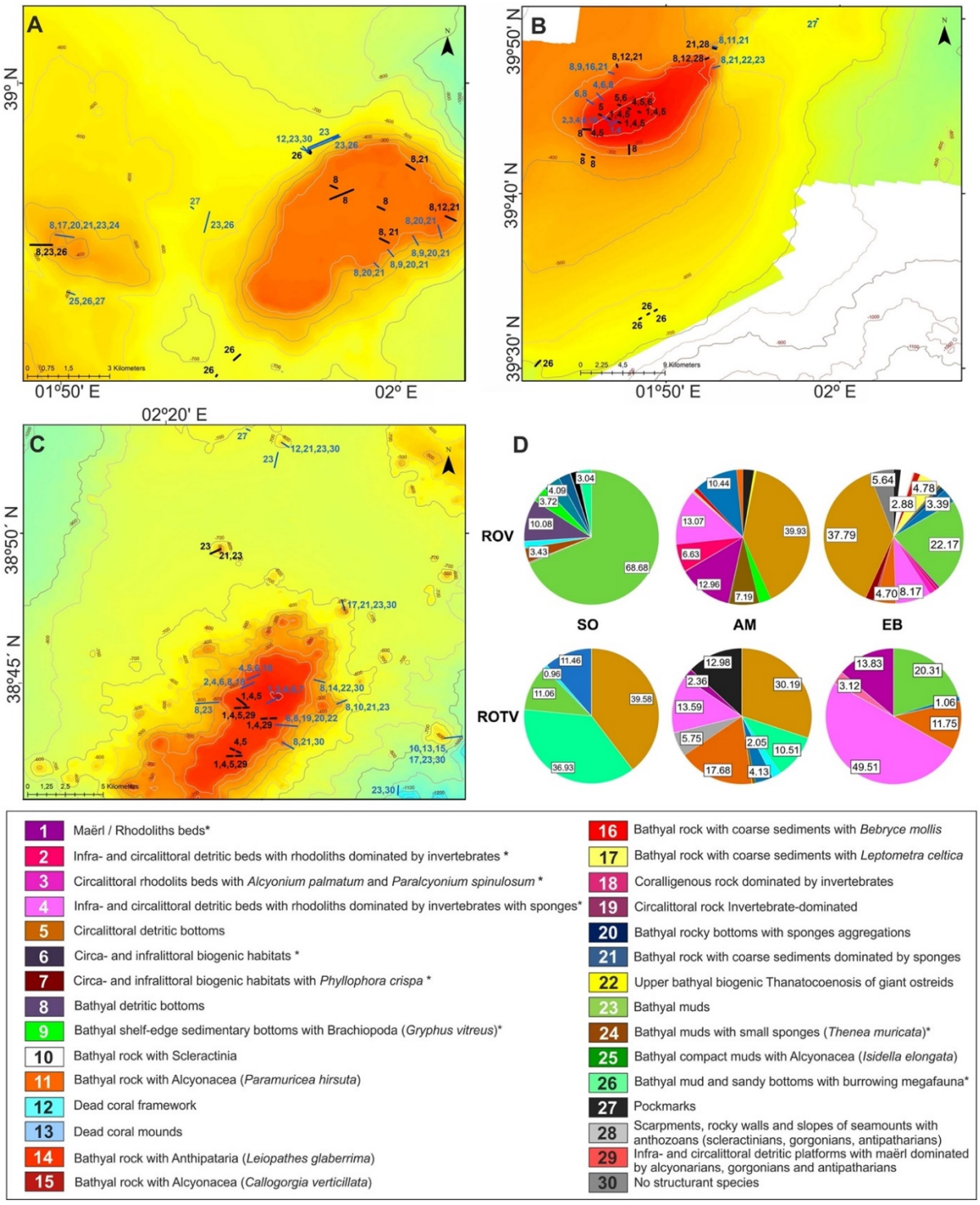

Figure 10. Video transects with ROTV and ROV developed in the (**A**) Ses Olives; (**B**) Ausias March, and (**C**) Emile Baudot seamounts, showing the code (1–29) of the categories of benthic habitats identified. Pie charts with the coverage percentage of the main habitats by seamount are also shown (**D**). (*) Full name, code, and level of habitats are detailed in Table 5.

5. Discussion

The present paper includes a preview of the results obtained during the INTEMARES project regarding the mapping and characterization of seafloor, benthic species, and habitats as well as fishing activity on the SO, AM, and EB seamounts and adjacent bottoms. This multidisciplinary approach has greatly improved the scientific knowledge on the

geological, biological, and habitat diversity of these seamounts in the Mallorca Channel, which constitutes the first step for their inclusion in the Natura 2000 network. It provides new baseline information on the diversity patterns in the area and useful details of the seascape distribution, which can be used for future ecological assessments.

5.1. Geodiversity

The new geomorphological mapping has enhanced between six and 20 times the bathymetric detail of the seabed. From this improvement, we differentiated, among the seamounts, 15 different morphological types: minor highs, ridges, tectonic depressions, fault scarps, pockmarks, volcanic cones, gullies, slide scars and mass-transport deposits, contourite moats, furrows and drifts, sediment waves, and numerous biogenic mounds. This great geomorphological variety of features shows the importance of the interplay of several geological (structural and fluid flow processes), oceanographic (bottom current related processes), and biogenic (bioaccumulation of reef-building organisms) processes in shaping the seafloor and influencing substrate types and benthic habitats of the Mallorca Channel.

The presence of biogenic mounds and mass-movement related features is widespread at the summits and flanks of all the seamounts and adjacent bottoms, with AM the most affected seamount by both processes. Biogenic mounds and patch settlements strongly depend on the availability of hard substrates [61] such as the rocky outcrops identified at these summits, occurring in at least half of the summit surface of AM and EB, but being less represented at the summit and upper flanks of SO. They were previously reported by OCEANA (2011, 2015) [13,14], although their distribution was more than double that described, probably due to the widest depth range analyzed in the present study. All seamounts have flat-topped summits and some develop terraced levels, suggesting that they were once islands that later on became submerged edifices associated with different mechanisms such as wave erosion at the sea surface, water mass interaction, or affected by subsidence [62,63]. These processes, together with other environmental conditions such as the hydrodynamic regime and the sufficient productivity, have modulated the morphology of these structures.

The seafloor surface affected by sedimentary instabilities is 12% of the study area (~600 km^2), a value double that of that previously estimated for the Balearic Promontory by Acosta (2005) [64]. At the same time, they are related to zones of fragility associated with structural and fluid flow processes such as active faulting, folding, and pockmark development, as has been suggested by Iglesias et al. (2010) and Palomino et al. (2011) [4,65] in the Cantabrian and Alboran seas, respectively.

Pockmarks have been categorized as habitat type 1180 "Submarine structures made by leaking gases" in the Habitats Directive 92/43/EEC, which has a restricted distribution in European waters, with the Mediterranean one of these areas where this habitat is located. However, it remains unrepresented within the Mediterranean Natura 2000 network [18]. Previous studies have identified some pockmarks in the Mallorca and Ibiza Channel and Iberian Peninsula area [66], with our results in line with these findings. However, we highlighted the presence of almost 4000 pockmarks that largely developed surrounding the three seamounts with deep bottoms up to 1000 m in depth. These pockmarks occur in areas with great sedimentary thickness, where the higher sedimentation rates favor the burial of organic matter and make it more prone to anaerobic digestion. In this sense, the location of the large pockmark fields displays the highest organic matter values in superficial sediments of the study area.

The formation of pockmarks has been univocally proposed in the literature as caused by the existence of fluid escape processes, water or gas, preferably gas such as methane from the subsoil [67] whose expulsion would favor the erosion of sediments. These seafloor depressions can also be affected by bottom currents, which may favor their erosion and genesis. In the Mallorca Channel, these fluid flow features can be found in different evolutionary phases, although in some cases, the occurrence of underneath acoustic chimneys

in the subsoil has been located in the high resolution parametric profiles. The origin of these acoustic masking features has been proposed in the literature as amplitude anomalies related to free gas that is migrating upward through the sediments toward the seabed (e.g., [68]).

Another feature to remark on is the volcanic cone field (up to 170 edifices) restricted to the flanks and adjacent bottoms of EB, a seamount that unlike SO and AM is of volcanic origin [11]. The presence of numerous volcanic cones suggests a multiple focused extrusion paths towards the seafloor. High-resolution sub-bottom profiles show low penetration on them, indicating the absence of a recent unconsolidated sedimentary cover, that point out to the availability of hard substrates at these structures for reef-forming organisms, as reported for the seamounts. Furthermore, volcanic cones and pockmarks are spatially interspersed along the periphery of EB, fact that could influence the fluid flow process development onto the seafloor.

5.2. Biodiversity, Communities, and Habitats

The flora and fauna inventoried, with up to 547 species or taxa, have also contributed to improve the knowledge of the biodiversity of the study area. In contrast to previous studies, developed exclusively from visual censuses and samples of benthic organisms using ROV [13,14,17], the combination of sampling methods used in the present study (epi-benthic sledge, bottom trawl, rock dredge, and ROV) has allowed us to cover not only a wide range of species including small-sized benthic organisms, species difficult to identify only from images and highly mobile nekton-benthic fishes, but also to achieve a more precise identification of them by obtaining more samples to be analyzed in the laboratory.

Some of the identified species up to date have been new to science and new records in the study area or even in the Mediterranean. This is the case of the discovery of the new genus of sponge Foraminospongia, whose type species F. balearica is one of the most abundant sponges at the AM and EB summits and the other two new sponge species F. minuta and Paratimea masuttii [69]. Moreover, new geographical records have been published for another 16 sponges [69] and one ophiuroid [70], with this last species also abundant in the study area. Some species have been found at depths where they had not been previously recorded, which was the case of two little known decapod crustaceans: the alpheids Alpheus platydactylus and Alpheus cf. dentipes. Up until now, the first species had been reported at depths of 120–791 m [71–73], but we collected a male and an ovigerous female at 88 m depth in the coralligenous bottoms of EB. The second was collected at a 305 m depth in SO, but this species had always been reported at shallow infra-littoral bottoms inside sponges, rock cavities, and among calcareous algae [71,74–77]. Although the species was identified as A. cf. dentipes according to Noël (1992) [78], these differences in bathymetry cause doubt about its specific assignment, pending future studies. The report of the sepiolid Stoloteuthis leucoptera in the fishing grounds adjacent to AM must also be pointed out. This species is a deep-sea cephalopod, whose presence in the Mediterranean is very rarely known [79].

These invertebrate groups are good examples of the limitations regarding the identification of species only from images. Since Pitcher et al. (2007) [80], the assessment of benthic species richness on seamounts can be strongly influenced by the sampling methodology applied, with extractive sampling yielding broader estimation of biodiversity. Moreover, with these sampling methods, it is possible to obtain individuals and perform the detailed morphological and genetic analyses needed for the description and identification of new species or records [81]. This is clear from the number of species inventoried exclusively using one or another sampling method. From the 537 species or taxa detected in the Mallorca Channel seamounts, only 110 have been detected using both images and one of the three sampling gears. The majority of these species have been exclusively detected using gears, up to 484, whereas only 54 of them were exclusively detected from the images. The most effective sampling gear was the beam trawl, with up to 184 species detected exclusively

using this gear, whereas 51 and 41 species were exclusively detected using bottom trawl and rock dredge, respectively.

However, ROV images are very useful for sampling rocky bottoms and to improve the information collected with epi-benthic sledge and bottom trawling on sedimentary bottoms. In rocky bottoms, images and samples from ROV can allow for the estimation of the standardized density of benthic flora and fauna and to detect highly mobile nekton-benthic species. This was the case of Trachyscorpia cristulata echinata and Pontinus kuhlii, observed in EB from our study and OCEANA (2011) [13], respectively. Both scorpionfishes are poorly known in the Mediterranean, probably because their preferential habitat is not accessible to the more conventional and widespread sampling in the area for nekto-benthic species, developed from bottom trawl gears. In fact, these findings represent the second report of both species in the Balearic Islands [82,83]. In the case of sedimentary bottoms, ROV or photogrammetric sledge images can provide information on the spatial distribution of benthic species (e.g., patchiness) and the tridimensional structure of habitats, thus providing a more realistic picture. All these results emphasize the importance of combining complementary sampling methods to assess the diversity of seamounts.

In most seamount studies, depth has been shown to be the most important environmental factor in determining the structure of benthic assemblages, which generates their distribution as bands encircling the seamounts [84,85]. Our results are not an exception, and the assemblages of benthic and nekton-benthic species identified both in sedimentary and rocky bottoms of the Mallorca Channel follow a clear bathymetric distribution, with different communities in the summit, flanks and base that is also related to the substrate type. Albeit to a lesser degree, we have also detected differences in epi-benthic species composition between the seamounts, both at summits, characterized by coarser sediment, high content in inorganic carbon, and low content in organic matter as well as in flanks and bases, mainly dominated by finer sediments, low content in organic carbon, and high content in organic matter. These differences were lower for the nekton-benthic assemblages in the trawl fishing grounds adjacent to AM and EB. This result should be highlighted considering the different level of exploitation of the fishing grounds compared. While AM has been exploited by the bottom trawl fleet targeted to red shrimp (A. antennatus) for more than 50 years [86], this fishery has not been developed in EB during the last two decades because of its large distance from any port, and more recently, the high fuel cost [44]. Despite this, the only difference that could be attributable to the impact of fishing is the slightly greater abundance of the elasmobranch G. melastomus observed in EB compared to AM (on average, 21.0 vs. 17.2 individuals/km^2, respectively), although the other elasmobranch Etmopterus spinax showed a contrary situation (on average, 6.2 vs. 1.2 individuals/km^2, respectively). In contrast, red shrimp did not show differences in its abundance, only in its length frequency.

The gradient of habitats found also followed the depth range. In the circalittoral summits of AM and EB, there are detritic bottoms with rhodolith beds and coralligenous outcrops, dominated by communities of sponges and alcyonarians and gorgonian anthozoans. As a consequence of the extreme transparency of the water in these areas, these rhodolith beds have been found quite well structured down to a 137 m depth, most likely the deepest depth of this habitat in the western Mediterranean. As above-mentioned, most of SO summit is flat and is covered by detritic bottoms, which is in contrast to the seafloor around this seamount, containing mud and sandy mud beds dominated by burrowing fauna, as occur in the Gulf of Cadiz [87]. Sponges and corals colonize the rocky bottoms of the flanks, in the upper slope of the three seamounts. These filtering species seem to be more frequent and abundant in the flanks facing the main current directions, probably as a consequence of a current-mediated increase in food availability, an aspect that should be further investigated in studies of habitat and species modeling. Other habitats in this bathymetric range were some crinoid beds and thanatocoenosis of giant ostreids, which seems to surround each seamount between 260 and 415 m in depth. In the less steep flaks and bathyal terraces of the upper and middle slope were muddy soft sediments

accumulating facies of the brachiopod G. vitreus, burrowing megafauna and/or dead coral debris. The deepest areas of the middle slope at the base of seamounts are dominated by the finest muddy sediments and the presence of pockmarks. In these bottoms, facies with the corals Callogorgia verticillata and Isidella elongata, the sponge Thenea muricata, and the bryozoan Kinetoskias sp. have also been found.

5.3. Fisheries

Currently, deep water bottom trawl fishing activity is developed on adjacent bottoms of SO and AM. The comparison of the epi-benthic and nekton-benthic assemblages and one of the main fishing resources (red shrimp) between these fishing grounds and a fishing ground adjacent to EB that has not been exploited by the trawling fleet for 20 years did not show clear differences. However, these results must be considered as very preliminary and further studies to assess the impact of fishing activities on species and habitats will be necessary.

These studies should also consider the direct impact of trawling gears on the seafloor, because bottom trawling has also been reported as an important driver of sediment resuspension, caused by the passage of the fishing gear through bottoms, becoming an important seafloor micro-morphology disturbing process in muddy and moderate-energy continental shelves [88] and a driver of deep seascape evolution [89,90]. Sediment resuspended, as a result of trawl fishing, also has a wide variety of additional effects including the smothering of feeding and respiratory organs [91], which can affect the settlement and feeding of the biota. Hence, the potential effect of these sediments reaching and settling in the seamounts should be assessed, considering the high diversity and density of filtering benthic species inhabiting both the sedimentary and rocky bottoms of the SO and AM seamounts and adjacent areas.

The potential impact of other demersal fishing gears should also be considered in these studies. This was the case for two commercial fleets operating with traps and bottom long-lines on the summits and flanks of the three seamounts and the recreational fleet operating with hand-lines. The activity and catches of this last fishery is largely unknown. Although traps and long-lines are more selective than bottom trawl and their impact is much less, it can still be significant not only on their target species, but also on benthic habitats [92]. Moreover, it must be taken into account that these fishing gears operate in areas not accessible to trawling.

5.4. Ecological Value of Mallorca Channel Seamounts

Most of these habitats are included in the Habitats Directive (HD) as being of community interest (habitat codes 1110, 1170, and 1180) and are of high ecological value, not only because of the high species diversity they house, some of which are threatened or declining, but also because some of them are considered as sensitive or vulnerable habitats and, for that reason, they have been protected by both environmental and fisheries regulations. That is the case of maërl or rhodoliths and coralligenous beds, which the Council Regulation No. 1967/2006, concerning management measures for the sustainable exploitation of fishery resources in the Mediterranean Sea, considers as protected habitats and prohibits fishing with bottom trawls on these bottoms. To implement this, in 2014, the Spanish Ministry for Agriculture, Fisheries, and Food declared the summits of AM and EB as fishing protection zones in which trawling was forbidden. Until then, the AM summit had hosted some trawl fishing grounds, which are currently not exploited. Maërl/rhodolith beds have also been considered as Essential Fish Habitats because they are necessary for the development of critical life stages of exploited fish species, and require special protection to improve stock status and the long-term sustainability of fisheries [93].

Some of the inventoried species are considered of conservation interest, according to Annex IV of the HD (species that need strict protection), Annex II of the Barcelona Convention (endangered or threatened species), and the Spanish List of Wild Species under Special Protection Regime (Law 42/2007 on Natural Heritage and Biodiversity), which include

species, subspecies, and populations deserving of attention and particular protection based on the scientific, ecological, and/or cultural value due to its uniqueness, rarity, or degree of threat as well as species that appear as protected in directives and international conventions ratified by Spain, and the Balearic Catalog of Threatened and Special Protection Species (Decree 75/2005). This is the case of the Corallinaceae red algae Lithothamnium coralloides and Phymatholithon calcareum, the sponges Axinella polypoides and Tethya sp., the gastropod mollusk Ranella olearium, and the corals Callogorgia verticillata, Dendrophyllia cornigera, and Madrepora oculata. Other anthozoans such as the bamboo coral I. elongata, the sea pen Funiculina quadrangularis, and the whip coral Viminella flagellum, not included in the previous regulations but catalogued by the International Union for the Conservation of Nature (IUCN) as Critical Endangered, Vulnerable and Near Threatened, respectively [94] have also been observed. In addition, the elasmobranch Centrophorus uyato, catalogued by IUCN as Endangered [95], has also been recorded. To these benthic and nekton-benthic species must be added especially protected pelagic species that have also been reported in the seamounts of the Mallorca Channel. This is the case of the sea turtle Caretta and the cetaceans Delphinus delphis, Stenella coeruleoalba, Tursiops truncates, and Physeter macrocephalus [13]. Recent studies have also suggested that these seamounts and the area around them are an important enclave for this last species and have reported the presence of two other cetaceans: Grampus griseus and Globicephala melaena (Unpublished data, Fundación TURSIOPS).

The high heterogeneity of habitats found is in concordance with previous studies in the area [13,14] and encompasses similar values in the nearby Menorca Channel [59,96–99] and other Mediterranean seamounts [100,101]. However, the number of habitats identified in the Mallorca Channel seamounts is higher than that of the Seco de los Olivos seamount [101,102], one of the closest and recently studied seamounts in the western Mediterranean. This could be due to the widest depth range analyzed, the special oceanographic characteristics of the SO, AM, and EB seamounts in between the Balearic and Algerian sub-basins [20], and the large heterogeneity of environments, both hydrographic and geo-morphological, as has been found in other seamounts [84,85,103]. Other explanatory factors may include biotic (e.g., availability of food or space for attachment and competition) and abiotic characteristics, taking into account the different origin of SO and AM, made up of carbonate materials like most of geological units of the Balearic Promontory, with respect to EB of volcanic origin, which increase the availability of different substrate types, promoting a wide variety of habitats.

Our results agree with Galil and Zibrowius (1998) [104] who suggested that Mediterranean seamounts can be considered as isolated refuges for relict populations of species that have disappeared from a previously larger distribution range [70] and that also provide an excellent habitat for rich communities of filter-feeding animals such as sponges [69]. This fact, together with the presence of species and habitats of special interest for their protection, justify the inclusion of the seamounts of the Mallorca Channel within the Natura 2000 network. This will complement the marine SCIs of the Balearic Islands because all of them are sited in coastal areas, with the only exception of the Menorca Channel, which also includes circa-littoral and bathyal bottoms [96,105]. This will also expand the SCIs that include seamounts in Mediterranean waters off Spain, until now represented only by the Seco de los Olivos in the Alboran Sea [101,102] and the deep-sea habitats corresponding to 1170 and 1180 types, which are not well-represented in the Mediterranean Natura 2000 network [18].

To do this, benthic species and habitat modeling as well as mapping of fishing and other human activities in the area (e.g., shipping) that can also affect sea turtles and cetaceans should be made. These studies, together with the assessment of their impact in terms of species and habitat degradation and loss of diversity, both geological and biological, will provide the required scientific information to propose the seamounts of the Mallorca Channel as a SCI and to provide advice to develop the management plan required

for its final declaration as a SAC, with the objective to maintain not only their biodiversity and ecosystems, but also the services they provide.

Author Contributions: Conceptualization, E.M.; Funding acquisition, E.M.; Methodology, E.M., O.S.-G., M.T.F., D.P., P.B., B.R., N.M.-C., S.K., C.L.-R., N.L.-G., E.M.-H., U.F.-A., F.F., F.O. and J.-T.V.; Species identification, M.T.F., S.J. and F.O. (algae), J.A.D. (sponges), E.M.-H., M.V. and S.R.-A. (crustaceans and mollusks), F.O. (echinoderms and fishes), M.T.F. and F.O. (ascidians), S.R.-A. (elasmobranchs), M.T.F., B.R., E.M.-H., U.F.-A., M.V., S.R.-A. and F.O. (other taxa); Formal analysis, O.S.-G., M.T.F., B.R., S.K., C.L.-R., N.L.-G., E.M.-H. and U.F.-A.; Data curation, All authors; Writing—original draft, E.M. and O.S.-G.; Writing—review & editing, All authors; Supervision, E.M., A.F. and J.-T.V. All authors have read and agreed to the published version of the manuscript.

Funding: This research was performed in the scope of the LIFE IP INTEMARES project, coordinated by the Biodiversity Foundation of the Ministry for the Ecological Transition and the Demographic Challenge. It receives financial support from the European Union's LIFE program (LIFE15 IPE ES 012). The MEDITS surveys are co-funded by the European Union through the European Maritime and Fisheries Fund (EMFF) within the National Program of collection, management, and use of data in the fisheries sector and support for scientific advice regarding the Common Fisheries Policy. J.A. Díaz and S. Ramírez-Amaro are supported by predoctoral and postdoctoral contracts, co-funded by the Regional Government of the Balearic Islands and the European Social Fund.

Institutional Review Board Statement: Not applicable.

Informed Consent Statement: Not applicable.

Data Availability Statement: Data are stored in the database of the Instituto Español de Oceanografía (IEO) for the INTEMARES project, some of which is available at the IEO marine geospatial information viewers and services: http://www.ieo.es/en/ideo (accessed on 15 December 2021).

Acknowledgments: We thank all participants who took part in the surveys INTEMARES_A22B_0718, INTEMARES_A22B_1019, INTEMARES_A22B_0720, INTEMARES_A22B_0820, MEDITS_ES_GSA5_2020, MEDITS_ES_GSA5_2021, and MEDITS-PITIÜSES-2021, as well as the captains and crew of the R/Vs Ángeles Alvariño, Sarmiento de Gamboa and Miguel Oliver.

Conflicts of Interest: The authors declare no conflict of interest.

Appendix A

Table A1. Characteristics of the sampling stations carried out with Shipek (SK) and Box–Corer (BC) dredges in the Mallorca Channel seamounts Ses Olives (SO), Ausias March (AM), and Emile Baudot (EB) as well as those of the central basin (CB) and the main pockmark fields (PK) during the INTEMARES project.

Code	Dredge	Area	Latitude (N)	Longitude (E)	Depth (m)
A22B_0718_SK025	SK	AM	38°44.32′	001°46.05′	110
A22B_0718_SK026	SK	AM	38°43.95′	001°46.58′	88
A22B_0718_SK027	SK	AM	38°43.87′	001°46.58′	86
A22B_0718_SK028	SK	AM	38°43.47′	001°46.85′	98
A22B_0718_SK029	SK	AM	38°43.37′	001°46.70′	99
A22B_0718_SK031	SK	AM	38°45.42′	001°46.34′	125
A22B_0718_SK033	SK	AM	38°46.96′	001°45.44′	324
A22B_0718_SK034	SK	AM	38°45.16′	001°47.01′	113
A22B_0718_SK035	SK	AM	38°45.67′	001°49.00′	103
A22B_0718_SK036	SK	AM	38°43.11′	001°53.45′	479

Table A1. *Cont.*

Code	Dredge	Area	Latitude (N)	Longitude (E)	Depth (m)
A22B_0718_SK038	SK	AM	38°45.89′	001°47.48′	131
A22B_0718_SK039	SK	AM	38°47.73′	001°47.66′	121
A22B_0718_SK040	SK	AM	38°45.30′	001°48.45′	98
A22B_0718_SK041	SK	AM	38°45.65′	001°49.60′	104
A22B_0718_SK042	SK	AM	38°45.35′	001°49.45′	105
A22B_0718_SK043	SK	AM	38°44.97′	001°49.51′	103
A22B_0718_SK045	SK	AM	38°44.86′	001°51.03′	132
A22B_0718_SK046	SK	AM	38°45.16′	001°50.89′	124
A22B_0718_SK047	SK	AM	38°45.63′	001°51.02′	121
A22B_0718_SK048	SK	AM	38°45.60′	001°51.68′	142
A22B_0718_SK049	SK	AM	38°45.08′	001°52.62′	436
A22B_1019_SK054	SK	AM	38°45.48′	001°47.71′	115
A22B_1019_SK056	SK	AM	38°46.64′	001°52.07′	134
A22B_1019_SK084	SK	AM	38°42.08′	001°45.77′	352
A22B_1019_SK092	SK	AM	38°42.28′	001°44.99′	385
A22B_1019_SK100	SK	AM	38°48.15′	001°44.75′	338
A22B_1019_SK102	SK	AM	38°4815′	001°44.98′	335
A22B_1019_SK106	SK	AM	38°4712′	001°51.38′	130
A22B_0820_SK18	SK	AM	38°51.26′	001° 55.29′	490
A22B_0820_BC20	BC	AM	38°48.48′	002°00.35′	667
A22B_0820_SK21	SK	AM	38°49.98′	001° 53.48′	506
A22B_0820_SK22	SK	AM	38°52.34′	001° 51.79′	430
A22B_0820_BC23	BC	AM	38°50.30′	001°45.87′	341
A22B_0820_SK31	SK	AM	38°40.22′	001° 47.86′	441
A22B_0820_SK33	SK	AM	38°42.19′	001° 57.34′	664
A22B_0718_SK053	SK	EB	38°44.21′	002°30.09	109
A22B_0718_SK054	SK	EB	38°44.21′	002°30.15	107
A22B_0718_SK055	SK	EB	38°44.23′	002°30.27	104
A22B_0718_SK056	SK	EB	38°44.37′	002°30.18	108
A22B_0718_SK057	SK	EB	38°44.43′	002°30.24	107
A22B_0718_SK059	SK	EB	38°44.11′	002°29.52	128
A22B_0718_SK064	SK	EB	38°44.94′	002°30.82	134
A22B_0718_SK065	SK	EB	38°43.17′	002°29.42	147
A22B_0718_SK070	SK	EB	38°41.83′	002°28.00	149
A22B_0718_SK071	SK	EB	38°41.17′	002°28.11	153
A22B_0718_SK072	SK	EB	38°42.05′	002°29.79	278
A22B_0718_SK073	SK	EB	38°42.44′	002°29.96	152
A22B_0718_SK074	SK	EB	38°42.45′	002°29.53	152
A22B_0718_BC080	BC	EB	38°46.86′	002°31.12′	320
A22B_0718_BC082	BC	EB	38°43.60′	002°28.25′	399

Table A1. *Cont.*

Code	Dredge	Area	Latitude (N)	Longitude (E)	Depth (m)
A22B_0718_SK084	SK	EB	38°43.17′	002°29.45′	147
A22B_0718_SK087	SK	EB	38°41.24′	002°26.61′	319
A22B_0718_SK089	SK	EB	38°45.09′	002°27.65′	583
A22B_1019_SK151	SK	EB	38°40.38′	002°26.57′	394
A22B_1019_SK152	SK	EB	38°40.56′	002°29.02′	486
A22B_1019_SK161	SK	EB	38°42.63′	002°27.61′	320
A22B_1019_SK162	SK	EB	38°41.94′	002°25.11′	575
A22B_1019_SK171	SK	EB	38°42.29′	002°28.28′	153
A22B_1019_SK172	SK	EB	38°42.04′	002°32.43′	727
A22B_1019_SK181	SK	EB	38°43.05′	002°30.43′	147
A22B_1019_SK183	SK	EB	38°43.38′	002°28.28′	423
A22B_1019_SK184	SK	EB	38°43.95′	002°31.90′	316
A22B_1019_SK185	SK	EB	38°44.05′	002°31.17′	125
A22B_0820_SK44	SK	EB	38°45.76′	002° 31.25′	326
A22B_0820_SK46	SK	EB	38°42.15′	002° 26.74′	307
A22B_0820_SK47	SK	EB	38°41.24′	002° 26.03′	308
A22B_0820_SK48	SK	EB	38°41.14′	002° 25.98′	349
A22B_0820_BC49	BC	EB	38°40.91′	002° 25.27′	285
A22B_1019_SK174	SK	CB	38°51.89′	002°19.68′	1060
A22B_1019_SK191	SK	CB	38°53.13′	002°22.51′	986
A22B_0820_SK02	SK	CB	38°05.48′	002°09.48′	946
A22B_0820_SK15	SK	CB	38°57.55′	002°05.48′	950
A22B_0820_SK37	SK	CB	38°52.80′	002° 05.91′	852
A22B_0820_SK38	SK	CB	38°52.62′	002° 08.09′	924
A22B_0820_SK39	SK	CB	38°50.90′	002°13.69′	1044
A22B_0718_SK002	SK	SO	38°57.84′	002°00.11′	286
A22B_0718_SK003	SK	SO	38°57.57′	001°58.45′	291
A22B_0718_SK004	SK	SO	38°59.35′	001°59.44′	627
A22B_0718_SK006	SK	SO	38°56.28′	001°57.99′	281
A22B_0718_SK007	SK	SO	38°55.78′	001°57.73′	265
A22B_0718_SK008	SK	SO	38°54.56′	001°57.19′	683
A22B_0718_SK009	SK	SO	38°54.31′	001°59.45′	661
A22B_0718_BC010	BC	SO	38°58.80′	001°59.06′	697
A22B_0718_SK013	SK	SO	38°59.36′	002°01.33′	1062
A22B_0718_SK015	SK	SO	38°57.43′	002°00.23′	282
A22B_0718_SK016	SK	SO	38°57.18′	002°00.28′	302
A22B_0718_SK017	SK	SO	38°56.52′	002°00.49′	510
A22B_1019_SK005	SK	SO	38°57.60′	001°59.40′	292
A22B_1019_SK006	SK	SO	38°57.15′	001°58.21′	298
A22B_1019_SK016	SK	SO	38°55.36′	001°57.38′	452

Table A1. *Cont.*

Code	Dredge	Area	Latitude (N)	Longitude (E)	Depth (m)
A22B_1019_SK024	SK	SO	38°56.92′	001°59.68′	296
A22B_1019_SK026	SK	SO	38°56.18′	001°58.93′	446
A22B_0820_SK17	SK	SO	38°53.64′	001° 56.18′	688
A22B_0718_SK012	SK	PK	38°59.86′	001°59.24′	793
A22B_1019_SK030	SK	PK	38°54.98′	002°01.06′	786
A22B_1019_SK031	SK	PK	38°54.99′	002°00.93′	780
A22B_1019_SK038	SK	PK	38°57.85′	001°56.58′	617
A22B_1019_SK039	SK	PK	38°58.14′	001°56.15′	633
A22B_1019_SK110	SK	PK	38°55.51′	001°55.33′	667
A22B_1019_SK117	SK	PK	38°57.33′	001°51.75′	587
A22B_1019_SK118	SK	PK	38°57.42′	001°52.11′	638
A22B_1019_BC119	BC	PK	38°59.80′	001°53.90′	607
A22B_1019_SK121	SK	PK	39°00.80′	001°56.11′	710
A22B_0820_SK05	SK	PK	39°05.44′	001°57.70′	723
A22B_0820_BC08	BC	PK	38°58.77′	001°56.97′	656
A22B_0820_BC10	BC	PK	38°59.20′	001°53.79′	597
A22B_0820_BC12	BC	PK	38°53.38′	001°59.53′	749
A22B_0820_SK16	SK	PK	38°56.34′	002°01.88′	778
A22B_1019_SK042	SK	PK	38°32.80′	001°48.44′	628
A22B_1019_SK043	SK	PK	38°32.96′	001°48.72′	633
A22B_1019_BC068	BC	PK	38°33.05′	001°48.92′	630
A22B_1019_SK069	SK	PK	38°33.19′	001°49.10′	630
A22B_1019_BC070	BC	PK	38°32.95′	001°49.05′	629
A22B_1019_BC076	BC	PK	38°35.74′	001°47.50′	564
A22B_1019_SK077	SK	PK	38°36.01′	001°47.82′	556
A22B_1019_BC078	BC	PK	38°35.68′	001°47.53′	560
A22B_0820_BC26	BC	PK	38°40.87′	001°41.01′	390
A22B_0820_SK30	SK	PK	38°38.47′	001°43.42′	429
A22B_0820_SK32	SK	PK	38°36.18′	001°53.16′	624
A22B_0718_BC076	BC	PK	38°45.58′	002°25.86′	726
A22B_0718_SK078	SK	PK	38°47.57′	002°27.27′	721
A22B_0718_BC079	BC	PK	38°50.07′	002°27.81′	770
A22B_1019_SK131	SK	PK	38°48.11′	002°26.09′	739
A22B_1019_SK139	SK	PK	38°48.97′	002°29.68′	735
A22B_1019_SK140	SK	PK	38°49.41′	002°28.52′	431
A22B_1019_SK164	SK	PK	38°49.52′	002°30.81′	759
A22B_1019_BC190	BC	PK	38°53.73′	002°29.43′	755
A22B_0820_SK45	SK	PK	38°45.77′	002°33.88′	761
A22B_0820_SK51	SK	PK	38°40.68′	002°25.95′	316
A22B_0820_SK52	SK	PK	38°38.56′	002°18.78′	1017

Table A1. *Cont.*

Code	Dredge	Area	Latitude (N)	Longitude (E)	Depth (m)
A22B_0820_SK53	SK	PK	38°38.65′	002°29.22′	1005
A22B_0820_BC54	BC	PK	38°39.37′	002°22.60′	905
A22B_0820_SK57	SK	PK	38°53.03′	002°27.82′	744
A22B_0820_SK58	SK	PK	38°49.90′	002°24.65′	798
A22B_0820_SK59	SK	PK	38°48.57′	002°21.21′	993
A22B_0820_SK60	SK	PK	38°47.45′	002°19.92′	985
A22B_0820_SK62	SK	PK	38°43.83′	002°20.19′	895

Appendix B

Table A2. Characteristics of the sampling stations carried out with rock dredges in the Mallorca Channel seamounts Ses Olives (SO), Ausias March (AM), and Emile Baudot (EB) during the INTEMARES project. Bathymetric interval shows the initial and final depths of the haul.

			Setting		Hauling		
Code	Area	Date	Latitude (N)	Longitud (E)	Latitude (N)	Longitud (E)	Depth (m)
A22B_0718_DR_014	SO	28 July 2018	38°58.97′	001°59.97′	38°58.74′	001°59.98′	479–278
A22B_0718_DR_018	SO	28 July 2018	38°57.36′	002°01.09′	38°57.41′	002°00.83′	263–235
A22B_0718_DR_019	SO	28 July 2018	38°57.01′	001°59.55′	38°57.13′	001°59.45′	278–285
A22B_0718_DR_023	AM	30 July 2018	38°44.54′	001°46.66′	38°44.40′	001°46.85′	106–92
A22B_0718_DR_024	AM	30 July 2018	38°43.98′	001°46.54′	38°43.99′	001°46.28′	90
A22B_0718_DR_052	EB	3 August 2018	38°44.23′	002°30.03′	38°44.21′	002°30.20′	109–107
A22B_0718_DR_058	EB	3 August 2018	38°43.93′	002°29.11′	38°44.00′	002°29.25′	131–126
A22B_0718_DR_062	EB	4 August 2018	38°45.80′	002°34.33′	38°45.56′	002°34.37′	600–556
A22B_0718_DR_067	EB	4 August 2018	38°41.54′	002°27.56′	38°41.66′	002°27.97′	144–151
A22B_0718_DR_068	EB	4 August 2018	38°41.91′	002°28.76′	38°42.16′	002°28.59′	125–135
A22B_0718_DR_086	EB	7 August 2018	38°40.65′	002°25.73′	38°40.65′	002°25.95′	337–309
A22B_1019_DR_003	SO	11 October 2019	38°58.66′	001°59.29′	38°58.55′	001°59.23′	287–257
A22B_1019_DR_008	SO	11 October 2019	38°57.65′	002°00.89′	38°57.70′	002°00.97′	253–227
A22B_1019_DR_009	SO	11 October 2019	38°57.68′	002°00.99′	38°57.63′	002°00.92′	253–242
A22B_1019_DR_014	SO	12 October 2019	38°55.61′	001°57.63′	38°55.69′	001°57.61º	266–250
A22B_1019_DR_015	SO	12 October 2019	38°55.58′	001°57.65′	38°55.68′	001°57.59′	268–241
A22B_1019_DR_114	SO	23 October 2019	38°56.99′	001°53.23′	38°56.93′	001°53.03′	428–385
A22B_1019_DR_051	AM	15 October 2019	38°44.15′	001°49.14′	38°44.22′	001°49.19′	105
A22B_1019_DR_052	AM	15 October 2019	38°44.18′	001°47.64′	38°44.27′	001°47.70′	91–89
A22B_1019_DR_053	AM	15 October 2019	38°45.05′	001°47.68′	38°44.95′	001°47.79′	107–96
A22B_1019_DR_095	AM	19 October 2019	38°47.82′	001°52.56′	38°47.74′	001°52.38′	289–217
A22B_1019_DR_097	AM	19 October 2019	38°48.28′	001°52.91′	38°48.35′	001°52.61′	458–352
A22B_1019_DR_103	AM	21 October 2019	38°47.43′	001°47.17′	38°47.27′	001°47.22′	310–241
A22B_1019_DR_128	EB	24 October 2019	38°49.32′	002°28.66′	38°49.45′	002°28.50′	607–446
A22B_1019_DR_132	EB	25 October 2019	38°46.66′	002°27.99′	38°46.60′	002°28.07′	560–524
A22B_1019_DR_137	EB	25 October 2019	38°44.85′	002°30.28′	38°44.83′	002°30.19′	124,114
A22B_1019_DR_144	EB	26 October 2019	38°42.78′	002°27.72′	38°42.65′	002°27.82′	321–286
A22B_1019_DR_147	EB	26 October 2019	38°42.23′	002°28.91′	38°42.26′	002°29.03′	126–123

Table A2. *Cont.*

			Setting		Hauling		
Code	**Area**	**Date**	**Latitude (N)**	**Longitud (E)**	**Latitude (N)**	**Longitud (E)**	**Depth (m)**
A22B_1019_DR_165	EB	28 October 2019	38°46.97′	002°31.10′	38°46.88′	002°31.13′	320–312
A22B_1019_DR_176	EB	29 October 2019	38°45.28′	002°31.50′	38°45.23′	002°31.48′	144–141
A22B_0720_DR_003	SO	21 July 2020	38°56.67′	001°59.94′	38°56.74′	001°59.77′	455–288
A22B_0720_DR_004	SO	21 July 2020	38°56.39′	001°59.03′	38°56.30′	001°59.05′	440–350
A22B_0720_DR_007	SO	21 July 2020	38°58.76′	001°59.01′	38°58.56	001°59.14′	384–255
A22B_0720_DR_008	SO	21 July 2020	38°58.165′	002°00.67′	38°58.20′	002°00.43′	355–295
A22B_0720_DR_009	SO	21 July 2020	38°58.79′	002°00.85′	38°59.04′	002°00.50′	673–657
A22B_0720_DR_012	SO	22 July 2020	38°55.91′	001°56.09′	38°55.87′	001°56.43′	664–609
A22B_0720_DR_014	SO	22 July 2020	38°55.51′	001°58.13′	38°55.91′	001°57.88′	395–270
A22B_0720_DR_015	SO	22 July 2020	38°56.38′	001°59.59′	38°56.60′	001°59.35′	428–287
A22B_0720_DR_019	AM	23 July 2020	38°43.83′	001°45.57′	38°43.77′	001°45.72′	112–94
A22B_0720_DR_020	AM	23 July 2020	38°42.87′	001°46.47′	38°43.19′	001°46.47′	137–104
A22B_0720_DR_027	AM	24 July 2020	38°47.55′	001°52.83′	38°47.48′	001°52.53′	226–195
A22B_0720_DR_028	AM	24 July 2020	38°45.95′	001°51.87′	38°46.06′	001°51.76′	142–133
A22B_0720_DR_030	AM	24 July 2020	38°47.31′	001°47.01′	38°46.97′	001°47.13′	276–204
A22B_0720_DR_034	AM	25 July 2020	38°46.03′	001°49.09′	38°45.92′	001°49.24′	121–105
A22B_0720_DR_042	EB	26 July 2020	38°43.54′	002°29.28′	38°43.63′	002°29.10′	139
A22B_0720_DR_043	EB	26 July 2020	38°44.41′	002°30.66′	38°44.55′	002°30.56′	116
A22B_0720_DR_046	EB	26 July 2020	38°42.31′	002°30.75′	38°42.52′	002°30.71′	367–235
A22B_0720_DR_047	EB	26 July 2020	38°43.84′	002°29.40′	38°43.94′	002°29.28′	127
A22B_0720_DR_053	EB	27 July 2020	38°44.01′	002°30.72′	38°44.14′	002°30.41′	107–102
A22B_0720_DR_054	EB	27 July 2020	38°43.33′	002°30.90′	38°43.52′	002°30.73′	216–124
A22B_0720_DR_057	EB	27 July 2020	38°41.72′	002°21.88′	38°41.56′	002°22.10′	665–488
A22B_0720_DR_058	EB	27 July 2020	38°41.66′	002°29.36′	38°41.70′	002°29.27′	195–138
A22B_0720_DR_059	EB	28 July 2020	38°42.62′	002°36.41′	38°42.85′	002°36.48′	620–550
A22B_0720_DR_060	EB	28 July 2020	38°42.59′	002°36.63′	38°42.71′	002°36.29′	686–597
A22B_0720_DR_061	EB	28 July 2020	38°40.70′	002°35.37′	38°40.94′	002°35.27′	1191–1066

Appendix C

Table A3. Table characteristics of the sampling stations carried out with beam trawl in the Mallorca Channel seamounts Ses Olives (SO), Ausias March (AM), and Emile Baudot (EB) during the INTEMARES project.

			Setting			Hauling			Sampling	
Code	**Area**	**Date**	**Hour**	**Latitude (N)**	**Longitud (E)**	**Hour**	**Latitude (N)**	**Longitud (E)**	**Surface (m^2)**	**Depth (m)**
A22B_1019_BT_002	SO	11 October 2019	7:34	38°57.85′	001°58.78′	7:52	38°57.49′	001°58.49′	654	295
A22B_1019_BT_004	SO	11 October 2019	9:25	38°57.71′	001°59.81′	9:43	38°57.55′	001°59.19′	619	293
A22B_1019_BT_007	SO	11 October 2019	11:23	38°57.33′	001°59.90′	11:41	38°57.65′	001°59.32′	520	291
A22B_1019_BT_010	SO	11 October 2019	14:25	38°56.79′	001°57.71′	14:43	38°56.67′	001°57.65′	477	288
A22B_1019_BT_012	SO	12 October 2019	6:52	38°56.36′	001°59.14′	7:12	38°55.67′	001°58.64′	613	453
A22B_1019_BT_013	SO	12 October 2019	7:39	38°55.50′	001°57.03′	8:01	38°54.98′	001°58.14′	758	504
A22B_1019_BT_027	SO	13 October 2019	6:12	38°56.85′	002°00.76′	6:32	38°56.48′	001°59.84′	480	491
A22B_1019_BT_028	SO	13 October 2019	7:38	38°56.75′	002°01.16′	7:55	38°57.29′	002°01.32	487	449
A22B_1019_BT_029	SO	13 October 2019	8:26	38°56.44′	002°01.63′	8:51	38°55.59′	002°01.32′	272	764

Table A3. *Cont.*

Code	Area	Date	Setting			Hauling			Sampling	
			Hour	Latitude (N)	Longitud (E)	Hour	Latitude (N)	Longitud (E)	Surface (m^2)	Depth (m)
A22B_1019_BT_036	SO	13 October 2019	15:51	38°57.19′	001°56.11′	16:18	38°57.99′	001°56.67′	590	619
A22B_1019_BT_049	AM	15 October 2019	7:07	38°43.33′	001°49.37′	7:19	38°43.80′	001°50.09′	697	124
A22B_1019_BT_050	AM	15 October 2019	7:49	38°43.42′	001°47.90′	8:00	38°43.58′	001°48.39′	524	102
A22B_1019_BT_055	AM	15 October 2019	10:44	38°45.44′	001°47.56′	10:48	38°45.56′	001°47.78′	425	114
A22B_1019_BT_058	AM	15 October 2019	12:40	38°46.54′	001°52.09′	12:53	38°47.10′	001°52.33′	642	139
A22B_1019_BT_065	AM	16 October 2019	6:19	38°35.57′	001°53.45′	6:47	38°36.83′	001°54.40′	1679	631
A22B_1019_BT_075	AM	17 October 2019	8:46	38°34.72′	001°45.22′	9:17	38°35.52′	001°46.80′	2057	551
A22B_1019_BT_079	AM	17 October 2019	13:37	38°39.07′	001°50.42′	14:11	38°40.02′	001°51.82′	1850	501
A22B_1019_BT_089	AM	18 October 2019	14:10	38°40.71′	001°41.94′	14:44	38°41.45′	001°43.28′	2040	410
A22B_1019_BT_093	AM	19 October 2019	6:03	38°48.40′	001°48.03′	6:32	38°48.89′	001°50.45′	1531	376
A22B_1019_BT_094	AM	19 October 2019	6:54	38°48.85′	001°51.06′	7:21	38° 50.02′	001° 51.21′	2123	409
A22B_1019_BT_099	AM	19 October 2019	12:25	38°46.20′	001°48.91′	12:42	38°46.50′	001°49.60′	1241	131
A22B_1019_BT_101	AM	21 October 2019	7:34	38°48.70′	001°42.88′	7:58	38°47.83′	001°42.40′	1056	320
A22B_1019_BT_104	AM	21 October 2019	11:12	38°45.62′	001°50.77′	11:25	38° 46.09′	001°51.14′	524	116
A22B_1019_BT_109	SO	23 October 2019	6:39	38°53.67′	001°55.37′	7:15	38°55.12′	001°56.12′	2086	715
A22B_1019_BT_113	SO	23 October 2019	10:25	38°54.41′	001°56.72′	11:05	38°53.66′	001°58.61′	1991	697
A22B_1019_BT_122	SO	24 October 2019	7:42	39°00.54′	001°55.57′	8:18	38°59.61′	001°57.40′	2148	693
A22B_1019_BT_123	SO	24 October 2019	8:54	38°58.27′	001°55.85′	9:30	38°59.97′	001°56.56′	2222	675
A22B_1019_BT_124	EB	24 October 2019	13:37	38°45.11′	002°31.16′	13:45	38°45.35′	002°31.14′	387	146
A22B_1019_BT_125	EB	24 October 2019	14:18	38°45.61′	002°31.66′	14:36	38°46.06′	002°30.98′	630	314
A22B_1019_BT_135	EB	25 October 2019	14:05	38°44.91′	002°29.66′	14:16	38°44.53′	002°29.27′	815	153
A22B_1019_BT_136	EB	25 October 2019	14:49	38°42.85′	002°29.51′	15:00	38°43.23′	002°29.37′	689	143
A22B_1019_BT_143	EB	26 October 2019	10:19	38°47.46′	002°30.78′	10:51	38°47.82′	002°29.47′	1271	686
A22B_1019_BT_148	EB	26 October 2019	15:10	38°41.45′	002°28.18′	15:20	38°41.15′	002°28.03′	641	147
A22B_1019_BT_149	EB	26 October 2019	15:49	38°40.76′	002°27.48′	16:08	38°40.96′	002°26.83′	614	277
A22B_1019_BT_156	EB	27 October 2019	11:23	38°48.48′	002°25.14′	12:03	38°49.89′	002°25.70′	1360	759
A22B_1019_BT_157	EB	27 October 2019	14:00	38°41.41′	002°26.95′	14:20	38°42.20′	002°27.09′	1135	288
A22B_1019_BT_158	EB	27 October 2019	14:57	38°42.97′	002°29.65′	15:07	38°42.94′	002°29.11′	524	143
A22B_1019_BT_166	EB	28 October 2019	14:47	38°44.48′	002°28.48′	15:08	38°43.74′	002°28.03′	1295	433
A22B_1019_BT_167	EB	28 October 2019	15:44	38°42.54′	002°29.77′	15:55	38°42.22′	002°29.50′	655	151
A22B_1019_BT_175	EB	29 October 2019	11:47	38°46.07′	002°30.15′	12:08	38°46.53′	002°31.10′	1182	412
A22B_1019_BT_177	EB	29 October 2019	14:22	38°44.23′	002°28.89′	14:34	38°43.79′	002°28.90′	644	156
A22B_1019_BT_178	EB	29 October 2019	15:09	38°43.21′	002°27.37′	15:35	38°43.32′	002°26.27′	1262	555
A22B_1019_BT_188	EB	30 October 2019	13:18	38°49.11′	002°28.94′	13:44	38°50.01′	002°30.21′	2497	753
A22B_0718_BT_001	SO	27 July 2018	6:40	38°56.80′	001°58.54′	7:03	38°57.38′	001°59.39′	849	290
A22B_0718_BT_005	SO	27 July 2018	13:58	38°58.62′	001°59.88′	14:18	38°58.12′	001°59.24′	760	259
A22B_0718_BT_020	SO	28 July 2018	16:52	38°56.10′	001°58.52′	17:11	38°56.10′	001°57.73′	691	275
A22B_0718_BT_021	SO	28 July 2018	18:48	38°56.59′	001°57.03′	19:08	38°57.26′	001°57.31′	603	489
A22B_0718_BT_022	AM	30 July 2018	10:03	38°44.57′	001°46.25′	10:12	38°44.42′	001°45.89′	692	105
A22B_0718_BT_030	AM	30 July 2018	14:12	38°45.47′	001°45.58′	14:26	38°45.84′	001°46.01′	621	242
A22B_0718_BT_032	AM	30 July 2018	13:32	38°46.70′	001°44.90′	13:49	38°47.09′	001°45.45′	684	319
A22B_0718_BT_037	AM	31 July 2018	8:05	38°45.85′	001°47.26′	8:15	38°45.96′	001°47.58′	694	124
A22B_0718_BT_044	AM	31 July 2018	11:02	38°44.46′	001°50.85′	11:13	38°44.85′	001°50.95′	728	122
A22B_0718_BT_050	AM	31 July 2018	14:22	38°42.27′	001°52.18′	14:45	38°42.95′	001°52.57′	729	445
A22B_0718_BT_051	EB	3 August 2018	10:30	38°44.84′	002°30.52′	10:41	38°44.98′	002°30.91′	713	127
A22B_0718_BT_060	EB	3 August 2018	17:18	38°43.38′	002°29.64′	17:29	38°43.09′	002°29.34′	637	137
A22B_0718_BT_063	EB	4 August 2018	10:54	38°45.96′	002°34.56′	11:25	38°46.50′	002°35.72′	729	759
A22B_0718_BT_066	EB	4 August 2018	14:06	38°41.42′	002°28.44′	14:19	38°41.12′	002°28.03′	618	146
A22B_0718_BT_069	EB	4 August 2018	16:00	38°41.98′	002°28.21′	16:12	38°41.73′	002°27.86′	755	146
A22B_0718_BT_077	EB	6 August 2018	9:24	38°46.24′	002°26.01′	9:50	38°46.95′	002°26.65′	740	704

Table A3. *Cont.*

Code	Area	Date	Setting			Hauling			Sampling	
			Hour	Latitude (N)	Longitud (E)	Hour	Latitude (N)	Longitud (E)	Surface (m^2)	Depth (m)
A22B_0718_BT_085	EB	7 August 2018	8:12	38°41.92′	002°26.71′	8:31	38°41.29′	002°26.62′	624	299
A22B_0718_BT_088	EB	7 August 2018	11:00	38°45.48′	002°27.75′	11:23	38°44.74′	002°27.44′	698	574
A22B_0720_BT_001	SO	21 July 2020	6:12	38°57.67′	002°00.64′	6:33	38°58.25′	002°00.00′	1443	281
A22B_0720_BT_002	SO	21 July 2020	7:09	38°57.29′	002°00.40′	7:31	38°56.96′	001°59.60′	1229	298
A22B_0720_BT_005	SO	21 July 2020	11:31	38°56.57′	001°57.25′	11:56	38°55.90′	001°56.60′	1172	405
A22B_0720_BT_006	SO	21 July 2020	12:39	38°57.46′	001°57.06′	13:16	38°58.28′	001°58.16′	1901	556
A22B_0720_BT_010	SO	22 July 2020	6:06	38°54.47′	001°56.28′	6:45	38°55.45′	001°56.80′	1900	697
A22B_0720_BT_011	SO	22 July 2020	7:49	38°55.64′	001°55.99′	8:26	38°54.37′	001°55.46′	1848	715
A22B_0720_BT_013	SO	22 July 2020	11:27	38°56.48′	001°56.00′	12:01	38°57.71′	001°56.30′	1768	607
A22B_0720_BT_016	AM	23 July 2020	7:00	38°43.40′	001°47.04′	7:14	38°43.25′	001°46.64′	949	99
A22B_0720_BT_017	AM	23 July 2020	7:52	38°45.39′	001°47.08′	8:11	38°45.08′	001°46.60′	1067	112
A22B_0720_BT_018	AM	23 July 2020	8:41	38°45.05′	001°46.55′	8:57	38°45.27′	001°46.90′	165	113
A22B_0720_BT_021	AM	23 July 2020	14:17	38°44.92′	001°50.16′	14:34	38°45.32′	001°50.49′	477	105
A22B_0720_BT_026	AM	24 July 2020	9:11	38°47.16′	001°50.76′	9:27	38°47.10′	001°51.44′	281	127
A22B_0720_BT_029	AM	24 July 2020	12:43	38°46.24′	001°47.57′	13:07	38°46.03′	001°46.52′	1068	195
A22B_0720_BT_031	AM	24 July 2020	14:26	38°48.05′	001°48.19′	15:24	38°47.72′	001°47.08′	1138	348
A22B_0720_BT_033	AM	25 July 2020	6:57	38°46.73′	001°47.67′	7:19	38°47.37′	001°48.27′	1173	225
A22B_0720_BT_035	AM	25 July 2020	8:52	38°44.42′	001°43.79′	9:23	38°43.80′	001°42.75′	849	352
A22B_0720_BT_037	AM	25 July 2020	11:15	38°42.86′	001°51.53′	11:49	38°42.05′	001°50.73′	1200	363
A22B_0720_BT_038	EB	26 July 2020	6:09	38°43.72′	002°27.69′	6:38	38°42.52′	002°27.67′	846	511
A22B_0720_BT_039	EB	26 July 2020	7:49	38°44.84′	002°28.28′	8:13	38°44.21′	002°27.84′	936	483
A22B_0720_BT_044	EB	26 July 2020	11:57	38°39.11′	002°29.45′	12:34	38°38.97′	002°27.70′	1142	680
A22B_0720_BT_045	EB	26 July 2020	13:40	38°42.52′	002°29.74′	14:01	38°42.27′	002°29.40′	178	150
A22B_0720_BT_052	EB	27 July 2020	8:30	38°45.54′	002°31.59′	8:53	38°45.95′	002°30.62′	1267	297
A22B_0720_BT_055	EB	27 July 2020	11:42	38°39.98′	002°28.99′	12:08	38°40.24′	002°27.81′	673	473
A22B_0720_BT_062	EB	28 July 2020	12:20	38°43.25′	002°27.82′	12:47	38°44.00′	002°27.68′	894	508

Appendix D

Table A4. Characteristics of the sampling stations carried out with the experimental bottom trawl GOC-73 in the fishing grounds adjacent to the Mallorca Channel seamounts Ausias March (AM) and Emile Baudot (EB) during the INTEMARES project.

Code	Area	Date	Setting			Hauling			Sampling	
			Hour	Latitude (N)	Longitude (E)	Hour	Latitude (N)	Longitude (E)	Surface (km^2)	Depth (m)
A22B_1019_GOC_040	AM	14 October 2019	6:46	38°36.89′	001°55.19′	8:30	38°33.31′	001°50.91′	0.103084	631
A22B_1019_GOC_044	AM	14 October 2019	11:40	38°30.34′	001°45.14′	13:25	38°33.05′	001°51.71′	0.102621	663
A22B_1019_GOC_066	AM	16 October 2019	7:36	38°40.94′	001°56.27′	9:10	38°36.23′	001°53.57′	0.106566	619
A22B_1019_GOC_154	EB	27 October 2019	9:10	38°52.46′	002°27.08′	10:30	38°51.79′	002°26.11′	0.071558	760
A22B_1019_GOC_155	EB	27 October 2019	6:47	38°51.92′	002°33.42′	8:10	38°48.95′	002°25.94′	0.071789	755
A22B_1019_GOC_173	EB	29 October 2019	6:53	38°47.34′	002°13.04′	8:40	38°51.19′	002°16.90′	0.093264	1028
A22B_1019_GOC_186	EB	30 October 2019	9:20	38°53.16′	002°34.81′	11:00	38°49.24′	002°30.41′	0.103130	759
MEDITS_0620_GOC_108	EB	24 June 2020	5:53	38°52.52′	002°27.06′	7:11	38°48.31′	002°25.72′	0.075247	746
MEDITS_0620_GOC_109	EB	24 June 2020	7:54	38°47.45′	002°24.32′	9:16	38°51.73′	002°26.08′	0.073746	754
MEDITS_0620_GOC_110	EB	24 June 2020	10:52	38°46.89′	002°26.75′	12:14	38°49.73′	002°31.30′	0.079473	732
MEDITS_0621_GOC_235	EB	23 June 2021	5:56	38°53.15′	002°34.78′	7:19	38°49.64′	002°30.99′	0.088226	757
MEDITS_0621_GOC_236	EB	23 June 2021	8:08	38°52.58′	002°30.34′	9:30	38°48.92′	002°26.92′	0.088505	747

Table A4. *Cont.*

Code	Area	Date	Setting			Hauling			Sampling	
			Hour	Latitude (N)	Longitud (E)	Hour	Latitude (N)	Longitud (E)	Surface (m^2)	Depth (m)
MEDITS_0821_GOC_003	AM	18 August 2021	11:25	38°34.27′	001°39.32′	12:48	38°34.47′	001°44.80′	0.095555	542
MEDITS_0821_GOC_004	AM	18 August 2021	13:44	38°31.08′	001°43.56′	15:03	38°32.72′	001°48.91′	0.950162	627
MEDITS_0821_GOC_009	AM	19 August 2021	13:01	38°56.65′	001°49.37′	14:30	38°53.04′	001°53.47′	0.113673	459
MEDITS_0821_GOC_032	AM	25 August 2021	5:59	38°39.40′	001°55.89′	7:19	38°43.95′	001°56.83′	0.087158	615
MEDITS_0821_GOC_033	AM	25 August 2021	8:05	38°45.83′	001°53.62′	9:26	38°41.67′	001°52.06′	0.100025	460
MEDITS_0821_GOC_034	AM	25 August 2022	10:59	38°39.17′	001°40.08′	12:10	38°42.67′	001°42.62′	0.088374	393
MEDITS_0821_GOC_035	AM	25 August 2021	12:55	38°45.88′	001°46.13′	13:45	38°46.91′	001°49.38′	0.053231	237

Appendix E

Table A5. Characteristics of the sampling stations carried out with the TASIFE photogrammetric sledge (ROTV) in the Mallorca Channel seamounts Ses Olives (SO), Ausias March (AM), and Emile Baudot (EB) during the INTEMARES project.

Code	Area	Date	Initial				Final				Sampling Area (m^2)
			Hour	Latitude (N)	Longitude (E)	Depth (m)	Hour	Latitude (N)	Longitude (E)	Depth (m)	
TR017	SO	12 October 2019	11:21	38°57.994′	01°58.627′	283	11:36	38°57.936′	01°58.622′	288	534.00
TR018	SO	12 October 2019	11:51	38°57.788′	01°59.094′	288	12:08	38°57.726′	01°59.238′	287	602.16
TR019	SO	12 October 2019	12:27	38°57.587′	01°59.551′	287	12:42	38°57.514′	01°59.720′	286	540.34
TR020	SO	12 October 2019	13:25	38°58.410′	02°00.127′	280	13:45	38°58.298′	02°00.308′	302	711.18
TR021	SO	12 October 2019	14:18	38°57.399′	02°00.888′	230	14:40	38°57.303′	02°01.091′	326	799.34
TR022	SO	12 October 2019	15:17	38°56.960′	01°59.600′	284	15:37	38°56.862′	01°59.802′	292	687.32
TR032	SO	13 October 2019	12:07	38°58.668′	01°58.213′	587	12:12	38°58.715′	01°58.160′	612	360.52
TR033	SO	13 October 2019	12:50	38°58.600′	01°58.240′	579	12:58	38°58.678′	01°58.205′	693	326.72
TR034	SO	13 October 2019	13:31	38°58.632′	01°58.243′	580	13:36	38°58.660′	01°58.205′	599	187.81
TR035	SO	13 October 2019	14:13	38°58.617′	01°58.233′	583	14:24	38°58.662′	01°58.170′	621	335.32
TR045	AM	14 October 2019	14:57	38°32.801′	01°48.446′	624	15:12	38°32.875′	01°48.568′	624	544.34
TR046	AM	14 October 2019	15:35	38°33.073′	01°48.918′	579	15:50	38°33.140′	01°49.035′	622	545.80
TR047	AM	14 October 2019	16:09	38°33.277′	01°49.333′	619	16:24	38°33.354′	01°49.468′	617	609.81
TR059	AM	15 October 2019	14:03	38°44.644′	01°48.533′	94	14:18	38°44.695′	01°48.388′	92.	629.58
TR060	AM	15 October 2019	14:48	38°44.846′	01°47.938′	90	15:03	38°44.898′	01°47.791′	94	638.56
TR061	AM	15 October 2019	15:21	38°45.040′	01°47.380′	106	15:36	38°45.092′	01°47.231′	107	728.32
TR062	AM	15 October 2019	16:07	38°47.397′	01°44.038′	88	16:22	38°44.099′	01°47.248′	87	593.34
TR063	AM	15 October 2019	16:40	38°44.265′	01°46.819′	90	16:55	38°44.322′	01°46.675′	90	634.50
TR064	AM	15 October 2019	17:14	38°44.486′	01°46.263′	110	17:29	38°44.544′	01°46.121′	111	623.60
TR071	AM	16 October 2019	16:41	38°30.436′	01°42.765′	669	17:01	38°30.340′	01°42.666′	699	355.56
TR072	AM	16 October 2019	17:03	38°30.328′	01°42.655′	699	17:23	38°30.195′	01°42.537′	716	678.44
TR073	AM	16 October 2019	17:24	38°30.188′	01°42.532′	717	17:34	38°30.121′	01°42.471′	727	342.86
TR080	AM	17 October 2019	15:21	38°42.782′	01°47.863′	151	15:41	38°42.619′	01°47.867′	225	633.50
TR081	AM	17 October 2019	15:43	38°42.607′	01°47.867′	229	16:03	38°42.441′	01°47.872′	265	638.76
TR082	AM	17 October 2019	16:05	38°42.435′	01°47.872′	269	16:25	38°42.259′	01°47.876′	293	638.72
TR086	AM	18 October 2019	9:04	38°43.671′	01°45.650′	95	9:24	38°43.676′	01°45.436′	657	656.98
TR087	AM	18 October 2019	9:26	38°43.676′	01°45.429′	159	9:46	38°43.681′	01°45.200′	657	657.48
TR090	AM	18 October 2019	15:40	38°42.058′	01°45.867′	346	15:55	38°42.095′	01°45.716′	500	499.58
TR091	AM	18 October 2019	16:19	38°42.293′	01°45.146′	367	16:34	38°42.248′	01°45.146′	482	481.60
TR096	AM	19 October 2019	9:23	38°48.338′	01°52.670′	339	9:43	38°48.285′	01°52.880′	691	691.42
TR098	AM	19 October 2019	11:27	38°47.691′	01°52.250′	198	11:47	38°47.777′	01°52.443′	668	667.84

Table A5. *Cont.*

			Initial				Final				
Code	**Area**	**Date**	**Hour**	**Latitude (N)**	**Longitude (E)**	**Depth (m)**	**Hour**	**Latitude (N)**	**Longitude (E)**	**Depth (m)**	**Sampling Area (m^2)**
TR107	AM	21 October 2019	13:58	38°47.246′	01°47.193′	234	14:18	38°47.403′	01°47.147′	303	671.60
TR111	SO	23 October 2019	8:59	38°54.672′	01°56.847′	664	9:19	38°54.562′	01°56.722′	665	1113.30
TR112	SO	23 October 2019	9:47	38°54.206′	01°56.389′	681	9:52	38°54.244′	01°56.375′	680	271.34
TR115	SO	23 October 2019	14:16	38°56.829′	01°53.156′	394	14:36	38°56.827′	01°52.944′	484	889.36
TR116	SO	23 October 2019	14:38	38°56.827′	01°52.922′	492	14:58	38°56.829′	01°52.714′	576	946.00
TR126	EB	24 October 2019	15:34	38°49.437′	02°28.508′	426	15:54	38°56.827′	01°52.944′	580	880.22
TR127	EB	24 October 2019	15:55	38°49.352′	02°28.323′	593	16:15	38°49.269′	02°28.175′	713	943.64
TR133	EB	25 October 2019	12:59	38°43.847′	02°29.414′	128	13:19	38°43.970′	02°29.267′	125	731.20
TR134	EB	25 October 2019	13:22	38°43.256′	02°29.094′	125	13:42	38°44.095′	02°29.094′	134	724.98
TR145	EB	26 October 2019	13:38	38°42.146′	02°29.219′	131	13:53	38°42.208′	02°29.082′	123	525.56
TR146	EB	26 October 2019	14:02	38°42.245′	02°29.000′	123	14:17	38°42.307′	02°28.862′	130	516.90
TR159	EB	27 October 2019	15:52	38°43.770′	02°29.525′	126	16:12	38°43.762′	02°29.313′	128	661.86
TR160	EB	27 October 2019	16:20	38°43.758′	02°29.227′	128	16:40	38°43.751′	02°29.017′	148	656.76
TR168	EB	28 October 2019	16:28	38°42.043′	02°29.260′	138	16:48	38°42.037′	02°29.048′	131	656.56
TR169	EB	28 October 2019	16:58	38°42.034′	02°28.945′	123	17:18	38°42.027′	02°28.738′	128	631.40
TR179	EB	29 October 2019	16:32	38°43.368′	02°29.966′	131	16:52	38°43.375′	02°30.170′	124	644.68
TR180	EB	29 October 2019	17:04	38°43.378′	02°30.293′	126	17:24	38°43.383′	02°30.506′	126	660.68

Appendix F

Table A6. Characteristics of the sampling stations carried out with the ROV Liropus 2000 in the Mallorca Channel seamounts Ses Olives (SO), Ausias March (AM), and Emile Baudot (EB) during the INTEMARES project.

			Initial				Final				
Code	**Area**	**Date**	**Hour**	**Latitude (N)**	**Longitude (E)**	**Depth (m)**	**Hour**	**Latitude (N)**	**Longitude (E)**	**Depth (m)**	**Sampling Area (m^2)**
R1_1	SO	21 August 2020	12:38:25	38°58.98′	001°58.78′	608	14:47:27	38°58.72′	001°58.18′	637	784,624
R1_2	SO	21 August 2020	15:33:42	38°58.73′	001°58.18′	642	16:21:43	38°58.99′	001°58.78′	611	1,086,012
R1_3	SO	21 August 2020	16:31:04	38°58.96′	001°58.78′	800	16:57:00	38°58.92′	001°58.67′	601	188,041
R2_1	SO	22 August 2020	8:40:40	38°58.95′	001°58.81′	580	9:48:47	38°58.69′	001°58.20′	611	1,559,742
R2_2	SO	22 August 2020	10:28:07	38°58.76′	001°58.08′	672	11:34:43	38°58.65′	001°58.20′	604	229,906
R3	SO	23 August 2020	7:50:31	38°58.65′	001°58.20′	605	11:42:20	38°58.67′	001°58.13′	640	241,508
R4_1	SO	23 August 2020	13:58:13	38°56.38′	001°59.58′	423	15:40:40	38°56.47′	001°59.48′	280	154,396
R4_2	SO	23 August 2020	16:14:04	38°56.59′	001°59.86′	454	17:10:32	38°56.73′	001°59.75′	289	299,956
R5_1	SO	24 August 2020	8:09:24	38°56.82′	002°00.35′	443	9:24:59	38°57.00′	002°00.24′	298	323,297
R5_2	SO	24 August 2020	10:07:51	38°56.96′	002°00.81′	374	11:28:24	38°57.21′	002°00.74′	254	385,623
R6_1	SO	24 August 2020	13:38:50	38°57.07′	001°56.14′	606	14:45:44	38°57.47′	001°56.24′	605	912,376
R6_2	SO	24 August 2020	15:39:11	38°57.53′	001°55.93′	645	16:53:33	38°57.57′	001°55.87′	624	101,768
R7	AM	25 August 2020	7:42:33	38°45.74′	001°46.01′	242	9:48:00	38°45.37′	001°46.36′	120	799,572
R8	AM	25 August 2020	10:46:55	38°44.44′	001°46.34′	107	12:53:06	38°44.13′	001°46.73′	86	719,893
R9	AM	25 August 2020	13:40:29	38°43.92′	001°46.74′	85	15:10:00	38°44.18′	001°47.24′	85	925,759
R10	AM	25 August 2020	16:05:07	38°45.38′	001°45.41′	251	17:17:51	38°45.10′	001°45.84′	128	687,313
R11	AM	26 August 2020	7:08:53	38°46.96′	001°46.68′	299	8:51:42	38°46.85′	001°47.00′	197	528,920
R12	AM	26 August 2020	10:06:05	38°47.30′	001°53.08′	445	11:39:18	38°47.19′	001°52.68′	215	504,425
R13	AM	26 August 2020	12:39:20	38°48.37′	001°52.95′	456	14:11:54	38°48.43′	001°52.65′	344	435,245
R14	AM	26 August 2020	15:44:22	38°49.99′	001°58.75′	647	16:39:05	38°50.00′	001°58.67′	630	113,915
R15	EB	27 August 2020	6:48:54	38°42.29′	002°31.12′	546	8:17:14	38°42.52′	002°30.71′	233	708,701

Table A6. *Cont.*

Code	Area	Date	Initial				Final				Sampling Area (m^2)
			Hour	Latitude (N)	Longitude (E)	Depth (m)	Hour	Latitude (N)	Longitude (E)	Depth (m)	
R16	EB	27 August 2020	9:11:44	38°43.10′	002°31.25′	401	12:01:00	38°43.15′	002°30.46′	143	1,243,278
R17	EB	27 August 2020	13:04:58	38°44.03′	002°33.01′	593	14:58:32	38°43.89′	002°32.67′	363	475,220
R18	EB	27 August 2020	16:03:34	38°44.75′	002°31.87′	500	17:05:37	38°44.76′	002°31.85′	341	557,222
R19	EB	28 August 2020	7:01:25	38°40.64′	002°34.84′	1140	8:45:34	38°40.97′	002°34.86′	1015	524,461
R20	EB	28 August 2020	10:38:16	38°42.74′	002°37.14′	895	13:20:57	38°42.67′	002°36.51′	523	765,042
R21	EB	28 August 2020	15:02:34	38°47.61′	002°32.83′	719	16:57:40	38°47.26′	002°32.94′	417	661,131
R22	EB	29 August 2020	8:23:53	38°43.90′	002°27.63′	537	8:22:57	38°43.95′	002°28.46′	287	996,950
R23	EB	29 August 2020	9:21:25	38°44.45′	002°29.24′	165	11:27:16	38°44.66′	002°29.72′	129	738,266
R24	EB	29 August 2020	12:40:32	38°44.76′	002°29.46′	151	14:25:19	38°44.95′	002°29.90′	130	682,976
R25	EB	29 August 2020	15:31:19	38°43.91′	002°30.16′	114	17:06:42	38°44.14′	002°30.60′	96	652,233
R26_1	EB	30 August 2020	8:19:50	38°52.35′	002°30.43′	740	9:32:20	38°52.89′	002°30.56′	738	950,914
R26_2	EB	30 August 2020	10:24:19	38°53.08′	002°30.95′	732	11:50:26	38°53.25′	002°30.68′	515	374,714
R27	EB	30 August 2020	13:13:58	38°53.73′	002°29.43′	753	14:42:44	38°53.67′	002°29.56′	700	150,203
R28	SO	31 August 2020	7:10:43	38°55.84′	001°53.59′	610	8:35:27	38°55.90′	001°53.43′	587	176,282
R29	SO	31 August 2020	9:49:08	85°6.974′	001°53.57′	422	11:41:24	38°57.02′	001°53.20′	387	424,614

Appendix G

Table A7. Inventory of species or taxa identified so far from the sampling developed in the Ses Olives, Ausias March, and Emile Baudot seamounts and adjacent bottoms of the Mallorca Channel (Balearic Islands, western Mediterranean) during the INTEMARES project, with beam trawl (BT), the GOC-73 experimental bottom trawl (GOC), rock dredge (RD), and remote operated vehicle (ROV). The area and depth in which the species or taxa have been found as well as their frequency of occurrence are also shown. (*) Not been taken into account for biodiversity estimations, since they may be species or taxa repetitions.

	Area				Sampling method		
	SO	**AM**	**EB**	**Depth (m)**	**BT**	**GOC**	**RD**	**ROV**
CHLOROPHYTA								
***Palmophyllum crassum* (Naccari) Rabenhorst, 1868**		X	X	90–128	3		15	X
Chlorophyceae		X	X	87–146				X
OCHROPHYTA								
Halopteris filicina (Grateloup) Kützing, 1843		X	X	89–105			5	X
Zanardinia typus (Nardo) P.C.Silva, 2000		X		85–106				X
Zonaria tournefortii (J.V.Lamouroux) Montagne, 1846		X		85–106				X
RHODOPHYTA								
Aeodes marginata (Roussel) F.Schmitz, 1894		X		90			7	
Cryptonemia tuniformis (Bertoloni) Zanardini, 1868		X	X	90–124	7		6	
Corallinaceae		X	X	98–152	37		59	
cf. *Lithophyllum stictiforme* (J.E. Areschoug) Hauck, 1877		X	X	85–106				X
Lithophyllum spp.		X		85–100			7	X
Lithothamnion spp.				85–135	37			X
cf. *Lithothamnion valens* Foslie, 1909		X		85–100				X
Phymatolithon spp.		X	X	85–135	37			X
cf. *Mesophyllum alternans* (Foslie) Cabioch & M.L. Mendoza, 1998		X		85–86				X
cf. *Mesophyllum lichenoides* (J.Ellis) Me.Lemoine, 1928		X	X	85–135				X
Spongites fruticulosus Kützing, 1841		X		85–91			7	X
Spongites spp.		X	X	85–135	41			X
cf. *Peyssonnelia rosa-marina* Boudouresque & Denizot, 1973		X	X	85–135				X
Peyssonnelia spp. Decaisne, 1841		X	X	85–135	7			X
Phyllophora crispa (Hudson) P.S. Dixon, 1964		X	X	90–124			6	X

Table A7. *Cont.*

	Area				Sampling method			
	SO	**AM**	**EB**	**Depth (m)**	**BT**	**GOC**	**RD**	**ROV**
PORIFERA								
Aaptos aaptos (Schmidt, 1864)		X	X	108–117	3		6	X
Ancorinidae sp. 1	X	X	X	100–511	26		20	X
Ancorinidae sp. 2		X	X	105–150	10			
Ancorinidae sp. 3		X	X	105–150	3			
Ancorinidae sp. 4			X	125–125			3	
Ancorinidae spp. *	X	X	X	85–576				X
Astrophorina sp. 1			X	117–117			5	
Astrophorina sp. 2		X	X	113–150	5			
Astrophorina sp. 3	X			305–305			8	
Axinella polypoides Schmidt, 1862		X	X	98–99	7			X
Axinella spatula Sitjà & Maldonado, 2014		X		152–152	3			
Axinella verrucosa (Esper, 1794)		X		98–127	3		3	
Axinella sp. 1		X	X	153–328	3	7		
Axinella sp. 2		X	X	113–395	10			
Axinella sp. 3			X	150–150	3			
Axinella sp. 4		X		99–99	3			
Axinella sp. 5		X	X	113–150	3			
Axinella sp. 6		X		99–112	7			
Axinella spp. *		X	X	85–362				X
Biemna sp.		X		113–113	3			
Bubaris sp. 1	X	X	X	143–523	22		12	
Bubaris sp. 2		X		98–98	3			
Calcarea sp. 1	X	X	X	105–297	6			
Calcarea sp. 2		X	X	105–150	3			
Calcarea sp. 3		X		99–99	3			
Calyx cf. *tufa* (Ridley & Dendy, 1886)		X		112–113	7			X
Cladocroce sp.			X	277–412	10			X
Cladorhiza abyssicola Sars, 1872	X	X	X	377–715	13			
Clathrina sp.		X		121–121			7	
Craniella sp.			X	117–117			5	
Crella (*Crella*) sp.		X		105–105	3			
Crella (*Yvesia*) sp.		X		112–112	3			
Darwinellidae sp.		X	X	99–277	23		14	
Desmacella annexa Schmidt, 1870	X	X	X	112–756	25	17		
Desmacella inornata (Bowerbank, 1866)	X	X	X	116–757	40	7	8	
Desmacella sp.	X			607–607	4			
Dictyonella sp.		X		105–105	3			
Dictyonella spp.		X	X	98–143	5		9	

Table A7. *Cont.*

	Area				Sampling method			
	SO	**AM**	**EB**	**Depth (m)**	**BT**	**GOC**	**RD**	**ROV**
Diplastrella bistellata (Schmidt, 1862)		X		105–105	3			X
Dragmatella aberrans (Topsent, 1890)	X	X	X	127–412	22		14	
Dysidea sp.			X	117–117			5	
Eurypon sp.		X		99	3			
Foraminospongia balearica Díaz, Ramírez-Amaro & Ordines, 2021		X	X	87–170	40		25	X
Foraminospongia minuta Díaz, Ramírez-Amaro & Ordines, 2021	X			288–318			8	
Geodiidae sp. 1		X	X	98–150	7		5	X
Geodiidae sp. 2		X	X	99–127	14		5	X
Geodiidae sp. 3			X	150–150	3			
Geodiidae sp. 4		X	X	105–105	3			
Geodiidae sp. 5		X		105–105	3			
Geodiidae sp. 6		X	X	105–150	3			
Geodiidae sp. 7			X	141–166			10	
Geodiidae sp. 8		X	X	98–147	8		14	
Geodiidae sp. 9			X	146–146	3			
Spongosorites spp. *		X	X	100–286				X
Halichondriidae sp. 1			X	105–105			5	
Halichondriidae sp. 2			X	511–511	3			
Haliclona (Soestella) fimbriata Bertolino & Pansini, 2015	X			143–133				X
Haliclona poecillastroides (Vacelet, 1969)	X	X	X	98–402	20		20	X
Haliclona (*Rhizoniera*) *rhizophora* (Vacelet, 1969)	X	X	X	225–405	5			
Haliclona sp. 1		X		99–99	3			
Haliclona sp. 2		X		127–127	3			
Haliclona sp. 3		X		99–99	3			
Haliclona sp. 4			X	150–150	3			
Haliclona sp. 5			X	150–150	3			
Haliclona sp. 6		X	X	105–150	3			
Haliclona sp. 7		X		105–105	3			
Haliclona sp. 8		X		105–105	3			
Haliclona (*Flagellia*) sp.			X	143–146	6			
Haliclona (*Halichoclona*) sp.		X	X	116–402	10			
Hamacantha spp. *	X	X	X	248–676				X
Hamacantha (Hamacantha) sp.		X	X	143–412	16		7	
Hamacantha (Vomerula) falcula (Bowerbank, 1874)		X		98–402	14			
Hamacantha (Vomerula) sp. 1		X		267–267			7	
Hamacantha (Vomerula) sp. 2	X	X	X	150–508	13			

Table A7. *Cont.*

	Area				Sampling method			
	SO	**AM**	**EB**	**Depth (m)**	**BT**	**GOC**	**RD**	**ROV**
Hamacantha (Vomerula) sp. 3			X	674–674	3			
Hemiasterella elongata Topsent, 1928		X	X	113–473	7		7	
Hexadella sp.		X	X	98–277	25		12	
Hymedesmia (*Hymedesmia*) sp. 1		X		99–113	7			
Hymedesmia (*Hymedesmia*) sp. 2		X		105–105	3			
Hymedesmia (*Hymedesmia*) sp. 3			X	473–473	3			
Keratosa spp. *			X	106				X
Keratosa sp. 1			X	143–150	10			
Keratosa sp. 2			X	105–150	19		10	
Latrunculia sp.		X	X	121–141			6	
Melonanchora emphysema (Schmidt, 1875)		X		121–121			7	
Pachastrella sp. *		X		106				X
Pachastrellidae sp. 1		X	X	104–113	3		3	
Pachastrellidae sp. 2	X			274–274			8	
Pachastrellidae sp. 3		X	X	105–235			12	
Pachastrellidae sp. 4			X	538–538			5	X
Paratimea massutii Díaz, Ramírez–Amaro & Ordines, 2021			X	155–167	3			
Penares sp. *		X	X	85–87				X
Penares helleri (Schmidt, 1864)		X	X	100–460	23	7	6	X
Petrosia (Petrosia) raphida Boury-Esnault, Pansini & Uriz, 1994		X	X	98–395	18			
Petrosia (Strongylophora) vansoesti Boury-Esnault, Pansini & Uriz, 1994		X	X	98–297	13		10	
Petrosia ficiformis (Poiret, 1789)		X	X	98–150	10		5	X
Phakellia hirondellei Topsent, 1890		X	X	135–147	3		3	
Phakellia robusta Bowerbank, 1866	X	X	X	150–297	5		12	X
Phakellia ventilabrum (Linnaeus, 1767)			X	140			1	X
Phakellia sp.	X		X	128–242			9	
Poecillastra sp. *		X	X	150–370				X
Poecillastra compressa (Bowerbank, 1866)	X	X	X	98–511	40		25	X
Polymastia spp. *		X	X	237–573				X
Polymastia sp. 1			X	473–473	3			
Polymastia sp. 2		X		99–99	3			
Polymastia sp. 3	X		X	288–674	11			
Porifera *	X	X	X	85–116				X
Prosuberites sp. 1		X		99–99	3			
Pseudotrachya hystrix (Topsent, 1890)		X		138–209			14	

Table A7. *Cont.*

	Area				Sampling method			
	SO	**AM**	**EB**	**Depth (m)**	**BT**	**GOC**	**RD**	**ROV**
Rhabdobaris implicata Pulitzer-Finali, 1983			X	117–117			5	
Rhizaxinella pyrifera (Delle Chiaje, 1828)		X		225–402	10	7		
Rhizaxinella sp. 1		X	X	150–348	3			
Rhizaxinella sp. 2	X			281–715	8			
Scopalinidae		X		99–112	7			
Spinularia sp.	X	X	X	195–688	5			
Spongosorites sp. 1		X		99–99	3			X
Spongosorites sp. 2		X		127–127	3			X
Spongosorites sp. 3		X		127–127	3			
Stylocordyla pellita (Topsent, 1904)		X	X	297–538	3		6	X
Stylocordyla spp. *	X	X	X	286–687				X
Suberites domuncula (Olivi, 1792)		X		328–328		7		
Sympagella sp. 1		X		352–352	3			
Tethya sp.		X		105–134	3			X
Tetractinellida *			X	133–169				X
Thenea muricata (Bowerbank, 1858)	X	X	X	122–740	48	20	7	X
Timea sp.		X		98–127	10			
Topsentia sp. 1		X		105–105	3			
Topsentia sp. 2		X		112–112	3			
Tretodictyum reiswigi Boury-Esnault, Vacelet & Chevaldonné, 2017	X		X	143–511	23			X
Tretodictyum spp. *	X	X	X	236–534				X
Vulcanellidae sp.	X	X	X	127–303	3		9	X
CNIDARIA								
Acanthogorgia sp. *		X	X	133–337				X
Actiniaria *			X	546				X
Actiniidae *		X	X	590–818				X
Adamsia carcinopados (Müller, 1776)		X	X	98–277	30		5	
Adamsia palliata (Fabricius, 1779)		X		98–127	10			
Alcyonium acaule Marion, 1878		X		105	3			
Alcyonium coralloides (Pallas, 1766)			X	105–128			15	
Alcyonium palmatum Pallas, 1766		X	X	160			5	X
Alcyonium sp. *			X	100–144				X
Anthozoa *	X	X	X	146–854				X
Amphianthus dornii (Koch, 1878)	X			678	4			
Bathypathes sp.			X	858–875				X
Bebryce mollis Philippi, 1842		X	X	100–412	12		18	X
Calliactis parasitica (Couch, 1842)	X	X	X	98–328	23	12	5	

Table A7. *Cont.*

	Area				Sampling method			
	SO	**AM**	**EB**	**Depth (m)**	**BT**	**GOC**	**RD**	**ROV**
Callogorgia verticillata (Pallas, 1766)			X	117–887			10	X
Callogorgia sp. *			X	143–134				X
Caryophyllia smithii Stokes & Broderip, 1828	X			290	4			
Caryophyllia(Caryophyllia) calveri Duncan, 1873			X	531–684				X
Caryophyllia sp. *	X		X	542–874				X
Cerianthus membranaceus (Gmelin, 1791)		X		159–299				X
Ceriantharia	X	X	X	258–753				X
Chironephthya mediterranea López-González, Grinyó & Gili, 2014		X		226–258				X
Dendrophyllia sp.	X			642				X
Dendrophyllia cornigera (Lamarck, 1816)		X	X	297–372				X
Ellisella flagellum (Johnson, 1863)			X	128–293			15	X
Eunicella singularis cf. (Esper, 1791)		X	X	96–112				X
Funiculina quadrangularis (Pallas, 1766)		X	X	137–146	6	7		X
Hydrozoa *		X	X	88–106				X
Isidella elongata (Esper, 1788)	X		X	146–715	12		8	X
Lafoea dumosa (Fleming, 1820)	X		X	312–757	4		5	
Leiopathes glaberrima (Esper, 1792)			X	500				X
Madrepora oculata Linnaeus, 1758		X		338–372				X
cf. *Muriceides lepida* Carpine & Grasshoff, 1975		X		173–255				X
cf. *Nicella granifera* (Kölliker, 1865)	X	X	X	145–887				X
Paralcyonium spinulosum (Delle Chiaje, 1822)		X	X	88–144				X
Paramuricea hirsuta (Gray, 1857)		X		344–380				X
Parazoanthus sp. Haddon & Shackleton, 1891	X		X	603–644				X
Pelagia noctiluca (Forsskål, 1775)	X	X	X	153–1028	18	87		
Savalia savaglia (Bertoloni, 1819)			X	625–843				X
Swiftia pallida cf.Madsen, 1970		X	X	272–716				X
Villogorgia bebrycoides (Koch, 1887)			X	128–141			10	
Virgularia mirabilis (Müller, 1776)			X	129			5	
ANNELIDA								
Bonellia viridis Rolando, 1822	X	X	X	88–561				X
Euarche tubifex Ehlers, 1887	X	X	X	105–551	23		6	
Hyalinoecia tubicola (O.F. Müller, 1776)	X	X	X	98–405	28		20	X

Table A7. *Cont.*

	Area				Sampling method			
	SO	**AM**	**EB**	**Depth (m)**	**BT**	**GOC**	**RD**	**ROV**
Laetmonice hystrix (Savigny in Lamarck, 1818)	X	X	X	105–290	11			
Lanice conchilega (Pallas, 1766)	X	X	X	103–624	15		12	X
Pomatoceros triqueter (Linnaeus, 1758)	X	X	X	105–445	25			
Sabella pavonina Savigny, 1822		X		88				X
Serpula vermicularis Linnaeus, 1767			X	146	3			
Serpulidae *		X	X	93–530				X
Vermiliopsis infundibulum (Philippi, 1844)		X		90			7	
CRUSTACEA								
Acanthephyra eximia Smith, 1884			X	759		7		
Acanthephyra pelagica (Risso, 1816)			X	732–1028	3	40		
Achaeus cranchii Leach, 1817 [in Leach, 1815–1875]	X	X		113–242	3		8	
Aegaeon lacazei (Gourret, 1887)	X	X	X	124–688	21	13		
Alpheus cf. *dentipes* Guérin, 1832	X			305		7		
Alpheus glaber (Olivi, 1792)	X	X	X	112–474	23		7	
Alpheus macrocheles (Hailstone, 1835)			X	160			5	
Alpheus platydactylus Coutière, 1897	X	X	X	105–609	9	1	14	
Anamathia rissoana (P. Roux, 1828 [in P. Roux, 1828–1830])	X			607–680	12			
Anapagurus laevis (Bell, 1845 [in Bell, 1844–1853])	X	X	X	105–556	49		7	
Aristaeomorpha foliacea (Risso, 1827 in [Risso, 1826–1827])			X	756		7		
Aristeus antennatus (Risso, 1816)		X	X	542–1089	3	63		X
Atelecyclus rotundatus (Olivi, 1792)			X	146	3			
Bathynectes maravigna (Prestandrea, 1839)			X	543–750				X
Calappa granulata (Linnaeus, 1758)	X	X	X	105–365	25	7	9	X
Calocaris macandreae Bell, 1846 [in Bell, 1844–1853]	X	X	X	288–770	31	13		
Chlorotocus crassicornis (A. Costa, 1871)	X	X	X	275–510	20	33		
Crustacea *			X	1068–1086				X
Cymonomus granulatus (Norman in C. W. Thomson, 1873)	X	X	X	259–483	20			
Dardanus arrosor (Herbst, 1796)	X	X	X	98–328	23	13	5	X
Dardanus sp. *		X		215				X
Derilambrus angulifrons (Latreille, 1825)		X	X	122–150	7			
Distolambrus maltzami (Miers, 1881)		X	X	98–412	43			

Table A7. *Cont.*

	Area				Sampling method			
	SO	**AM**	**EB**	**Depth (m)**	**BT**	**GOC**	**RD**	**ROV**
Dorhynchus thomsoni C. W. Thomson, 1873	X	X	X	112–688	8			
Ebalia cranchii Leach, 1817 [in Leach, 1815–1875]	X			290–303	4		8	
Ebalia deshayesi H. Lucas, 1846	X	X	X	105–548	23			
Ebalia edwardsii O.G. Costa, 1838 [in O.G. Costa & A. Costa, 1838–1871]		X		98	3			
Ebalia nux A. Milne-Edwards, 1883	X	X	X	124–680	60		9	
Ebalia tuberosa (Pennant, 1777)	X	X	X	100–674	26		7	
Ergasticus clouei A. Milne-Edwards, 1882	X	X	X	105–757	65		5	
Ethusa mascarone (Herbst, 1785)			X	314	3			
Eurynome aspera (Pennant, 1777)		X	X	98–548	37			
Eusergestes arcticus (Krøyer, 1855)	X	X	X	444–770	14	47		X
Galathea nexa Embleton, 1836		X		100–631	3		7	
Galathea sp. *			X	636				X
Gennadas elegans (Smith, 1882)	X	X	X	147–1028	11	40		
Geryon longipes A. Milne-Edwards, 1882	X	X	X	460–770	19	77	8	X
Goneplax rhomboides (Linnaeus, 1758)	X	X	X	290–510	8	20		
Homola barbata (Fabricius, 1793)			X	511	3			
Idotea metallica Bosc, 1802		X		122	3			
Inachus dorsettensis (Pennant, 1777)	X	X	X	98–729	42	7	7	
Inachus leptochirus Leach, 1817 [in Leach, 1815–1875]	X	X	X	99–328	15	7		
Inachus sp. *		X		85				X
Latreillia elegans P. Roux, 1830 [in P. Roux, 1828–1830]	X	X	X	124–680	3			
Ligur ensiferus (Risso, 1816)		X		459–510		20		
Liocarcinus depurator (Linnaeus, 1758)	X	X	X	105–365	11			
Liocarcinus zariquieyi (Gordon, 1968)		X		105–135	14			
Lophogaster typicus M. Sars, 1857	X	X	X	105–757	66	20	8	
Macropipus tuberculatus (P. Roux, 1830 [in P. Roux, 1828–1830])	X	X	X	105–548	20	7		X
Macropodia linaresi Forest & Zariquiey Álvarez, 1964		X		127	3			
Macropodia longipes (A. Milne-Edwards & Bouvier, 1899)		X		135	3			
Meganyctiphanes norvegica (M. Sars, 1857)	X			275–290	8			
Monodaeus couchii (RQ Couch, 1851)	X	X	X	98–760	53	17	15	

Table A7. *Cont.*

	Area				Sampling method			
	SO	**AM**	**EB**	**Depth (m)**	**BT**	**GOC**	**RD**	**ROV**
Munida intermedia A. Milne-Edwards & Bouvier, 1899		X	X	348–574	7	27		X
Munida perarmata A. Milne Edwards & Bouvier, 1894	X	X	X	277–768	14	53		
Munida speciosa von Martens, 1878	X	X	X	99–697	27			
Munida spp. *	X	X	X	107–1068				X
Natantia *	X		X	298–843				x
Natatolana borealis (Lilljeborg, 1851)		X	X	116–412	13			
Nephrops norvegicus (Linnaeus, 1758)	X	X	X	328–627	7	60		X
Paguroidea *	X	X	X	140–283				X
Paguristes eremita (Linnaeus, 1767)			X	127	3			
Pagurus alatus J.C. Fabricius, 1775	X	X	X	352–680	16	7		X
Pagurus anachoretus Risso, 1827 in [Risso, 1826–1827]	X	X	X	116–275	BT	6		
Pagurus prideaux Leach, 1815 [in Leach, 1815–1875]		X	X	98–277	30		5	
Palicus caronii (P. Roux, 1830 [in P. Roux, 1828–1830])		X	X	122–147	3			
Palinurus elephas (JC. Fabricius, 1787)			X	107				X
Palinurus mauritanicus Gruvel, 1911	X	X		285–386				X
Parapenaeus longirostris (H. Lucas, 1846)	X	X	X	267–542	18	47	7	X
Paromola cuvieri (Risso, 1816)	X	X	X	444–759		37		X
Parthenopoides massena (P. Roux, 1830 [in P. Roux, 1828–1830])		X	X	105–153	28			
Pasiphaea multidentata Esmark, 1866	X	X	X	147–768	7	70		
Pasiphaea sivado (Risso, 1816)		X	X	444–732	3	13		
Philocheras bispinosus (Hailstone, 1835)	X			680	4			
Philocheras echinulatus (M. Sars, 1862)	X	X	X	290–688	16	7		
Phronima sedentaria (Forskål, 1775)	X	X	X	135–1028	13	50		
Phrosina semilunata Risso, 1822			X	768–1028		13		
Plesionika acanthonotus (Smith, 1882)	X	X	X	150–768	19	67		X
Plesionika antigai Zariquiey Álvarez, 1955	X	X	X	147–511	34	13	9	X
Plesionika edwardsii (J.F. Brandt in von Middendorf, 1851)	X	X	X	249–510	4	13	8	X
Plesionika gigliolii (Senna, 1902)	X	X	X	148–631	15	53	22	X
Plesionika heterocarpus (A. Costa, 1871)	X	X	X	237–619	14	47		
Plesionika martia (A. Milne-Edwards, 1883)	X	X	X	393–768	20	87		X
Plesionika narval (J.C. Fabricius, 1787)	X	X	X	241–459	9	7	25	

Table A7. *Cont.*

	Area				Sampling method			
	SO	**AM**	**EB**	**Depth (m)**	**BT**	**GOC**	**RD**	**ROV**
Plesionika spp. *	X	X	X	200–1072				X
Polycheles typhlops Heller, 1862	X	X	X	459–768	21	73		
Pontophilus norvegicus (M. Sars, 1861)			X	729–768		27		
Pontophilus spinosus (Leach, 1816)		X		445	3			
Processa canaliculata Leach, 1815 [in Leach, 1815–1875]	X	X	X	114–548	25	27		
Processa macrophthalma Nouvel & Holthuis, 1957			X	146	6			
Processa nouveli Al-Adhub & Williamson, 1975	X	X	X	127–510	15	13		
Reptantia *			X	340				X
Rissoides desmaresti (Risso, 1816)		X		444–510	3	13		
Robustosergia robusta (Smith, 1882)	X	X	X	542–1028	11	70		
Rocinella dumerilii (Lucas, 1849)		X	X	147–674	8			
Scalpellum (Linnaeus, 1767)		X		99	3			
Scyllarus pygmaeus (Spence Bate, 1888)		X		90			7	
Solenocera membranacea (Risso, 1816)	X	X	X	122–511	20	257		
Spinolambrus macrochelos (Herbst, 1790 [in Herbst, 1782–1790])		X	X	127–137	5			
Thia scutellata (Fabricius, 1793)		X		122	3			
MOLLUSCA								
Abra longicallus (Scacchi, 1835)	X	X	X	195–740	23			
Abralia veranyi (Rüppell, 1844)		X		393–460		27		
Addisonia excentrica (Tiberi, 1855)		X		116	3			
Aequipecten commutatus (Monterosato, 1875)			X	412	3			
Alloteuthis media (Linnaeus, 1758)		X		619		7		
Anadara carbuloides (Monterosato, 1881)		X		112–113	7			
Ancistrocheirus lesueurii (d'Orbigny [in Férussac & d'Orbigny], 1842)		X		600		7		
Ancistroteuthis lischtensteinii (Férussac [in Férussac & d'Orbigny], 1835)		X	X	627–747		10		
Anomia ephippium Linnaeus, 1758			X	274			5	
Anomiidae		X		105–122	11			
Aporrhais serresiana (Michaud, 1828)	X	X	X	319–640	12	7		
Aptyxis syracusana (Linnaeus, 1758)		X		116	3			
Arcopella balaustina (Linnaeus, 1758)		X		195	3			
Arcidae	X	X	X	100–577	7		33	
Atrina pectinata (Linnaeus, 1767)		X		107				X
Baptodoris cinnabarina Bergh, 1884	X	X	X	122–688	12			

Table A7. *Cont.*

	Area				Sampling method			
	SO	**AM**	**EB**	**Depth (m)**	**BT**	**GOC**	**RD**	**ROV**
Bathypolypus sponsalis (P. Fischer & H. Fischer, 1892)		X	X	444–770	3	20		
Bivalvia *			X	802				X
Calliostoma conulum (Linnaeus, 1758)			X	288	3			
Calliostoma granulatum (Born, 1778)	X	X	X	105–412	28		8	
Calliostoma gubbioli Nofroni, 1984	X	X		275–397	4		7	
Calliostoma zizyphinum (Linnaeus, 1758)		X	X	225–483	7			
Callumbonela suturale (Philippi, 1836)		X	X	153–365	5			
Capulus ungaricus (Linnaeus, 1758)		X	X	127–147	3			
Cardiomya costellata (Deshayes, 1835)	X	X		113–607	13			
Cephalopoda *		X	X	380–402				X
Cetomya neaeroides (Seguenza, 1877)	X			298–449	1		1	
Clavatulidae		X		116–365	10			
Clelandella miliaris (Brocchi, 1814)	X	X		135–474	4			
Colidae			X	574	1			
Comarmondia gracilis (Montagu, 1803)			X	127	3			
Cuspidaria cuspidata (Olivi, 1792)	X	X	X	127–474	12			
Cuspidaria rostrata (Spengler, 1793)	X	X	X	114–759	40			
Cymbulia peronii Blainville, 1818	X	X	X	113–768	11	23		
Danilia tinei (Calcara, 1839)		X		127	3			
Delectopecten vitreus (Gmelin, 1791)	X		X	640–674	4			
Eledone cirrhosa (Lamarck, 1798)		X		122–446	7	7		X
Eledone sp. *		X		260–342				X
Emarginula adriatica O.G. Costa, 1830			X	128–141			10	
Epitonium celesti (Aradas, 1854)			X	150–412	6			
Euspira fusca (Blainville, 1825)	X	X	X	242–474	12		8	
Fusinus pulchellus (Philippi, 1840)		X	X	105–395	12			
Gastropteron rubrum (Rafinesque, 1814)		X		105–242	7			
Gracilipurpura rostrata (Olivi, 1792)		X	X	127–483	10			
Heteroteuthis dispar (Rüppell, 1844)			X	732		7		
Histioteuthis bonnellii (Férussac, 1834)		X		444–663		47		
Histioteuthis reversa (Verrill, 1880)		X	X	600–757		33		
Illex coindetii (Vérany, 1839)		X		237–542		33		
Japonactaeon pusillus (Forbes, 1844)	X			556	4			
Kaloplocamus ramosus (Cantraine, 1835)			X	141			5	
Karnekampia sulcata (O.F. Müller, 1776)		X	X	127–348	5			
Lima (Linnaeus, 1758)		X		105	3			

Table A7. *Cont.*

	Area				Sampling method			
	SO	**AM**	**EB**	**Depth (m)**	**BT**	**GOC**	**RD**	**ROV**
Lima sp. *			X	1068				X
Limaria tuberculata (Olivi, 1792)		X		267			7	
Loligo forbesii Steenstrup, 1856		X		328–460		20		
Lyonsiidae	X			609–697	8			
Manupecten pesfelis (Linnaeus, 1758)		X	X	122–127	3			
Mimachlamys varia (Linnaeus, 1758)	X			290			8	
Mitrella gervillii (Payraudeau, 1826)			X	577			5	
Neorossia caroli (Joubin, 1902)		X		444–459		13		
Neopycnodonte sp. Stenzel, 1971	X	X	X	299–412				X
Nucula nitidiosa Winckworth, 1930		X		320–365	7			
Ocenebra erinaceus (Linnaeus, 1758)		X		225	3			
Octopus salutii Vérany, 1839		X		328–601		20		
Octopus vulgaris Cuvier, 1797			X	169				X
Octopodoidea *			X	324				X
Onchidella celtica (Audouin & Milne-Edwards, 1832)	X			242			8	
Orania fusulus (Brocchi, 1814)			X	129			5	
Pagodula echinata (Kiener, 1839)	X	X	X	267–680	11		7	
Palliolum incomparabile (Risso, 1826)		X	X	127–508	3			
Palliolum tigerinum (O.F. Müller, 1776)		X		116	3			
Parvamussium fenestratum (Forbes, 1844)		X	X	127–511	8			
Peltodoris sp.			X	133				X
Philine monterosati Monterosato, 1874	X	X	X	98–740	21			
Pleurobranchaea meckeli (Blainville, 1825)		X		114	3			
Policordia gemma (A. E. Verrill, 1880)			X	577			5	
Poromya granulata (Nyst & Westendorp, 1839)		X		122–352	21			
Pseudamussium clavatum (Poli, 1795)		X	X	105–352	27			
Ranella olearium (Linnaeus, 1758)			X	137–412	35			
Raphitomidae	X	X	X	225–574	7			
Rhinoclama nitens (Locard, 1898)	X			482–523	8			
Rondeletiola minor (Naef, 1912)		X		320	3			
Rossia macrosoma (Delle Chiaje, 1830)		X	X	328–548	3	12		
Scaeurgus unicirrhus (Delle Chiaje [in Férussac & d'Orbigny], 1841)		X	X	105–143	3			
Scaphander lignarius (Linnaeus, 1758)	X	X	X	122–445	7			
Sepia elegans Blainville, 1827		X	X	105–299	15			X
Sepia orbignyana Férussac [in d'Orbigny], 1826		X	X	146–237	3	7		
Sepietta oweniana (d'Orbigny, 1841)	X	X	X	112–542	29	47		

Table A7. *Cont.*

	Area				Sampling method			
	SO	**AM**	**EB**	**Depth (m)**	**BT**	**GOC**	**RD**	**ROV**
Sepiolidae *	X		X	340–620				X
Similipecten similis (Laskey, 1811)	X	X		105–298	11			
Spisula subtruncata (da Costa, 1778)	X			259	4			
Spondylidae			X	137			5	
Stoloteuthis leucoptera (Verrill, 1878)		X		459		7		
Taonius pavo (Lesueur, 1821)			X	1028		7		
Tectonatica rizzae (Philippi, 1844)	X	X		105–445	7			
Todarodes sagittatus (Lamarck, 1798)		X	X	328–770		47		
Todaropsis eblanae (Ball, 1841)		X		460		7		
Trophonopsis barvicensis (G. Johnston, 1825)	X			259	4			
Trophonopsis muricata (Montagu, 1803)		X		319	3			
Tropidomya abbreviata (Forbes, 1843)		X	X	122–402	13			
Turbinidae			X	508	3			
Xenophora crispa (König, 1825)		X	X	122–297	5			
ECHINODERMATA								
Amphipholis squamata (Delle Chiaje, 1828)	X			680	4			
Amphiura chiajei Forbes, 1843	X	X	X	114–445	11		7	
Amphiura filiformis (O.F. Müller, 1776)	X	X	X	146–508	25		6	
Anseropoda placenta (Pennant, 1777)		X	X	98–195	32		7	
Antedon mediterranea (Lamarck, 1816)		X	X	127–153	7			
Asteroidea sp. 1		X	X	105–153	15			
Asteroidea sp. 2			X	412–770	13	7		
Asteroidea sp. 3		X	X	114–147	7			
Asteroidea *			X	150				X
Astropecten irregularis (Pennant, 1777)		X	X	113–445	17	13		
Astropecten sp. *		X		242–342				X
Brissopsis atlantica mediterranea Mortensen, 1913	X	X		500–609	4			
Ceramaster grenadensis (Perrier, 1881)			X	760		7		
Chaetaster longipes (Bruzelius, 1805)		X	X	91–548	27		9	X
Cidaris cidaris (Linnaeus, 1758)	X	X	X	105–574	35	7	5	X
Crinoidea *	X		X	380–500				X
Echinaster sepositus (Retzius, 1783)		X		85–105				X
Echinocyamus pusillus (O.F. Müller, 1776)	X	X	X	127–275	7			
Echinodea *	X	X	X	188–610				X
Echinus melo Lamarck, 1816	X		X	147–278	4			X
Gracilechinus acutus (Lamarck, 1816)	X	X	X	112–680	22	20		X
Hacelia attenuata Gray, 1840		X		90–121	17		21	X

Table A7. *Cont.*

	Area				Sampling method			
	SO	**AM**	**EB**	**Depth (m)**	**BT**	**GOC**	**RD**	**ROV**
Holothuria forskali Delle Chiaje, 1824		X		99	3			X
Holothuria tubulosa Gmelin, 1791		X	X	105–127	3		5	X
Holothuria sp. *		X		85				X
Holothuroidea *			X	169–724				X
Leptometra celtica (M'Andrew & Barrett, 1857)	X	X	X	114–680	12			X
Luidia ciliaris (Philippi, 1837)		X	X	105–242	10		5	
Luidia sarsii Düben & Koren in Düben, 1844	X	X	X	98–548	39			
Marthasterias glacialis (Linnaeus, 1758)	X	X	X	98–395	25		8	
Mesothuria intestinalis (Ascanius, 1805)		X	X	225–759	8	7		X
Oestergrenia digitata (Montagu, 1815)	X	X		242–472	9			
Ophiacantha setosa (Bruzelius, 1805)			X	141			5	
Ophiactis balli (W. Thompson, 1840)	X		X	160–298			6	
Ophiocten abyssicolum (Forbes, 1843)	X	X	X	98–548	26			
Ophiomyces grandis Lyman, 1879	X	X	X	122–548	36		7	
Ophiopsila annulosa (M. Sars, 1859)		X	X	116–153	13			
Ophiopsila aranea Forbes, 1843		X	X	105–319	20			
Ophiothrix fragilis (Abildgaard in O.F. Müller, 1789)	X	X		114–259	7			
Ophiothrix quinquemaculata (Delle Chiaje, 1828)	X			278	4			
Ophiura (Dictenophiura) carnea Lütken, 1858	X	X	X	105–511	43		15	
Ophiura albida Forbes, 1839	X			298	4			
Ophiura grubei Heller, 1863		X	X	105–288	13			
Ophiuroieda sp. 1	X	X		410–556	6			
Ophiuroieda sp. 2			X	141			5	
Ophiuroieda sp. 3			X	150	3			
Ophiuroieda sp. 4	X			303–305			17	
Parastichopus regalis (Cuvier, 1817)		X	X	114–288	18	13		X
Peltaster placenta (Müller & Troschel, 1842)	X	X	X	105–412	37		11	X
Psammechinus microtuberculatus (Blainville, 1825)	X		X	146–290	7			
Pseudostichopus occultatus Marenzeller von, 1893	X	X	X	124–511	20		7	
Sclerasterias richardi (Perrier in Milne-Edwards, 1882)	X	X	X	105–548	38		10	X
Spatangus purpureus O.F. Müller, 1776	X	X	X	137–412	15	7		X
Stichopodidae	X			278–697	8			X
Tethyaster subinermis (Philippi, 1837)		X		195–328	3	7		

Table A7. *Cont.*

	Area				Sampling method			
	SO	**AM**	**EB**	**Depth (m)**	**BT**	**GOC**	**RD**	**ROV**
BRACHIOPODA								
Argyrotheca chordata (Risso, 1826)		X	X	90–473	28		56	
Brachiopoda *	X	X	X	99–432				X
Gryphus vitreus (Born, 1778)	X	X	X	116–764	59	20		X
Joania cordata (Risso, 1826)	X	X	X	127–290	5			
Mergelia truncata (Linnaeus, 1767)	X	X	X	90–511	22		50	
BRYOZOA								
Amphiblestrum lirulatum (Calvet, 1907)		X		402	3			
Bryozoa *			X	260–295				X
Hornera sp.			X	133				X
Kinetoskias sp.	X			591–622				X
Smittina cervicornis (Pallas, 1766)		X		105			5	X
THALIACEA								
Pyrosoma atlanticum Péron, 1804	X	X	X	137–1028	4	30		
Salpa spp.		X	X	393–757		57		
Salpa maxima Forskål, 1775		X	X	105–1028	10	13		X
Thaliacea *	X		X	131–599				X
ASCIDIACEA								
Ascidia involuta Heller, 1875		X		108			7	
Ascidia mentula Müller, 1776			X	117			5	X
Ascidiacea sp. 1 *	X	X	X	100–633				X
Ascidiacea sp. 2 *			X	143–150				X
Ascidiacea sp. 3 *		X	X	107–139				X
Ascidiacea sp. 4 *		X		104				X
Ascidiacea sp. 5 *		X		88–89				X
Ascidiacea sp. 6 *		X		86				X
Ascidiacea sp. 7 *	X			301–304				X
Ascidiacea sp. 8 *	X			314				X
Ascidiacea sp. 9 *		X	X	134–144				X
Clavelina dellavallei	X	X	X	88–349				X
Diazona violacea Savigny, 1816		X		90			7	X
Halocynthia papillosa		X		87–104				X
ELASMOBRANCHII								
Centrophorus uyato (Rafinesque, 1810)			X	738–760		27		
Dalatias licha (Bonnaterre, 1788)		X		542		7		
Dipturus oxyrinchus (Linnaeus, 1758)		X	X	328–757		10		
Etmopterus spinax (Linnaeus, 1758)		X	X	444–757		50		
Galeus melastomus Rafinesque, 1810	X	X	X	328–760	4	83		X
Leucoraja naevus (Müller & Henle, 1841)		X		237		7		

Table A7. *Cont.*

	Area				Sampling method			
	SO	**AM**	**EB**	**Depth (m)**	**BT**	**GOC**	**RD**	**ROV**
Raja clavata Linnaeus, 1758		X	X	103–451	3	13		X
Raja polystigma Regan, 1923		X		85–237		7		X
Scyliorhinus canicula (Linnaeus, 1758)		X		88–459		33		X
Squalus blainville (Risso, 1827)		X		85–328		13		X
ACTINOPTERI								
Acantholabrus sp.		X		298				X
Actinopteri *	X		X	394–760				X
Alepocephalus rostratus Risso, 1820			X	759		7		
Anthias (Linnaeus, 1758)	X	X	X	235			7	X
Arctozenus risso (Bonaparte, 1840)		X	X	510–747		20		
Argentina sphyraena Linnaeus, 1758		X		328–393		13		
Argyropelecus hemigymnus Cocco, 1829	X	X	X	288–1028	14	83		
Arnoglossus imperialis (Rafinesque, 1810)		X	X	105–147	12			X
Arnoglossus laterna (Walbaum, 1792)		X	X	122–153	8			
Arnoglossus rueppelii (Cocco, 1844)	X	X	X	105–511	21	7	5	X
Arnoglossus thori Kyle, 1913		X	X	98–147	5			
Arnoglossus sp. *		X		169–290				X
Aulopus filamentosus (Bloch, 1792)		X	X	89–311				X
Bathophilus nigerrimus Giglioli, 1882			X	760		7		
Bathypterois mediterraneus Bauchot, 1962			X	756–759		20		X
Benthocometes robustus (Goode & Bean, 1886)		X		615		7		
Benthosema glaciale (Reinhardt, 1837)	X	X	X	292–768	6	37		
Blennius ocellaris Linnaeus, 1758		X		100			7	
Buenia massutii Kovacic, Ordines & Schliewen, 2017		X		105–116	17			
Callanthias ruber (Rafinesque, 1810)			X	160			5	X
Callionymus maculatus Rafinesque, 1810	X	X	X	122–299	8			
Capros aper (Linnaeus, 1758)	X	X	X	105–770	16	53		X
Cataetyx alleni (Byrne, 1906)			X	729		7		
Centracanthus cirrus Rafinesque, 1810		X		237		7		
Centrolophus niger (Gmelin, 1789)			X	747		7		
Cepola macrophthalma (Linnaeus, 1758)			X	150	3			
Ceratoscopelus maderensis (Lowe, 1839)	X	X	X	290–760	4	27		
Chauliodus sloani Bloch & Schneider, 1801	X	X	X	290–1028	4	47		
Chelidonichthys cuculus (Linnaeus, 1758)		X	X	98–328	20	13		

Table A7. *Cont.*

	Area				Sampling method			
	SO	**AM**	**EB**	**Depth (m)**	**BT**	**GOC**	**RD**	**ROV**
Chelidonichthys lastoviza (Bonnaterre, 1788)		X	X	85–127				X
Chlopsis bicolor Rafinesque, 1810		X		328–444		13		
Chlorophthalmus agassizi Bonaparte, 1840	X	X	X	277–750	8	17		X
Coelorinchus caelorhincus (Risso, 1810)	X	X	X	328–574	12	47		X
Conger conger (Linnaeus, 1758)	X	X	X	328–760	4	47		X
Coris sp.			X	102				X
Cubiceps gracilis (Lowe, 1843)			X	732		7		
Cyclothone braueri Jespersen & Tåning, 1926	X			715	4			
Deltentosteus quadrimaculatus (Valenciennes, 1837)			X	412	3			
Diaphus holti Tåning, 1918		X	X	459–757		13		
Diaphus rafinesquii (Cocco, 1838)			X	757		7		
Diplecogaster bimaculata (Bonnaterre, 1788)		X	X	98–500	20			
Dysomma brevirostre (Facciolà, 1887)		X		444–510		13		
Echiodon dentatus (Cuvier, 1829)		X		459		7		
Electrona risso (Cocco, 1829)		X		459		7		
Epigonus constanciae (Giglioli, 1880)		X	X	444–511	3	7		
Epigonus denticulatus Dieuzeide, 1950		X	X	393–759		30		
Epigonus telescopus (Risso, 1810)			X	732–757		20		
Epigonus sp. *	X			283				X
Gadella maraldi (Risso, 1810)		X	X	444–760		27		
Gadiculus argenteus Guichenot, 1850	X	X	X	277–542	14	47		X
Gadidae *	X			306				X
Gaidropsarus biscayensis (Collett, 1890)	X	X	X	147–768	15	23		
Glossanodon leioglossus (Valenciennes, 1848)		X		237–459	3	13		X
Gnathophis mystax (Delaroche, 1809)		X	X	112–288	3			X
Gobiidae *		X	X	129–603				X
Gymnesigobius medits Kovačić, Ordines, Ramirez-Amaro & Schliewen, 2019			X	395–511	6			
Helicolenus dactylopterus (Delaroche, 1809)	X	X	X	259–732	18	30	5	X
Hoplostethus mediterraneus Cuvier, 1829	X	X	X	444–768	9	80		X
Hygophum benoiti (Cocco, 1838)		X	X	393–1028		23		
Hymenocephalus italicus Giglioli, 1884	X	X	X	393–768	5	87		X
Lampanyctus crocodilus (Risso, 1810)		X	X	444–1028	3	87		X
Lampanyctus pusillus (Johnson, 1890)		X	X	288–770	6	27		

Table A7. *Cont.*

	Area				Sampling method			
	SO	**AM**	**EB**	**Depth (m)**	**BT**	**GOC**	**RD**	**ROV**
Lebetus guilleti (Le Danois, 1913)		X		225	3			
Lepidion lepidion (Risso, 1810)			X	747–768		47		X
Lepidopus caudatus (Euphrasen, 1788)		X		328–460		27		
Lepidorhombus boscii (Risso, 1810)	X	X	X	195–600	14	53		X
Lepidorhombus whiffiagonis (Walbaum, 1792)		X	X	225–615	3	20		X
Lepidorhombus sp. *	X	X	X	240				X
Lepidotrigla cavillone (Lacepède, 1801)		X		105–114	10			
Lepidotrigla dieuzeidei Blanc & Hureau, 1973		X		124–328	3	13		
Lepidotrigla sp. *		X		287				X
Lestidiops sphyrenoides (Risso, 1820)		X		393		7		
Lobianchia dofleini (Zugmayer, 1911)	X	X	X	393–1028	5	60		
Lophius budegassa Spinola, 1807		X	X	113–510	5	33		
Lophius piscatorius Linnaeus, 1758		X	X	146–760	3	17		
Lophius sp. *		X		103				X
Macroramphosus scolopax (Linnaeus, 1758)		X	X	112–328	3	13		
Maurolicus muelleri (Gmelin, 1789)		X		328		7		
Merluccius merluccius (Linnaeus, 1758)		X		237–663	3	67		
Microchirus variegatus (Donovan, 1808)		X		114	3			
Micromesistius poutassou (Risso, 1827)		X		328		7		X
Molva dypterygia (Pennant, 1784)		X		393–459		20		
Mora moro (Risso, 1810)			X	759	3			
Muraena helena			X	99				X
Myctophum punctatum Rafinesque, 1810		X	X	444–768	3	23		X
Naucrates ductor (Linnaeus, 1758)			X	1028		7		
Nettastoma melanurum Rafinesque, 1810	X	X	X	600–760	4	40		X
Nezumia aequalis (Günther, 1878)	X	X	X	460–760	8	70		X
Notacanthus bonaparte Risso, 1840	X	X	X	600–729	4	13		X
Notoscopelus elongatus (Costa, 1844)		X	X	328–759		23		
Ophidion barbatum Linnaeus, 1758		X		122	3			
Pagellus bogaraveo (Brünnich, 1768)		X		342–446				X
Peristedion cataphractum (Linnaeus, 1758)	X	X	X	143–328	4	13		X
Phycis blennoides (Brünnich, 1768)	X	X	X	288–768	11	87		X
Polyacanthonotus rissoanus (De Filippi & Verany, 1857)			X	759		7		

Table A7. *Cont.*

	Area				Sampling method			
	SO	**AM**	**EB**	**Depth (m)**	**BT**	**GOC**	**RD**	**ROV**
Polyprion americanus (Bloch & Schneider, 1801)			X	802–813				X
Protogrammus alboranensis Fricke, Ordines, Farias & García-Ruiz, 2016		X	X	105–195	13		10	
Scorpaena elongata Cadenat, 1943		X		393–444		13		
Scorpaena loppei Cadenat, 1943		X		99			7	
Scorpaena scrofa Linnaeus, 1758		X	X	105–276				X
Serranus cabrilla (Linnaeus, 1758)		X	X	100–133				X
Stomias boa boa (Risso, 1810)		X	X	393–770		47		
Symbolophorus veranyi (Moreau, 1888)		X	X	393–756		10		
Symphurus ligulatus (Cocco, 1844)	X	X	X	600–732	3	20		X
Symphurus nigrescens Rafinesque, 1810	X	X	X	290–548	7	33		X
Symphurus sp. *		X	X	242–760				X
Synchiropus phaeton (Günther, 1861)	X	X	X	122–489	16	20		X
Trachurus picturatus (Bowdich, 1825)		X		237–600		20		
Trachurus trachurus (Linnaeus, 1758)		X		237–542		53		
Trachyrincus scabrus (Rafinesque, 1810)		X	X	631–754		13		
Trachyscorpia cristulata echinata (Köhler, 1896)			X	826				X
Trigla lyra Linnaeus, 1758		X	X	237–393	7	20		X
Triglidae *		X	X	107–169				X
Vinciguerria attenuata (Cocco, 1838)		X		459		7		

Appendix H

Table A8. SIMPER results of the assemblages (see codes in Figure 7) identified from multi-variant analysis of samples obtained with beam trawl, rock dredge, and experimental bottom trawl in the Ses Olives, Ausias March, and Emile Baudot seamounts and adjacent area of the Mallorca Channel (Balearic Islands, western Mediterranean), showing the average standardized biomass (B: g/500m^2), abundance (A: individuals/km^2) and occurrence (Occurr), the similarity (Sim), and the percentage contribution to the similarity (%Sim) of the main species or taxa contributing up to 90% of within-group similarity. Both abundance and biomass values were square root transformed.

Species	**B**	**Sim**	**%Sim**	**Σ%Sim**
BT-a (Sim: 24.0 %)				
Corallinaceae	4.62	2.47	10.07	10.07
Inachus dorsettensis	1.46	0.94	3.84	13.91
Poecillastra compressa	1.79	0.82	3.36	17.27
Ergasticus clouei	1.19	0.82	3.34	20.61
Gryphus vitreus	1.59	0.76	3.11	23.72
Anapagurus laevis	1.20	0.74	3.04	26.76

Table A8. *Cont.*

Species	B	Sim	%Sim	Σ%Sim
Distolambrus maltzami	1.01	0.73	2.99	29.74
Hexadella sp.	2.63	0.72	2.95	32.69
Dardanus arrosor	1.16	0.67	2.74	35.44
Cidaris cidaris	1.24	0.60	2.45	37.88
Peltaster placenta	1.21	0.59	2.42	40.30
Porifera sp. 1	1.50	0.56	2.3	42.61
Chelidonichthys cuculus	1.25	0.44	1.81	44.41
Pagurus prideaux	0.87	0.44	1.80	46.21
Pomatoceros triqueter	0.86	0.43	1.76	47.97
Ebalia tuberosa	0.86	0.41	1.69	49.66
Anseropoda placenta	0.73	0.41	1.67	51.34
Lophogaster typicus	0.67	0.39	1.58	52.92
Parthenopoides massena	0.82	0.39	1.58	54.5
Luidia sarsii	0.79	0.38	1.54	56.05
Eurynome aspera	0.73	0.37	1.51	57.56
Sclerasterias richardi	0.74	0.36	1.47	59.03
Chaetaster longipes	0.82	0.36	1.46	60.49
Chelonaplysilla psammophyla	1.11	0.34	1.40	61.90
Penares helleri	1.30	0.34	1.40	63.29
Argyrotheca chordata	1.19	0.34	1.37	64.67
Axinella spp.	0.94	0.32	1.31	65.97
Marthasterias glacialis	0.73	0.31	1.27	67.25
Pseudamussium clavatum	0.56	0.28	1.16	68.40
Ancorinidae spp.	1.10	0.28	1.14	69.54
Calappa granulata	1.02	0.27	1.10	70.64
Ebalia nux	0.70	0.26	1.06	71.70
Haliclona poecillastroides	0.96	0.26	1.04	72.75
Mergelia truncata	0.94	0.25	1.01	73.76
Monodaeus couchii	0.62	0.23	0.94	74.71
Macropipus tuberculatus	0.55	0.23	0.94	75.65
Gracilechinus acutus	0.51	0.21	0.84	76.49
Petrosia (Petrosia) raphida	1.02	0.20	0.83	77.32
Ranella olearium	0.81	0.19	0.77	78.09
Axinellidae	0.70	0.19	0.76	78.85
Calyx sp.	1.20	0.18	0.72	79.57
Hyalinoecia tubicola	0.81	0.17	0.69	80.26
Astrophorina sp. 2	0.88	0.16	0.65	80.91
Ebalia deshayesi	0.37	0.16	0.65	81.56
Ophiomyces grandis	0.49	0.15	0.60	82.17
Calliostoma granulatum	0.41	0.13	0.52	82.69
Polychaeta	0.42	0.13	0.51	83.20

Table A8. *Cont.*

Species	B	Sim	%Sim	Σ%Sim
Dragmatella aberrans	0.72	0.12	0.50	83.70
Ophiopsila aranea	0.35	0.12	0.47	84.17
Arnoglossus imperialis	0.49	0.11	0.46	84.64
Philine monterosati	0.32	0.11	0.45	85.09
Sepia elegans	0.41	0.11	0.44	85.53
Arnoglossus rueppelii	0.50	0.11	0.43	85.97
Parastichopus regalis	0.48	0.11	0.43	86.40
Diplecogaster bimaculata	0.35	0.10	0.42	86.81
Petrosia ficiformis	0.86	0.10	0.41	87.23
Desmacella inornata	0.66	0.10	0.39	87.61
Cuspidaria rostrata	0.33	0.09	0.38	88.00
Porifera sp. 2	0.83	0.09	0.38	88.38
Ophiura (Dictenophiura) carnea	0.25	0.09	0.38	88.75
Vulcanella aberrans	0.69	0.08	0.35	89.10
Lanice conchilega	0.43	0.08	0.34	89.44
Aphroditidae	0.30	0.08	0.21	89.78
Marginaster capreensis	0.43	0.08	0.34	90.11
BT-b (Sim: 21.9%)				
Lophogaster typicus	1.08	1.60	7.32	7.32
Ebalia nux	0.94	1.47	6.75	14.08
Desmacella inornata	1.38	1.35	6.18	20.25
Gryphus vitreus	1.58	1.12	5.14	25.39
Thenea muricata	0.92	1.02	4.66	30.05
Plesionika antigai	0.88	0.96	4.40	34.46
Ergasticus clouei	0.70	0.82	3.74	38.20
Ophiura (Dictenophiura) carnea	0.65	0.70	3.22	41.42
Desmacella annexa	0.69	0.50	2.30	43.72
Sepietta oweniana	0.68	0.44	2.03	45.75
Pseudostichopus occultatus	0.74	0.40	1.83	47.58
Monodaeus couchii	0.40	0.38	1.76	49.34
Parapenaeus longirostris	0.58	0.36	1.63	50.97
Plesionika martia	0.49	0.35	1.61	52.58
Antalis sp.	0.40	0.35	1.60	54.18
Ophiomyces grandis	0.54	0.34	1.58	55.75
Alpheus glaber	0.47	0.33	1.51	57.26
Chlorotocus crassicornis	0.49	0.32	1.47	58.74
Cuspidaria rostrata	0.31	0.32	1.47	60.21
Amphiura filiformis	0.38	0.31	1.40	61.61
Bathyarca philippiana	0.35	0.29	1.35	62.96
Helicolenus dactylopterus	0.66	0.28	1.26	64.22
Anapagurus laevis	0.33	0.26	1.20	65.42

Table A8. *Cont.*

Species	B	Sim	%Sim	Σ%Sim
Hyalinoecia tubicola	0.54	0.24	1.09	66.51
Polychaeta sp. 1	0.42	0.23	1.06	67.57
Lepidorhombus boscii	0.57	0.23	1.05	68.62
Luidia sarsii	0.36	0.22	1.01	69.63
Processa canaliculata	0.38	0.22	0.99	70.62
Poecillastra compressa	0.44	0.22	0.99	71.61
Bubaris sp.	0.50	0.20	0.94	72.55
Plesionika gigliolii	0.42	0.19	0.88	73.43
Porifera sp. 1	0.54	0.19	0.24	74.30
Munida speciosa	0.34	0.18	0.84	75.14
Plesionika heterocarpus	0.35	0.18	0.81	75.96
Gadiculus argenteus	0.35	0.17	0.76	76.72
Cymonomus granulatus	0.23	0.16	0.73	77.45
Ophiocten abyssicolum	0.30	0.16	0.72	78.17
Solenocera membranacea	0.30	0.15	0.70	78.87
Aegaeon lacazei	0.27	0.15	0.68	79.55
Pagurus alatus	0.23	0.14	0.66	80.21
Abra longicallus	0.21	0.14	0.63	80.84
Synchiropus phaeton	0.35	0.13	0.59	81.43
Coelorinchus caelorhincus	0.29	0.13	0.58	82.02
Dragmatella aberrans	0.37	0.13	0.58	82.60
Philocheras echinulatus	0.24	0.12	0.57	83.17
Calliostoma granulatum	0.24	0.12	0.56	83.73
Sipunculidae sp. 1	0.25	0.12	0.25	84.28
Sclerasterias richardi	0.23	0.12	0.55	84.83
Cidaris	0.28	0.12	0.55	85.38
Hamacantha (Vomerula) sp.	0.30	0.12	0.55	85.92
Inachus dorsettensis	0.25	0.11	0.51	86.44
Sipunculidae sp. 2	0.33	0.11	0.51	86.94
Polychaeta sp 2	0.23	0.11	0.49	87.43
Euspira fusca	0.29	0.11	0.48	87.92
Processa nouveli	0.23	0.10	0.46	88.38
Anthozoa	0.22	0.10	0.46	88.84
Arnoglossus rueppelii	0.29	0.10	0.44	89.28
Chlorophthalmus agassizi	0.31	0.10	0.44	89.72
Aporrhais serresiana	0.29	0.09	0.42	90.14
BT-c (Sim: 33.4%)				
Geryon longipes	1.83	6.31	18.91	18.91
Polycheles typhlops	1.38	5.56	16.67	35.58
Calocaris macandreae	1.20	4.57	13.70	49.28
Plesionika acanthonotus	0.78	2.50	7.48	56.76

Table A8. *Cont.*

Species	B	Sim	%Sim	Σ%Sim
Antalis sp	0.68	1.81	5.41	62.18
Munida perarmata	0.67	1.61	4.84	67.01
Monodaeus couchii	0.49	1.18	3.52	70.53
Eusergestes arcticus	0.45	1.16	3.48	74.01
Thenea muricata	0.56	1.00	3.01	77.02
Nezumia aequalis	0.67	0.96	2.87	79.89
Isidella elongata	0.89	0.79	2.36	82.25
Gryphus vitreus	0.68	0.76	2.26	84.51
Plesionika martia	0.57	0.70	2.09	86.60
Gennadas elegans	0.29	0.55	1.66	88.26
Abra longicallus	0.32	0.45	1.34	89.60
Robustosergia robusta	0.30	0.43	1.30	90.90
RD-a (Sim: 21.84%)				
Corallinaceae	0.95	7.40	30.45	30.45
Megerlia truncata	0.90	5.63	23.15	53.60
Argyrotheca cordata	0.75	3.97	16.34	69.94
Porifera	0.65	2.18	8.98	78.92
Axinella spp.	0.40	0.80	3.27	82.20
Hyalinoecia tubicola	0.30	0.52	2.16	84.35
Cnidaria	0.30	0.34	1.41	85.76
Palmophyllum crassum	0.25	0.26	1.07	86.83
Jaspis spp.	0.25	0.20	0.84	87.67
Bebryce mollis	0.20	0.19	0.80	88.47
Viminella sp.	0.15	0.19	0.79	89.26
Monodaeus couchii	0.20	0.15	0.62	90.60
RD-b (Sim: 15.35%)				
Plesionika gigliolii	0.67	5.26	34.29	34.29
Asperarca nodulosa	0.58	4.74	30.87	65.16
Plesionika antigai	0.33	1.10	7.18	72.34
Ebalia nux	0.33	0.79	5.13	77.47
Plesionika narval	0.25	0.66	4.28	81.74
Bathyarca philippiana	0.25	0.61	3.95	85.69
Argyrotheca chordata	0.25	0.45	2.91	88.60
Ophiura (Dictenophiura) carnea	0.25	0.31	2.04	90.64
D-c (Sim: 23.63%)				
Porifera	1.00	12.41	52.54	52.54
Asperarca nodulosa	0.60	2.72	11.50	64.04
Callyspongiidae	0.50	1.76	7.46	71.50
Haliclona poecillastroides	0.50	1.65	7.00	78.50
Hamacantha sp.	0.40	1.37	5.80	84.29
Jaspis spp.	0.40	1.10	4.67	88.96
Cnidaria	0.30	0.50	2.13	91.09

Table A8. *Cont.*

Species	B	Sim	%Sim	Σ%Sim
GOC-a (Sim: 57.07%)				
Plesionika acanthonotus	17.8	7.5	12.2	12.2
Plesionika martia	16.25	6.31	10.26	22.45
Nezumia aequalis	18.29	6.16	10.01	32.46
Geryon longipes	16.05	6.01	9.77	42.23
Aristeus antennatus	18.47	5.38	8.75	50.99
Galeus melastomus	19.32	5.25	8.53	59.52
Hymenocephalus italicus	12.48	4.57	7.44	66.96
Polycheles typhlops	8.88	3.79	6.15	73.11
Robustosergia robusta	8.87	3.08	5.01	78.11
Phycis blennoides	6.79	2.6	4.22	82.34
Hoplostethus mediterraneus	8.65	2.46	4	86.33
Pasiphaea multidentata	7.68	1.69	2.74	89.07
Gennadas elegans	4.86	1.24	2.02	91.09
GOC-b (Sim: 52.07%)				
Plesionika martia	37.10	6.77	11.94	11.94
Phycis blennoides	30.66	5.48	9.67	21.62
Hymenocephalus italicus	34.49	5.20	9.17	30.78
Pasiphaea sivado	30.24	4.10	7.23	38.02
Nephrops norvegicus	16.57	3.74	6.6	44.62
Hoplostethus mediterraneus	29.46	3.50	6.17	50.78
Helicolenus dactylopterus	17.77	3.42	6.04	56.82
Parapenaeus longirostris	31.43	2.94	5.19	62.01
Processa canaliculata	14.44	2.84	5.01	67.03
Chlorotocus crassicornis	12.31	2.47	4.36	71.39
Munida perarmata	10.57	1.94	3.42	74.81
Gaidropsarus biscayensis	8.12	1.80	3.17	77.98
Coelorinchus caelorhincus	20.71	1.43	2.52	80.50
Gadiculus argenteus	22.21	1.43	2.52	83.02
Lepidorhombus boscii	11.13	1.24	2.18	85.20
Calocaris macandreae	9.66	1.04	1.83	87.03
Sepietta oweniana	18.15	1.01	1.78	88.81
Merluccius merluccius	8.28	1.01	1.78	90.59
GOC-c (Sim: 53.4%)				
Gadiculus argenteus	103.87	10.3	19.28	19.28
Chlorophthalmus agassizi	67.98	7.24	13.55	32.83
Coelorinchus caelorhincus	87.45	5.85	10.95	43.78
Parapenaeus longirostris	45.7	5.16	9.66	53.44
Scyliorhinus canicula	37.35	3.85	7.21	60.65
Sepietta oweniana	43.88	3.74	7	67.66
Helicolenus dactylopterus	66.52	3.58	6.7	74.36

Table A8. *Cont.*

Species	B	Sim	%Sim	Σ%Sim
Lepidorhombus boscii	20.56	1.79	3.35	77.71
Synchiropus phaeton	32.23	1.64	3.07	80.78
Galeus melastomus	30.43	1.3	2.43	83.21
Thenea muricata	10.29	1.23	2.31	85.52
Plesionika heterocarpus	25.14	1.09	2.04	87.56
Illex coindetii	9.23	1.02	1.91	89.48
Desmacella annexa	22.93	0.82	1.54	91.01

References

1. Coll, M.; Piroddi, C.; Steenbeek, J.; Kaschner, K.; Ben Rais Lasram, F.; Aguzzi, J.; Ballesteros, E.; Bianchi, C.N.; Corbera, J.; Dailianis, T.; et al. The Biodiversity of the Mediterranean Sea: Estimates, Patterns, and Threats. *PLoS ONE* **2010**, *5*, e11842. [CrossRef]
2. Borja, Á.; Elliott, M.; Carstensen, J.; Heiskanen, A.-S.; van de Bund, W. Marine management—Towards an integrated implementation of the European Marine Strategy Framework and the Water Framework Directives. *Mar. Pollut. Bull.* **2010**, *60*, 2175–2186. [CrossRef]
3. Clark, M.R.; Schlacher, T.A.; Rowden, A.A.; Stocks, K.I.; Consalvey, M. Science Priorities for Seamounts: Research Links to Conservation and Management. *PLoS ONE* **2012**, *7*, e29232. [CrossRef] [PubMed]
4. Palomino, D.; Vázquez, J.-T.; Ercilla, G.; Alonso, B.; López-González, N.; Díaz-Del-Río, V. Interaction between seabed morphology and water masses around the seamounts on the Motril Marginal Plateau (Alboran Sea, Western Mediterranean). *Geo-Mar. Lett.* **2011**, *31*, 465–479. [CrossRef]
5. Würtz, M.; Rovere, M.; Bo, M. Introducing the Mediterranean Seamount Atlas: General aspects. In *Atlas of the Mediterranean Seamounts and Seamount-like Structures*; Würtz, M., Rovere, M., Eds.; IUCN: Gland, Switzerland; Málaga, Spain, 2015; pp. 11–19.
6. *Report of the Technical Consultation on International Guidelines for the Management of Deep-Sea Fisheries in the High Seas*; FAO: Rome, Italy, 2009.
7. Gomez-Ballesteros, M.; Vazquez, J.T.; Palomino, D.; Rovere, M.; Bo, M.; Alessi, J.; Fiori, C.; Würtz, M. Seamounts and Seamount-like Structures of the Western Mediterranean. In *Atlas of the Mediterranean Seamounts and Seamount-like Structures*; Würtz, M., Rovere, M., Eds.; IUCN: Gland, Switzerland; Málaga, Spain, 2015; pp. 59–109.
8. Vazquez, J.T.; Alonso, B.; Fernandez-Puga, M.C.; Gomez-Ballesteros, M.; Iglesias, J.; Palomino, D.; Roque, C.; Ercilla, G.; Díaz del Río, V. Seamounts along the Iberian continental margins. *Bol. Geol. Min.* **2015**, *126*, 483–514.
9. Rodríguez, M.G.; Esteban, A. On the biology and fishery of Aristeus antennatus (Risso, 1816), (Decapoda, Dendrobranchiata) in the Ibiza Channel (Balearic Islands, Spain). *Sci. Mar.* **1999**, *63*, 27–37. [CrossRef]
10. Rodríguez, M.G.; Esteban, A.; Gil, J.L.P. Considerations on the biology of Plesionika edwardsi (Brandt, 1851) (Decapoda, Caridea, Pandalidae) from experimental trap catches in the Spanish western Mediterranean Sea. *Sci. Mar.* **2000**, *64*, 369–379. [CrossRef]
11. Acosta, J.; Muñoz, A.; Herranz, P.; Palomo, C.; Ballesteros, M.; Vaquero, M.; Uchupi, E. Geodynamics of the Emile Baudot Escarpment and the Balearic Promontory, western Mediterranean. *Mar. Pet. Geol.* **2001**, *18*, 349–369. [CrossRef]
12. Acosta, J.; Canals, M.; Carbo, A.; Martín, A.M.; Urgeles, R.; Muñoz-Martín, A.; Uchupi, E. Sea floor morphology and Plio-Quaternary sedimentary cover of the Mallorca Channel, Balearic Islands, western Mediterranean. *Mar. Geol.* **2004**, *206*, 165–179. [CrossRef]
13. *Montañas Submarinas de Las Islas Baleares: Canal de Mallorca. Propuesta de Protección Para Ausias March, Emile Baudot y Ses Olives*; OCEANA: Washington, DC, USA, 2011; p. 60, Unpublished work; Available online: https://oceana.org/sites/default/files/reports/OCEANA_Montanas_submarinas_baleares_Canal_mallorca_2011_0.pdf (accessed on 15 December 2021).
14. Expedition 2014 Balearic Islands Cabrera National Park and Mallorca Channel Seamounts; OCEANA: Washington, DC, USA. 2015, p. 21, Unpublished work. Available online: https://europe.oceana.org/sites/default/files/oceana_expedition2014_balearic_islands_eng_11.pdf (accessed on 20 December 2021).
15. Aguilar, R.; Correa, M.L.; Calcinai, B.; Pastor, X.; De La Torriente, A.; Garcia, S. First records of Asbestopluma hypogea Vacelet and Boury-Esnault, 1996 (Porifera, Demospongiae Cladorhizidae) on seamounts and in bathyal settings of the Mediterranean Sea. *Zootaxa* **2011**, *2925*, 33–40. [CrossRef]
16. Maldonado, M.; Aguilar, R.; Blanco, J.; Garcia, S.; Serrano, A.; Punzón, A. Aggregated Clumps of Lithistid Sponges: A Singular, Reef-Like Bathyal Habitat with Relevant Paleontological Connections. *PLoS ONE* **2015**, *10*, e0125378. [CrossRef]
17. Mastrototaro, F.; Chimienti, G.; Acosta, J.; Blanco, J.; Garcia, S.; Rivera, J.; Aguilar, R. Isidella elongata (Cnidaria: Alcyonacea) facies in the western Mediterranean Sea: Visual surveys and descriptions of its ecological role. *Eur. Zool. J.* **2017**, *84*, 209–225. [CrossRef]
18. Marín, P.; Aguilar, R.; Garcia, S.; Fournier, N. A Complementary Approach for the Mediterranean N2000 in Open and Deep Sea. 2011; p. 17, Unpublished work.

19. Acosta, J.; Canals, M.; López-Martínez, J.; Muñoz, A.; Herranz, P.; Urgeles, R.; Palomo, C.; Casamor, J.L. The Balearic Promontory geomorphology (western Mediterranean): Morphostructure and active processes. *Geomorphol.* **2003**, *49*, 177–204. [CrossRef]
20. Lehucher, P.M.; Beautier, L.; Chartier, M.; Martel, F.; Mortier, L.; Brehmer, P.; Millot, C.; Alberola, C.; Benzhora, M.; Taupier-Letage, I.; et al. Progress from 1989 to 1992 in understanding the circulation of the Western Med-iterranean Sea. *Oceanol. Acta* **1995**, *18*, 255–271.
21. Pinot, J.-M.; López-Jurado, J.; Riera, M. The CANALES experiment (1996-1998). Interannual, seasonal, and mesoscale variability of the circulation in the Balearic Channels. *Prog. Oceanogr.* **2002**, *55*, 335–370. [CrossRef]
22. Mertens, C.; Schott, F. Interannual Variability of Deep-Water Formation in the Northwestern Mediterranean. *J. Phys. Oceanogr.* **1998**, *28*, 1410–1424. [CrossRef]
23. Lafuente, J.; Jurado, J.L.L.; Lucaya, N.; Yañez, M.V.; Garcia, J. Circulation of water masses through the Ibiza Channel. *Oceanol. Acta* **1995**, *18*, 245–254.
24. Millot, C. Circulation in the Western Mediterranean Sea. *J. Mar. Syst.* **1999**, *20*, 423–442. [CrossRef]
25. Monserrat, S.; López-Jurado, J.; Marcos, M. A mesoscale index to describe the regional circulation around the Balearic Islands. *J. Mar. Syst.* **2008**, *71*, 413–420. [CrossRef]
26. Estr Estrada, M. Primary production in the northwestern Mediterranean. *Sci. Mar.* **1996**, *60* (Suppl. 2), 55–64.
27. Bosc, E.; Bricaud, A.; Antoine, D. Seasonal and interannual variability in algal biomass and primary production in the Mediterranean Sea, as derived from 4 years of SeaWiFS observations. *Glob. Biogeochem. Cycles* **2004**, *18*. [CrossRef]
28. Pinot, J.-M.; Tintoré, J.; Gomis, D. Multivariate analysis of the surface circulation in the Balearic Sea. *Prog. Oceanogr.* **1995**, *36*, 343–376. [CrossRef]
29. De Puelles, M.L.F.; Valencia, J.; Jansá, J.; Morillas, A. Hydrographical characteristics and zooplankton distribution in the Mallorca channel (Western Mediterranean): Spring 2001. *ICES J. Mar. Sci.* **2004**, *61*, 654–666. [CrossRef]
30. López-Jurado, J.; Marcos, M.; Monserrat, S. Hydrographic conditions affecting two fishing grounds of Mallorca island (Western Mediterranean): During the IDEA Project (2003–2004). *J. Mar. Syst.* **2008**, *71*, 303–315. [CrossRef]
31. Maynou, F.; Cartes, J.E. Community structure of bathyal decapod crustaceans off south-west Balearic Islands (western Mediterranean): Seasonality and regional patterns in zonation. *J. Mar. Biol. Assoc. U. K.* **2000**, *80*, 789–798. [CrossRef]
32. Cartes, J.; Maynou, F.; Morales-Nin, B.; Massutí, E.; Moranta, J. Trophic structure of a bathyal benthopelagic boundary layer community south of the Balearic Islands (southwestern Mediterranean). *Mar. Ecol. Prog. Ser.* **2001**, *215*, 23–35. [CrossRef]
33. Rueda, L.; Moranta, J.; Abelló, P.; Balbin, R.; Barbera, C.; De Puelles, M.F.; Olivar, M.; Ordines, F.; Ramon, M.; Torres, A.; et al. Body condition of the deep water demersal resources at two adjacent oligotrophic areas of the western Mediterranean and the influence of the environmental features. *J. Mar. Syst.* **2014**, *138*, 194–202. [CrossRef]
34. Carbonell, A.; Lloret, J.; Demestre, M. Relationship between condition and recruitment success of red shrimp (Aristeus antennatus) in the Balearic Sea (Northwestern Mediterranean). *J. Mar. Syst.* **2008**, *71*, 403–412. [CrossRef]
35. Massutí, E.; Monserrat, S.; Oliver, P.; Moranta, J.; López-Jurado, J.L.; Marcos, M.; Hidalgo, M.; Guijarro, B.; Carbonell, A.; Pereda, P. The influence of oceanographic scenarios on the population dynamics of demersal resources in the western Mediterranean: Hypothesis for hake and red shrimp off Balearic Islands. *J. Mar. Syst.* **2008**, *71*, 421–438. [CrossRef]
36. Barcelona, S.G.; De Urbina, J.M.O.; De La Serna, J.M.; Alot, E.; Macías, D. Seabird bycatch in Spanish Mediterranean large pelagic longline fisheries, 2000–2008. *Aquat. Living Resour.* **2010**, *23*, 363–371. [CrossRef]
37. Gordoa, A.; Rouyer, T.; Ortiz, M. Review and update of the French and Spanish purse seine size at catch for the Mediterranean bluefin tuna fisheries 1970–2010. *ICCAT Recl. Doc. Sci./Collect. Vol. Sci. Pap.* **2017**, *75*, 1622–1633. Available online: https://archimer.ifremer.fr/doc/00490/60191/ (accessed on 31 October 2021).
38. Jennings, S.; Lancaster, J.; Woolmer, A.; Cotter, J. Distribution, diversity and abundance of epibenthic fauna in the North Sea. *J. Mar. Biol. Assoc. U. K.* **1999**, *79*, 385–399. [CrossRef]
39. Reiss, H.; Kröncke, I.; Ehrich, S. Estimating the catching efficiency of a 2-m beam trawl for sampling epifauna by removal experiments. *ICES J. Mar. Sci.* **2006**, *63*, 1453–1464. [CrossRef]
40. Bertrand, J.A.; Gil de Sola, L.; Papaconstantinou, C.; Relini, G.; Souplet, A. The general specifications of the MEDITS surveys. *Sci. Mar.* **2002**, *66*, 9–17. [CrossRef]
41. Spedicato, M.T.; Massutí, E.; Mérigot, B.; Tserpes, G.; Jadaud, A.; Relini, G. The MEDITS trawl survey specifications in an ecosystem approach to fishery management. *Sci. Mar.* **2019**, *83*, 9–20. [CrossRef]
42. Dremière, P.Y.; Fiorentini, L.; Cosimi, G.; Leonori, I.; Sala, A.; Spagnolo, A. Escapement from the main body of the bottom trawl used for the Mediterranean international trawl survey (MEDITS). *Aquat. Living Resour.* **1999**, *12*, 207–217. [CrossRef]
43. Fiorentini, L.; Dremière, P.-Y.; Leonori, I.; Sala, A.; Palumbo, V. Efficiency of the bottom trawl used for the Mediterranean international trawl survey (MEDITS)Efficacité du chalut de fond utilisé pour le programme international d'évaluation des ressources halieutiques de Méditerranée (MEDITS). *Aquat. Living Resour.* **1999**, *12*, 187–205. [CrossRef]
44. Guijarro, B. Population Dynamics and Assessment of Exploited Deep Water Decapods off Balearic Islands (Western Mediterra-Nean): From Single to Multi-Species Approach. Ph.D. Thesis, University of the Balearic Islands, Palma, Spain, 2012. Available online: http://www.repositorio.ieo.es/e-ieo/handle/10508/10096 (accessed on 15 December 2021).
45. Hamilton, E.L. Geoacoustic modeling of the sea floor. *J. Acoust. Soc. Am.* **1980**, *68*, 1313–1340. [CrossRef]
46. Gafeira, J.; Long, D.; Diaz-Doce, D. Semi-automated characterisation of seabed pockmarks in the central North Sea. *Near Surf. Geophys.* **2012**, *10*, 301–312. [CrossRef]

47. Folk, R.L. The Distinction between Grain Size and Mineral Composition in Sedimentary-Rock Nomenclature. *J. Geol.* **1954**, *62*, 344–359. [CrossRef]
48. Heiri, O.; Lotter, A.F.; Lemcke, G. Loss on ignition as a method for estimating organic and carbonate content in sediments: Reproducibility and comparability of results. *J. Paleolimnol.* **2001**, *25*, 101–110. [CrossRef]
49. Sardà, F.; Calafat, A.; Flexas, M.M.; Tselepides, A.; Canals, M.; Espino, M.; Tursi, A. An introduction to Mediterranean deep-sea biology. *Sci. Mar.* **2004**, *68*, 7–38. [CrossRef]
50. Clarke, K.R.; Gorley, R.N. *PRIMER v6 User Manual/Tutorial (Plymouth Routines in Multivariate Ecological Research)*; PRI-MER-E: Plymouth, Auckland, New Zealand, 2006; p. 192.
51. Farriols, M.T.; Ordines, F.; Hidalgo, M.; Guijarro, B.; Massutí, E. N90 index: A new approach to biodiversity based on similarity and sensitive to direct and indirect fishing impact. *Ecol. Indic.* **2015**, *52*, 245–255. [CrossRef]
52. Farriols, M.T.; Ordines, F.; Somerfield, P.J.; Pasqual, C.; Hidalgo, M.; Guijarro, B.; Massutí, E. Bottom trawl impacts on Mediterranean demersal fish diversity: Not so obvious or are we too late? *Cont. Shelf Res.* **2017**, *137*, 84–102. [CrossRef]
53. Ordines, F.; Ramón, M.; Rivera, J.; Rodríguez-Prieto, C.; Farriols, M.T.; Guijarro, B.; Pasqual, C.; Massutí, E. Why long term trawled red algae beds off Balearic Islands (western Mediterranean) still persist? *Reg. Stud. Mar. Sci.* **2017**, *15*, 39–49. [CrossRef]
54. Farriols, M.T.; Ordines, F.; Massutí, E. N90, a Diversity Index Sensitive to Variations in Beta Diversity Components. *Diversity* **2021**, *13*, 489. [CrossRef]
55. Templado, J.; Ballesteros, E.; Galparsoro, I.; Borja, A.; Serrano, A.; Martín, L.; Brito, A. Inventario Español de Hábitats y Especies Marinos. In *Guía Interpretativa: Inventario Español de Hábitats Marinos*; Ministerio de Agricultura, Alimentación y Medio Ambiente (España): Madrid, Spain, 2012.
56. Gerovasileiou, V.; Akel, E.K.; Akyol, O.K.A.N.; Alongi, G.; Azevedo, F.; Babali, N.; Bakiu, R.; Bariche, M.; Bennoui, A.; Castriota, L.; et al. New Mediterranean Biodiversity Records (July, 2017). *Mediterr. Mar. Sci.* **2017**, *18*, 355–384. [CrossRef]
57. Domínguez, M.; Fontán, A.; Rivera, J.; Ramón, M. *Informe proyecto DRAGONSAL: Caracterización del ecosistema bentónico de la plataforma costera del área comprendida entre Sa Dragonera, Cabrera y el Cap de Ses Salines (Mallorca), Convenio específico de colaboración entre la Conselleria d'Agricultura*; Medi Ambient i Territori de les Illes Balears y el Instituto Español de Oceanografía: Palma, Spain, 2013; Unpublished work.
58. Moranta, J.; Barberá, C.; Druet, M.; Zaragoza, N. *Caracterización Ecológica de La Plataforma Continental (50–100 m) del Canal de Menorca, Informe Final LIFE+ INDEMARES (LIFE07/NAT/E/000732)*; Instituto de Ciencias del Mar–CSIC: Barcelona, Spain, 2014; Unpublished work.
59. Requena, S.; Gili, J.M. Caracterización ecológica del área marina del Canal de Menorca: Zonas profundas y semiprofundas (100–400 m), Informe Final LIFE+ INDEMARES (LIFE07/NAT/E/000732). 2014. Unpublished work. Available online: https://www.indemares.es/sites/default/files/informe_final_canal_de_menorca_csic.pdf (accessed on 15 December 2021).
60. Guijarro, B.; Ordines, F.; Pasqual, C.; Valls, M.; Quetglas, A.; Massutí, E. La pesca de ròssec al voltant de l'arxipèlag de Cabrera. In *Arxipèlag de Cabrera: Història Natural*; Grau, A.M., Fornós, J.J., Mateu, G., Oliver, P.A., Terrasa, B., Eds.; Monogr Soc Hist Nat Balears: Palma, Spain, 2020; Volume 30, pp. 375–391.
61. Roberts, J.M.; Wheeler, A.J.; Freiwald, A. Reefs of the Deep: The Biology and Geology of Cold-Water Coral Ecosystems. *Science* **2006**, *312*, 543–547. [CrossRef] [PubMed]
62. Turner, D.L.; Jarrard, R.D.; Forbes, R.B. Geochronology and origin of the Pratt-Welker Seamount Chain, Gulf of Alaska: A new pole of rotation for the Pacific Plate. *J. Geophys. Res. Space Phys.* **1980**, *85*, 6547–6556. [CrossRef]
63. Just, J.; Hübscher, C.; Betzler, C.; Lüdmann, T.; Reicherter, K. Erosion of continental margins in the Western Mediterranean due to sea-level stagnancy during the Messinian Salinity Crisis. *Geo-Mar. Lett.* **2010**, *31*, 51–64. [CrossRef]
64. Acosta, J. El Promontorio Balear: Morfología Submarina Y Recubrimiento Sedimentario. *Ph.D. Thesis*; University of Barcelona: Barcelona, Spain, 2005. Available online: https://dialnet.unirioja.es/servlet/tesis?codigo=234793&info=resumen&idioma=SPA (accessed on 30 July 2021).
65. Iglesias, J.; Ercilla, G.; García-Gil, S.; Judd, A.G. Pockforms: An evaluation of pockmark-like seabed features on the Landes Plateau, Bay of Biscay. *Geo-Mar. Lett.* **2009**, *30*, 207–219. [CrossRef]
66. Acosta, J.; Muñoz, A.; Herranz, P.; Palomo, C.; Ballesteros, M.; Vaquero, M.; Uchupi, E. Pockmarks in the Ibiza Channel and western end of the Balearic Promontory (western Mediterranean) revealed by multibeam mapping. *Geo-Mar. Lett.* **2001**, *21*, 123–130. [CrossRef]
67. Hovland, M.; Heggland, R.; De Vries, M.; Tjelta, T. Unit-pockmarks and their potential significance for predicting fluid flow. *Mar. Pet. Geol.* **2010**, *27*, 1190–1199. [CrossRef]
68. Plaza-Faverola, A.; Bünz, S.; Mienert, J. Repeated fluid expulsion through sub-seabed chimneys offshore Norway in response to glacial cycles. *Earth Planet. Sci. Lett.* **2011**, *305*, 297–308. [CrossRef]
69. Díaz, J.A.; Ramírez-Amaro, S.; Ordines, F. Sponges of Western Mediterranean seamounts: New genera, new species and new records. *PeerJ* **2021**, *9*, e11879. [CrossRef]
70. Ordines, F.; Ramírez-Amaro, S.; Fernandez-Arcaya, U.; Marco-Herrero, E.; Massutí, E. First occurrence of an Ophiohelidae species in the Mediterranean: The high abundances of Ophiomyces grandis from the Mallorca Channel seamounts. *J. Mar. Biol. Assoc. U. K.* **2019**, *99*, 1817–1823. [CrossRef]
71. Forest, J. Campagnes du Professeur Lacaze-Duthiers aux Baleares Juin 1953 et Aout 1954 Crustaces Decapodes. *Vie et Milieu* **1965**, *16*, 325–413. Available online: https://eurekamag.com/research/038/039/038039972.php (accessed on 15 December 2021).

72. Duris, Z. Penaeid and caridean shrimps collected during Soviet expeditions 1974-1980 to the Mediterranean area. In Proceedings of the 6th Col-loquium Crustacea Decapoda Mediterranea, Florence, Italy, 12–15 September 1996; pp. 34–35.
73. Abello, P.; Carbonell, A.; Torres, P. Biogeography of epibenthic crustaceans on the shelf and upper slope off the Iberian Peninsula Mediterranean coasts: Implications for the establishment of natural management areas. *Sci. Mar.* **2002**, *66*. [CrossRef]
74. Zariquiey Alvarez, R. Crustaceos Decapodos Ibericos. *Inv. Pesq.* **1968**, *32*, 1–83.
75. Garcia-Raso, J.E. Crustacea Decapoda (Excl. Sergestidae) From Ibero-Moroccan Waters. Results of Balgim-84 Expedition. *Bull. Mar. Sci.* **1996**, *58*, 730–752.
76. Box, A. Ecología de Caulerpales: Fauna y Biomarcadores. Ph.D. Thesis, University of the Balearic Islands, Palma, Spain, 2008.
77. Mateo-Ramírez, Á.; Urra, J.; Rueda, J.L.; Marina, P.; Raso, J.G. Decapod assemblages associated with shallow macroalgal communities in the northwestern Alboran Sea: Microhabitat use and temporal variability. *J. Sea Res.* **2018**, *135*, 84–94. [CrossRef]
78. Noël, P.Y. Clé préliminaire d'identification des Crustacea Decapoda de France et des principales autres espèces d'Europe. Secrétariat de la Faune et de la Flore. Muséum National d'Histoire Naturelle, Paris. *Collect. Patrim. Nat.* **1992**, *9*, 1–145.
79. Quetglas, A.; Ordines, F.; Gonzalez, M.; Zaragoza, N.; Mallol, S.; Valls, M.; De Mesa, A. Uncommon pelagic and deep-sea cephalopods in the Mediterranean: New data and literature review. *Mediterr. Mar. Sci.* **2013**, *14*, 69. [CrossRef]
80. Corals on seamounts. In *Seamounts: Ecology, Fisheries & Conservation*; Pitcher, T.J.; Morato, T.; Hart, P.J.B.; Clark, M.R.; Haggan, N.; Santos, R.S. (Eds.) Blackwell Publishing Ltd.: Oxford, UK, 2007; pp. 1–527. [CrossRef]
81. Williams, A.; Althaus, F.; Schlacher, T.A. Towed camera imagery and benthic sled catches provide different views of seamount benthic diversity. *Limnol. Oceanogr. Methods* **2015**, *13*, 62–73. [CrossRef]
82. Massutí, E.; Renones, O.; Carbonell, A. À propos de la présence de Trachyscorpia cristulata echinata (Koehler, 1896) en Méditerranée nord-occidentale. *Cybium* **1993**, *17*, 223–228.
83. Merella, P.; Alemany, F.; Grau, A. Nuevos datos sobre la presencia de Pontinus kuhlii (Bowdich, 1825) (Osteichthyes: Scorpaenidae) en el Mediterráneo Occidental. *Sci. Mar.* **1998**, *62*, 133–208. [CrossRef]
84. McClain, C.R.; Lundsten, L. Assemblage structure is related to slope and depth on a deep offshore Pacific seamount chain. *Mar. Ecol.* **2014**, *36*, 210–220. [CrossRef]
85. Du Preez, C.; Curtis, J.M.R.; Clarke, M.E. The Structure and Distribution of Benthic Communities on a Shallow Seamount (Cobb Seamount, Northeast Pacific Ocean). *PLoS ONE* **2016**, *11*, e0165513. [CrossRef]
86. Oliver, P.A. Los Recursos Pesqueros del Mediterráneo. Primera Parte: Mediterráneo Occidental. *Stud. Rev. GFCM* **1983**, *59*, 1–141.
87. Lozano, P.; Rueda, J.L.; Gallardo-Núñez, M.; Farias, C.; Urra, J.; Vila, Y.; Lopez-Gonzalez, N.; Palomino, D.; Sánchez-Guillamón, O.; Vázquez, J.T.; et al. Habitat distribution and associated biota in different geomorphic features within a fluid venting area of the Gulf of Cádiz (Southwestern Iberian Peninsula, Northeast Atlantic Ocean). In *Seafloor Geomorphology as Benthic Habitat*; Elsevier BV: Amsterdam, The Netherlands, 2020; pp. 847–861.
88. Palanques, A.; Guillén, J.; Puig, P. Impact of bottom trawling on water turbidity and muddy sediment of an unfished continental shelf. *Limnol. Oceanogr.* **2001**, *46*, 1100–1110. [CrossRef]
89. Puig, P.; de Madron, X.D.; Salat, J.; Schroeder, K.; Martín, J.; Karageorgis, A.P.; Palanques, A.; Roullier, F.; Lopez-Jurado, J.L.; Emelianov, M.; et al. Thick bottom nepheloid layers in the western Mediterranean generated by deep dense shelf water cascading. *Prog. Oceanogr.* **2013**, *111*, 1–23. [CrossRef]
90. Martin, J.; Puig, P.; Palanques, A.; Giamportone, A. Commercial bottom trawling as a driver of sediment dynamics and deep seascape evolution in the Anthropocene. *Anthropocene* **2014**, *7*, 1–15. [CrossRef]
91. Kaiser, M.J.; Collie, J.S.; Hall, S.J.; Jennings, S.; Poiner, I.R. Modification of marine habitats by trawling activities: Prognosis and solutions. *Fish Fish.* **2002**, *3*, 114–136. [CrossRef]
92. Clark, M.R.; Althaus, F.; Schlacher, T.; Williams, A.; Bowden, D.A.; Rowden, A. The impacts of deep-sea fisheries on benthic communities: A review. *ICES J. Mar. Sci.* **2016**, *73*, i51–i69. [CrossRef]
93. Scientific, Technical and Economic Committee for Fisheries Sub-Group Meeting on Sensitive and Essential Fish Habitats in the Mediterranean Sea (STECF/SGMED-06-01). 2006, p. 48, Unpublisher work. Available online: https://stecf.jrc.ec.europa.eu/documents/43805/122927/07-06_SG-MOS+07-02+-+Evaluation+of+Closed+Areas.pdf (accessed on 15 December 2021).
94. Bo, M.; Numa, C.; Otero, M.D.M.; Orejas, C.; Garrabou, J.; Cerrano, C.; Kružić, P.; Antoniadou, C.; Aguilar, R.; Kipson, S.; et al. Overview of the conservation status of Mediterranean anthozoa. In *Overview of the Conservation Status of Mediterranean Anthozoa*; IUCN: Málaga, Spain, 2017; p. 73. [CrossRef]
95. Finucci, B.; Bineesh, K.; Cotton, C.; Dharmadi, D.; Kulka, D.; Neat, F.; Pacoureau, N.; Rigby, C.; Tanaka, S.; Walker, T. Iucn Centrophorus uyato. In *IUCN Red List of Threatened Species*; IUCN: Málaga, Spain, 2019.
96. Barberá, C.; Moranta, J.; Ordines, F.; Ramón, M.; De Mesa, A.; Díaz-Valdés, M.; Grau, A.M.; Massutí, E. Biodiversity and habitat mapping of Menorca Channel (western Mediterranean): Implications for conservation. *Biodivers. Conserv.* **2012**, *21*, 701–728. [CrossRef]
97. Grinyó, J.; Gori, A.; Ambroso, S.; Purroy, A.; Calatayud, C.; Dominguez-Carrió, C.; Coppari, M.; Iacono, C.L.; López-González, P.J.; Gili, J.-M. Diversity, distribution and population size structure of deep Mediterranean gorgonian assemblages (Menorca Channel, Western Mediterranean Sea). *Prog. Oceanogr.* **2016**, *145*, 42–56. [CrossRef]
98. Grinyó, J.; Garriga, A.; Soler-Membrives, A.; Santín, A.; Ambroso, S.; López-González, P.J.; Díaz, D. Soft corals assemblages in deep environments of the Menorca Channel (Western Mediterranean Sea). *Prog. Oceanogr.* **2020**, *188*, 102435. [CrossRef]

99. Santín, A.; Grinyó, J.; Ambroso, S.; Uriz, M.J.; Gori, A.; Dominguez-Carrió, C.; Gili, J.-M. Sponge assemblages on the deep Mediterranean continental shelf and slope (Menorca Channel, Western Mediterranean Sea). *Deep. Sea Res. Part I Oceanogr. Res. Pap.* **2018**, *131*, 75–86. [CrossRef]
100. Bo, M.; Bertolino, M.; Borghini, M.; Castellano, M.; Harriague, A.C.; Di Camillo, C.G.; Gasparini, G.; Misic, C.; Povero, P.; Pusceddu, A.; et al. Characteristics of the Mesophotic Megabenthic Assemblages of the Vercelli Seamount (North Tyrrhenian Sea). *PLoS ONE* **2011**, *6*, e16357. [CrossRef]
101. De la Torriente, A.; Serrano, A.; Fernández-Salas, L.M.; García, M.; Aguilar, R. Identifying epibenthic habitats on the Seco de los Olivos Seamount: Species assemblages and environmental characteristics. *Deep. Sea Res. Part I Oceanogr. Res. Pap.* **2018**, *135*, 9–22. [CrossRef]
102. De La Torriente, A.; González-Irusta, J.M.; Aguilar, R.; Fernández-Salas, L.M.; Punzón, A.; Serrano, A. Benthic habitat modelling and mapping as a conservation tool for marine protected areas: A seamount in the western Mediterranean. *Aquat. Conserv. Mar. Freshw. Ecosyst.* **2019**, *29*, 732–750. [CrossRef]
103. Serrano, A.; Cartes, J.; Papiol, V.; Punzón, A.; García-Alegre, A.; Arronte, J.; Ríos, P.; Lourido, A.; Frutos, I.; Blanco, M. Epibenthic communities of sedimentary habitats in a NE Atlantic deep seamount (Galicia Bank). *J. Sea Res.* **2017**, *130*, 154–165. [CrossRef]
104. Galil, B.; Zibrowius, H. First benthos samples from Eratosthenes Seamount, eastern Mediterranean. *Senckenberg. Marit.* **1998**, *28*, 111–121. [CrossRef]
105. Grinyó, J.; Gori, A.; Greenacre, M.; Requena, S.; Canepa, A.; Iacono, C.L.; Ambroso, S.; Purroy, A.; Gili, J.-M. Megabenthic assemblages in the continental shelf edge and upper slope of the Menorca Channel, Western Mediterranean Sea. *Prog. Oceanogr.* **2018**, *162*, 40–51. [CrossRef]